EXPERIMENTAL SETUP AND PRELIMINARY RESULTS FOR ELECTRON BEAM REMEDIATION OF HEAVY HYDROCARBON CONTAMINATED SOILS

A Thesis

by

KENNETH WAYNE BRIGGS III

Submitted to the Office of Graduate and Professional Studies of
Texas A&M University
in partial fulfillment of the requirements for the degree of

MASTER OF SCIENCE

Chair of Committee,	David Staack
Committee Members,	Andrea Strzelec
	Suresh Pillai
Head of Department,	Andreas Polycarpou

May 2015

Major Subject: Mechanical Engineering

ABSTRACT

Electron beam soil remediation has been shown to be an effective method for reducing total petroleum hydrocarbon (TPH) of polluted soils. This is done through a combination of reaction mechanisms, including thermal effects, radiation induced chemistry, and physical effects. Based on preliminary experiments, electron beam (e-beam) reactors and reactor supports were designed for soil treatment. Initial screening experiments with manufactured soils indicated a dose-dependent TPH reduction to below 1% in some cases. Further experiments and commercial analysis of treated real soils for C5-C38 alkanes showed reductions to below 1% for Benchmark soils 1 & 2 and GSC1AOS soil. Maximum TPH reductions for real soils are 9.1% to 0.15% for GSC1AOS with an 1100kGy dosage, 2.9% to 1.2% for GSI14RD with a 720kGy dosage, 1.6% to 0.17% for BM1 with a 960 kGy dosage, 2.1% to 0.5% for BM2 with an 820kGy dosage, and 31.9% to 28% for BT Sludge with an 1100kGy dosage. Three additives, ethanol, potassium chloride (KCl), and citrus oil were tested in 5wt% amounts with BM1. 720kGy treated soils with additives showed a TPH reduction to less than 0.5%, lower than the predicted value of 0.69% from BM1 experiments without additives. TPH reduction due to e-beam treatment was shown to increase with dosage and treatment temperature but decrease with increasing moisture. Additionally, changes in the carbon number distribution indicate non-thermal effects from e-beam treatment and the production of hydrocarbon fractions available for removal by environmental exposure. Adding a condenser to the setup was shown to improve collection of separated liquids.

ACKNOWLEDGEMENTS

I would like to thank my advisor and committee chair, Dr. Staack, for his guidance, suggestions, and support during this research. I would also like to thank my committee members, Dr Strzelec and Dr. Pillai, for their support and all plasma engineering lab members for their suggestions and extensive assistance during this research. Thanks again to Dr. Pillai for use of the electron beam at the National Center for Electron Beam Research. I would also like to thank Chevron for funding both my research and education. Finally, I would like to thank my friends for their support and my family for their love and encouragement.

NOMENCLATURE

A	Absorbance
DRO	Diesel Range Organics
EPA	Environmental Protection Agency
GCMS	Gas Chromotography Mass Spectroscopy
GRO	Gasoline Range Organics
I	Spectral Intensity
ID	Inner Diameter
K	Kelvin
KCl	Potassium Chloride
kg	kilograms
kGy	kilogray
kJ	kilojoules
m	meters
MS	Mass Spectrometry
NCEBR	National Center for Electron Beam Research
PAH	Polycyclic Aromatic Hydrocarbons
psi	pounds per square inch
PVC	Polyvinyl Chloride
OD	Outer Diameter
ORO	Oil Range Organics

TPH	Total Petroleum Hydrocarbon
VOC	Volatile Organic Compound

TABLE OF CONTENTS

Page

LIST OF FIGURES

LIST OF TABLES

Page

1. INTRODUCTION

1.1 Motivation

Pollution of soils by organic hydrocarbons is a major global environmental issue. Pollution may occur quickly from large oil spills, or slowly through seepage of lighter liquid fractions at drill sites over decades, resulting in contamination of soil and groundwater [1]. The importance of this issue is self-evident, given the importance of soil as a natural resource, its role in maintaining life, and its low renewal rate. The implications of soil pollution are destruction of local ecosystems, contamination of drinking water and farmland, and millions of dollars in economic damage. To minimize the consequences of soil pollution, soil remediation technologies must be fast, efficient, and economically viable at large scales.

Of most immediate importance is remediation of soils contaminated with heavy hydrocarbons. Crude oils contain a wide range of hydrocarbon fractions, including light, medium, heavy, and very heavy compounds [2]. Lighter fractions are clear, highly viscous liquids that are naturally removed through environmental exposure and biodegradation. Very heavy components such as tar and asphaltenes are generally immobile and thus pose no threat to the environment. Medium to heavy fractions, however, do not degrade as quickly as light fractions, but are still mobile in soils. These pose the greatest threat for environmental damage, due to their ability to spread through large areas of soil, and, most importantly, into groundwater.

Most hydrocarbons are largely held on the top of the water table, since their insolubility in water prevents downward movement. The hydrocarbons will disperse

with the groundwater flow. This results in contamination of the water supply and the spread of toxic fumes into locations with access to public water supplies. Additionally, trace (non-organic) contaminants found in hydrocarbons may be deposited in the water and in soil along the hydrocarbon flow. These contaminants can poison drinking water, water for agriculture, and the soil itself. Thus, remediation of soil is not only necessary to reclaim the contaminated soil, but also to prevent contaminants from spreading to other locations and causing further damage.

1.2 Background

Ranges of hydrocarbon fractions are more rigorously defined as gasoline range organics (GRO), diesel range organics (DRO), and oil range organics (ORO). These ranges are defined for n-alkanes, or hydrocarbons that consist of only hydrogen and carbon atoms joined by single covalent bonds [3]. The chain length, or carbon number for these ranges is 5-12 (light fractions), 13-22 (medium fractions), and 23-40 (heavy fractions) respectively. They are graphically depicted in Figure 1 and define TPH. Thus, very heavy fractions (>C40) are excluded from quantitative analysis, though they may account for up to 40% of fractions present in crude oils.

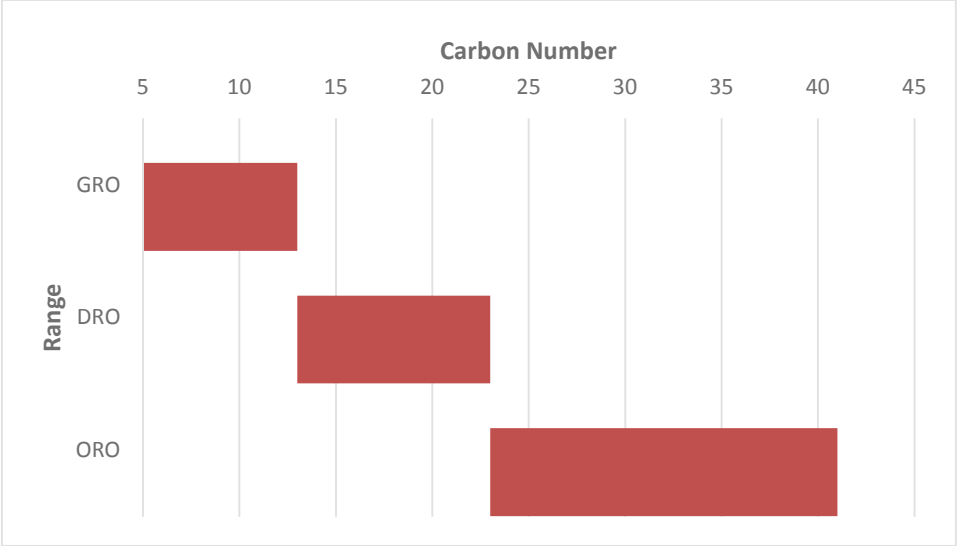

Figure 1: Carbon number ranges

TPH is typically the standard for evaluating contamination levels in US government regulations. Different state governments have varying soil clean-up standards ranging from roughly 0.01%-2.0% by soil mass. The most widely used and accepted standard is 1% soil TPH by mass [4]. Many remediation technologies, including, bioremediation, thermal desorption, solidification, and soil washing [5-7], attempt to achieve this clean-up level, but are typically time consuming, expensive, and often insufficient. Based on previous investigations of electron beam interactions with hydrocarbon compounds, it is believed that the use of electron beam technologies to induce chemical and physical changes in hydrocarbons could lead to sufficient reductions in contaminated soils [6, 8-10].

Electron beam processing uses electrons as a radiation source to generate physical and chemical changes in various substances. These changes depend on energy supplied to the material and material properties [11, 12]. Electron beam irradiation

processes are highly controllable and leave no residual radiation, lending them to many industrial applications including but not limited to bond cracking, cross-linking, polymer degradation, sterilization, pasteurization, and vulcanization [11, 12]. Previous research indicates that e-beams have great potential for applications in soil remediation. A concept for the setup of an e-beam soil remediation system is shown below.

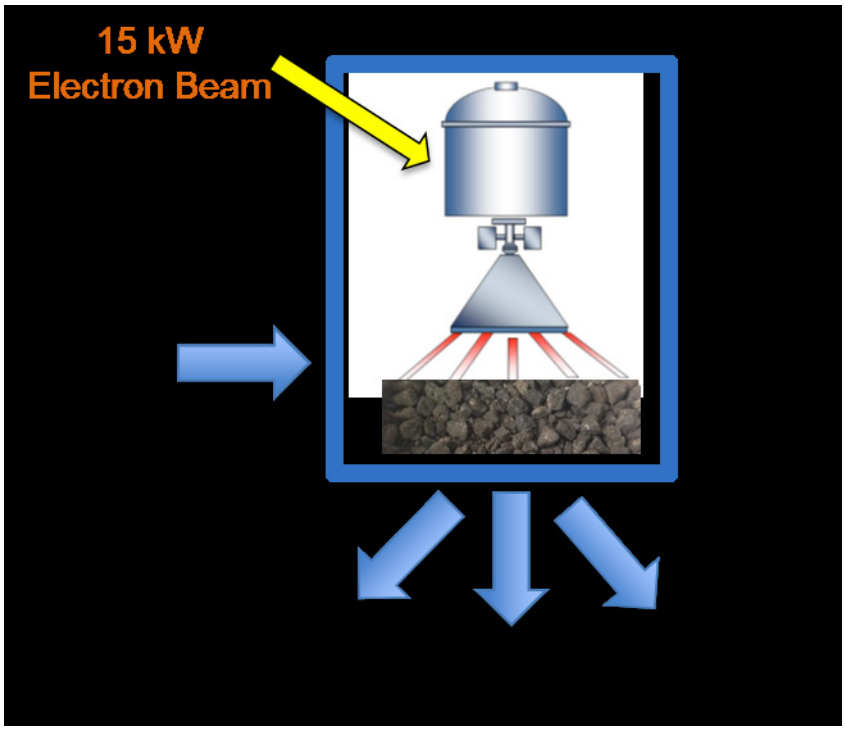

Figure 2: E-beam soil remediation concept

A variety of factors may play into the effectiveness of electron beam remediation of soils. Primary control variables are treatment temperature, soil moisture, soil composition, including additives, and dosage. Increasing the dosage would increase hydrocarbon removal efficiency since higher energy means higher temperatures and more energy provided for cracking hydrocarbon compounds. Higher temperatures are

advantageous since a variety of remediation techniques, most notably thermal desorption, rely on high temperatures alone and have demonstrated high contaminant removal efficiencies. Three types of reaction processes should occur during heating of soil contaminants: pyrolysis, combustion, and evaporation. Pyrolysis is thermochemical decomposition of organic material at elevated temperature in the absence of oxygen. Thermal cracking is a typical pyrolytic process. Combustion is a high temperature exothermic reaction between organic compounds and oxygen. Evaporation is physical change of a compound from a liquid to gaseous state.

Medium carbon chains that are not cracked may simply evaporate. Boiling point ranges for GRO, DRO, and ORO ranges are -0.2ºC – 216ºC, 234ºC – 367ºC, 379ºC – 524ºC respectively [13, 14]. Based on Equation 1, where D is dose in kGy, c is specific heat in kJ/kg*K, T is temperature in Kelvin, and h_{fg} is the enthalpy of vaporization of water, a 1 minute treatment from a 10MeV electron beam (roughly 480 kGy) on a dry soil should produce a temperature of roughly 400°C. This is a high enough temperature to boil most DRO range and some ORO range hydrocarbons. This equation assumes no heat transfer out of the system during treatment. This is reasonable since the energy generated by the beam is several orders of magnitude higher than the energy leaving the soil during treatment.

$$\Delta T = \frac{D - h_{fg}}{c} \tag{1}$$

This will not be the case for OROs as well as more complex alkenes or alkynes, which feature double and triple bonds between carbon atoms respectively. Most of these could undergo physical separation resulting from pyrolysis. Physical separation involves separation of compounds from denser ones and may be gravimetric flow or pressure driven. The GRO component of soil TPH could increase from cracking of OROs and heavy DROs. GROs and light DROs should evaporate or crack into compounds that are gas phase at room temperature, such as methane.

For very high dosages, an e-beam treatment system would also effectively act as an incinerator, combusting many compounds. Most hydrocarbons in the GRO – ORO ranges can be combusted with temperatures in the 870°C-1200°C range [4]. Based on estimates, a dosage of 1500 kGy would be sufficient to produce these temperatures for most soils.

Soil composition has a major effect on removal efficiency. Primary effects from moisture level result from the high specific heat of water (4.2 kJ/kg*K) compared to oil and soil, which results in water absorbing a large amount of the energy provided by the electron beam. Also, since water evaporates at low temperatures compared to hydrocarbons, all water must be evaporated before significant phase change of the contaminants occurs assuming uniform soil temperature. A large amount of energy goes towards overcoming enthalpy of vaporization of water as well. Consider 1 kg of a soil that is 60% solids, 10% oil, and 30%. The required energy to evaporate the water would be 678 kJ, while heating to boiling from room temperature (25^{o}C) would require an additional 94.5 kJ. Estimating the specific heats of soil and oil at 0.83kJ/kg*K and 2

kJ/kg*K respectively, the energy absorbed to reach 100ºC would be 37.4 kJ and 15 kJ respectively. Assuming the soil to be at uniform temperature across all phases, the required dosage to reach 100ºC and evaporate all water would be 850.5 kGy. Assuming a water content of 10% and 10% oil, this dosage reduces to 412.7kGy. Oil concentration also affects treatment efficiency. Experiments have shown that treatment efficiency tends to decrease logarithmically as oil concentration is reduced [9].

Additives, primarily salts and surfactants, can increase removal efficiency by reducing surface tension between liquids (water and oils) and solids, enhancing physical separation. This reduces the energy required to induce phase separation in a soil, and should result in greater TPH reductions than the same dosage without additives.

Another possible outcome is that the hydrocarbons will chemically bond with the soil. The energy of the electron beam should be enough to break up the covalent bonds that hold together most soils. This would allow radicalized hydrocarbons to possibly form covalent bonds with the soil. The high energy required for these reactions would indicate that the resulting bonds would not be broken in normal environmental conditions. This means that these hydrocarbon fractions would be inert and would not cause any environmental damage. This is effectively the application of the stabilization remediation technique to hydrocarbon polluted soils. Breaking up soil grains will further facilitate remediation as this exposes oils to treatment that otherwise would not be in less energetic techniques such as bioremediation.

Phase separation is a greatly desired outcome of treatment. Cracking and evaporation should result in the production of lighter, lower viscosity liquid products

that separate from the soil. These products will consist of lighter fractions in the C5-C16 range that may be removed through environmental exposure and other remediation techniques such as biodegradation.

There is a possibility that e-beam treatment of soils will produce toxic by-products. Non-equilibrium hydrocarbon products capable of reacting with the environment on time scales ranging from seconds to years could be made. Many of these have the potential to be carcinogenic. Conversely, treatment could result in breakdown of toxic components. Determination of the hazard level of products will require further research.

1.3 Objectives

The main objectives of this research are to demonstrate a proof of concept for electron beam remediation of hydrocarbon polluted soils and to show the impact of testing parameters such as dosage, treatment temperature, moisture, and additive concentration on TPH levels for various soils. Initial screening experiments will determine conceptual design of the experiment setup and a range of dosages. Further experiments will attempt to demonstrate reductions of TPH to <1% for a variety of manufactured and real soils while continuing optimization of the experiment setup.

Section 2 will provide a literature review of electron beams and general radiation concepts, soil remediation experiments, and irradiation of hydrocarbons. Section 3 will describe the process of developing the experimental setup. Preliminary e-beam treatment of some simple oil and sand mixtures was used to design the experimental operating apparatus and determine a range of treatment conditions. Section 4 will describe results

from different electron beam experiments, including soils manufactured from clay and sand and as-received soils provided by the research sponsor. Proof of concept was demonstrated using clay and sandy soil experiments along with analysis of water content and temperature effects. As-received soil experiments were used to develop a relationship for TPH reduction as a function of dosage and to test further setup modifications. Section 5 will summarize the results of the research and provide suggestions for possible future work.

2. LITERATURE REVIEW

2.1 Electron Beam Radiation Background

Electron beams can be defined as a stream of free electrons accelerated through a vacuum using an electromagnetic or electrostatic field[15]. They are generated in a vacuum using a voltage applied between an anode and a cathode. Electron beams, or cathode rays, were observed long before electrons were known to exist. Experiments conducted by Michael Faraday in the early 19^{th} century showed a glow between two charged electrodes proportional to gas density [16]. Further experiments by Hittorf and Plucker suggested that this glow was in fact a beam of charged particles that could be manipulated by electrostatic forces [17, 18]. This characterization of the glow as a beam was confirmed by JJ Thomson, who theorized that it consisted of subatomic particles he named electrons in 1897 [19].

With the physical properties of cathode rays established, i.e. a stream of negatively charged particles that respond to electromagnetic forces, many practical applications of cathode rays were devised along with better and more precise methods of controlling the energy and direction of these rays. High current beams with high energy densities were made available in the 1950s (O-type and M-type tubes), and allowed for development of industrial scale applications, such as bond cracking, cross-linking, polymer degradation, sterilization, pasteurization, and vulcanization [11, 12, 20]. Electron beam processing uses electrons as a radiation source to generate physical and chemical changes in various substances. These changes depend on energy supplied to the material and material properties [11, 12]. Figure 3 shows approximate dose ranges for

various applications [21]. These reactions occur due to the production of chemically reactive species from absorption of electron beam radiation [22].

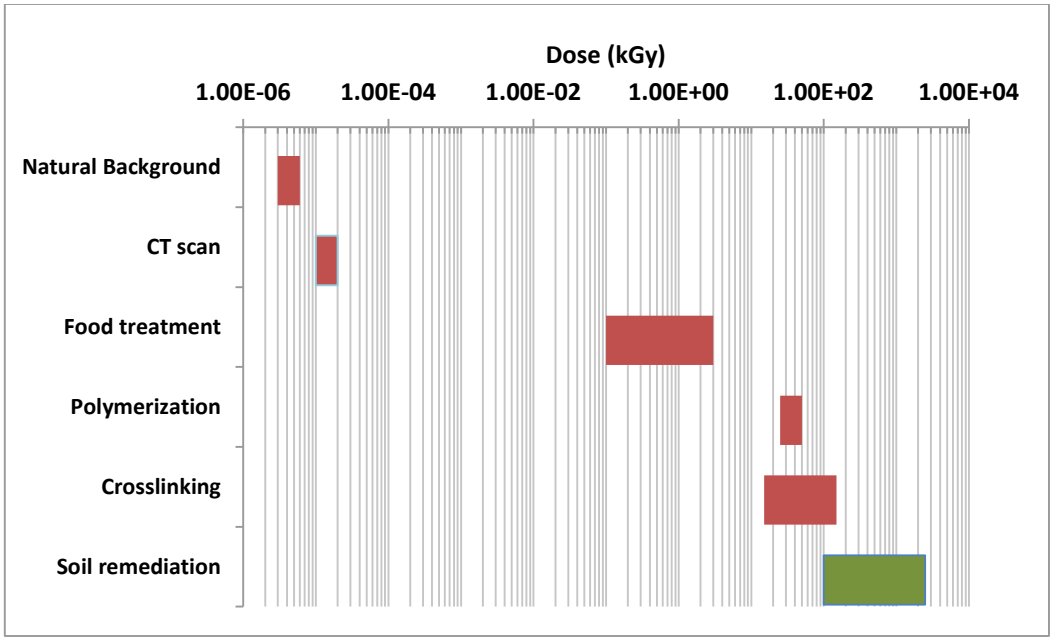

Figure 3: Typical dose ranges for industrial applications

The energy of electrons emitted by an e-beam is measured in electron volts, or the energy of one electron exposed to a potential of 1V [21]. The energy in Joules carried by each electron is determined by dividing the energy E in electron volts by the elementary charge:

$$E\ [J] = \frac{E\ [eV]}{1.602 \times 10^{-19} eV/J} \tag{2}$$

To determine the incident energy on the sample, some quantity related to the charge density must be known. This is typically beam current (I). Assuming steady-state current, the energy incident on the sample in Gray may be determined as shown below:

$$E_{incident} = \frac{I\Delta t(E\ [J])}{(1.602 \times 10^{-19})m} \tag{3}$$

where t is the irradiation time, m is the sample mass and $E_{incident}$ is the incident energy on the sample. This model has some error since not all energy from the beam will be incident on the sample. Also, beam current is not typically steady-state over the irradiation time. For this case, the charge ($I\Delta t$) is determined by integrating current over the irradiation time.

Dosimetry studies the physical quantities of concern for radiation deposition. Dose is typically defined as the energy imparted to a material resulting in chemical and physical changes in the material. This quantity is not the same as incident energy and requires knowledge of energy absorption at the molecular level, making it difficult to exactly measure. Typically, a dose absorber that experiences permanent physical changes after treatment is used for dosage determination. The dose obtained from this absorber is considered equivalent to the dose of the material of interest. This is a valid assumption for most materials. Dose is measured in units of Joules per kilogram, or Grays [23].

When an electron enters a medium, energy is imparted to the medium through Coulomb collisions with other electrons, which result in ionization of molecules and the

formation of chemically reactive radicals [23]. For 1-10 MeV beam energies, significant energy transfer results from these collisions but does not generate residual radiation [15]. In the meantime, initially ejected electrons (i.e. secondary electrons) collide with more molecules, eject more electrons (tertiary electrons) while forming radicals, and so on. This process continues until the initial kinetic energy of emitted electrons is dissipated [24]. The length of this process is characterized by the stopping power of the irradiated material, which is defined as the rate of energy loss per unit path length [24]. This quantity is a function of the material density, since a more closely packed material will induce more scattering. Due to formation of additional free electrons, the maximum applied dosage typically occurs somewhere in the interior of a material. In water, this occurs at depths of roughly 0.2cm, 1.2cm, and 3 cm for beam energies of 1 Mev, 5 MeV, and 10 MeV respectively [15].

2.2 Soil Remediation Techniques

Soil contamination is chemical degradation that severely limits the soil's environmental usefulness. This degradation is a function of the contaminant's bioavailability, mobility, and persistence. Bio-availability may be defined as the percentage of the contaminate freely available to cross the cellular membrane of an organism from the medium the organism inhabits [25], persistence refers to resistance of contaminants to environmental degradation [26], and mobility refers to a contaminants ability to move through the soil. Remediation techniques seek to change these contaminant characteristics through chemical, thermal, and/or biological means [27] in order to minimize damage to soils. The selection of an appropriate remediation

technique depends heavily on the extent and magnitude of contamination on site and the constituents present [7]. Confinement techniques that restrict contaminant mobility and/or decontamination techniques can be used to permanently remediate soils [27]. On-site and in-situ methods provide the most economical alternative, however all methods but thermal desorption are expensive, high energy, and have a long time frame [8]. Remediation techniques have been shown to be more effective when combined, as this allows targeting of many different constituents. Electron beam treatment could possibly enhance these techniques in this way [7].

Mobilization techniques attempt to use desorption to remove VOCs via phase separation [28]. Vapor extraction removes contaminants by filtering air through a well filled with soil. This is effective for light, highly mobile fractions. The contaminants must be volatile and have low water solubility, and must be above the water table. These conditions place severe limits on the technique; SVE extraction efficiency decreases to <10% when the GRO fraction is approximately 40% [7]. Soil flushing is designed to enhance in situ mobilization of contaminants using a fluid, typically water, to dissolve and mobilize contaminants in permeable soils [29]. This technique is mainly used for metal contaminants, but certain fluids, such as surfactants, make it applicable to organic compounds.

Immobilization encompasses a variety of techniques used to immobilize contaminants in soils as solid phase [30]. In-situ immobilization introduces treatment chemicals into the ground to confine contaminants and can confine 82-95% of metals [6]. Stabilization and solidification techniques convert contaminants into their most

environmentally stable form. Solidification reduces the mobility of hazardous substances through mixing with chemical reagents. This technique is only feasible for volatile organics. Heavier organics may be polymerized and bonded with the soil itself through vitrification, which uses extreme temperatures maintained for long periods to melt and harden organic contaminants [31].

Irradiation with microwave heating has been shown to be very effective for removal of volatile and semi-volatile hydrocarbons [8]. C10-C40 hydrocarbons were destroyed, desorbed, or co-evaporated with moisture. Reductions between 75% and 98% were reported [8]. Additionally, removal efficiencies of 90-95% for a 1000 W input for 60 minutes were reported for ex-situ treatment of 20 g soil samples. Removal efficiency appears to decrease with increasing water content [9].

Thermal techniques have been shown to be the most efficient. Two common techniques are thermal desorption and incineration. Thermal desorption heats soil to temperatures of 100-600^{o}C to volatilize contaminants and instigate phase separation [5, 6]. Temperatures of 150^{o}C have been shown to remove 95% and 75% of contaminants in sandy soils and clayey soils respectively for a 30 minute treatment [10]. For higher temperatures, removal of >99% of contaminants has been reported [32-34]. Desorption appears to improve with reduced water content and smaller particle size. Additionally, the rate of removal during treatment appears to decrease as contamination levels decrease [10]. Incineration uses temperatures of 870-1200^{o}C to combust contaminants in solids and liquids and can achieve reductions of >99.99% [6].

Bioremediation uses microscopic organisms to break down hydrocarbon compounds in soil into less harmful substances. Specific conditions may be required for different microbes. Bioremediation has been shown to provide 70%-80% removal of mineral oil [6, 35] and 95% removal of monocyclic aromatic hydrocarbons [6]. Additionally, 90% removal of diesel fuel in soil was reported after 4 weeks of treatment [35]. Removal rates from bioremediation are very economical. However, reductions of >95% are difficult, limiting use of bioremediation to sites with high levels of contamination (>50,000 ppm) [5].

Electrokinetic (EK) techniques use electrodes implanted in soil to cause ionic species to migrate to one electrode [36]. Migration is induced by the generation of H+OH radicals [37]. This technique is typically used to enhance other techniques such as ultrasonic (US) remediation. EK and ultrasonic US remediation technologies have been studied for PAH removal, with EK alone and EK and US removing 85% and 90% of PAHs respectively [38]. EK has also been combined with bioremediation, and has been shown to double removal efficiency over 100 days of treatment [39].

It is believed that electron beam treatment of soils would produce effects from incineration, thermal desorption, vitrification, oxidation, and irradiation. The energy from the beam would result in rapid heating. Compounds with very high boiling points would experience vitrification, high to medium boiling point compounds would volatilize as in thermal desorption, while lighter fractions would be incinerated. Oxidation and irradiation from e-beam energy would result in formation of radicals and bonding between soil and oil, effectively immobilizing these compounds. Volatilization

of compounds that initially have low mobility could be used to enhance other techniques dependent on this quantity, namely mobilization techniques and bioremediation.

2.3 Irradiation of Hydrocarbons and Soils

Two types of reactions may occur as a result of electron beam treatment in hydrocarbons. The hydrocarbon molecules may break up and recombine into larger molecules (polymerization), or permanently break into smaller molecules (cracking).

Cracking may be induced through heating, known as thermal cracking (TC) or through radiation absorption, known as radiation thermal cracking (RTC). TC begins with initiation, where the chemical bond between two carbon atoms in an organic molecule is broken. This results in an un-bonded electron, creating an electrically charged molecule known as a free radical. Interactions involving radicalized hydrocarbons drive the cracking process. Only a small fraction of the organic molecules will generate radicals. The next step is hydrogen abstraction. In this process, free radicals remove hydrogen atoms from other molecules. This transforms the second molecule into a free radical. Radical decomposition occurs when an organic radical breaks into a hydrogen radical and a stable alkene molecule. These mechanisms are shown below in Equations 4-7 for an n-decane molecule. Molecules preceeded by an "*" are radicalized molecules.

$$C_{10}H_{22} \rightarrow {}^{*}C_5H_{11} + {}^{*}C_5H_{11} \qquad \textbf{[Radical formation]} \qquad (4)$$

$$^{*}C_5H_{11} + C_{10}H_{22} \rightarrow C_5H_{12} + {}^{*}C_{10}H_{21} \quad \textbf{[H abstraction]} \quad (5)$$

$$^{*}CH_3 + C_{10}H_{22} \rightarrow CH_4 + {}^{*}C_{10}H_{21} \quad (6)$$

$$^{*}C_{10}H_{21} \rightarrow {}^{*}C_5H_{11} + C_5H_{10} \quad \textbf{[Radical Decomposition]} \quad (7)$$

The primary mechanism of radiation thermal cracking is dissociation of C-H bonds [40]. RTC has been demonstrated to be more effective for cracking of n-hexadecane [40, 41]. Chemical reactions occurring during RTC are shown below in Equations 8-10 [42]:

$$C_{10}H_{22} \rightarrow {}^{*}C_{10}H_{21} + {}^{*}H \quad \textbf{[Decyl and hydrogen radicals]} \quad (8)$$

$$^{*}H + {}^{*}n - C_{10}H_{21} \rightarrow H_2 + C_{10}H_{10} \quad \textbf{[Hydrogen and alkene formation]} \quad (9)$$

$$^{*}H + C_{10}H_{22} \rightarrow H_2 + {}^{*}C_{10}H_{21} \quad \textbf{[Hydrogen and decyl formation]} \quad (10)$$

This process could be coupled with TC, since a lot of heating would be expected during e-beam treatment, to create a highly efficient cracking process. However, to fully evaluate the effectiveness of radiation methods, the two mechanisms would need to be clearly distinguished. It is believed that high dose rates are beneficial at low temperatures, but RTC becomes less important than TC at high temperatures [40].

Polymerization results from recombination of radicalized hydrocarbon chains. During polymerization, a hydrocarbon molecule breaks up into free radicals with a free electron that may bond with other radicals. This process is repeated many times during one treatment, producing larger molecules [43]. This creates hydrocarbon compounds

with higher molecular weights that are less sensitive to changes in temperature. An example of polymerization is shown in equations 11-13. Polymerization typically occurs with heavy hydrocarbon molecules, but propane is used to simplfy the graphical depiction shown in Figure 4 [43]. Beam energies between roughly 25-50 kGy are used for polymerization according to Figure 3, much less than dosages used for soil remediation applications.

$$C_3H_8 \rightarrow {}^*C_3H_7 + {}^*H \qquad \textbf{[Radical Formation]} \qquad (11)$$

$${}^*C_3H_7 + C_2H_4 \rightarrow {}^*C_5H_{11} \qquad \textbf{[Chain Propagation]} \qquad (12)$$

$${}^*C_3H_7 + {}^*C_3H_7 \rightarrow C_6H_{14} \qquad \textbf{[Termination]} \qquad (13)$$

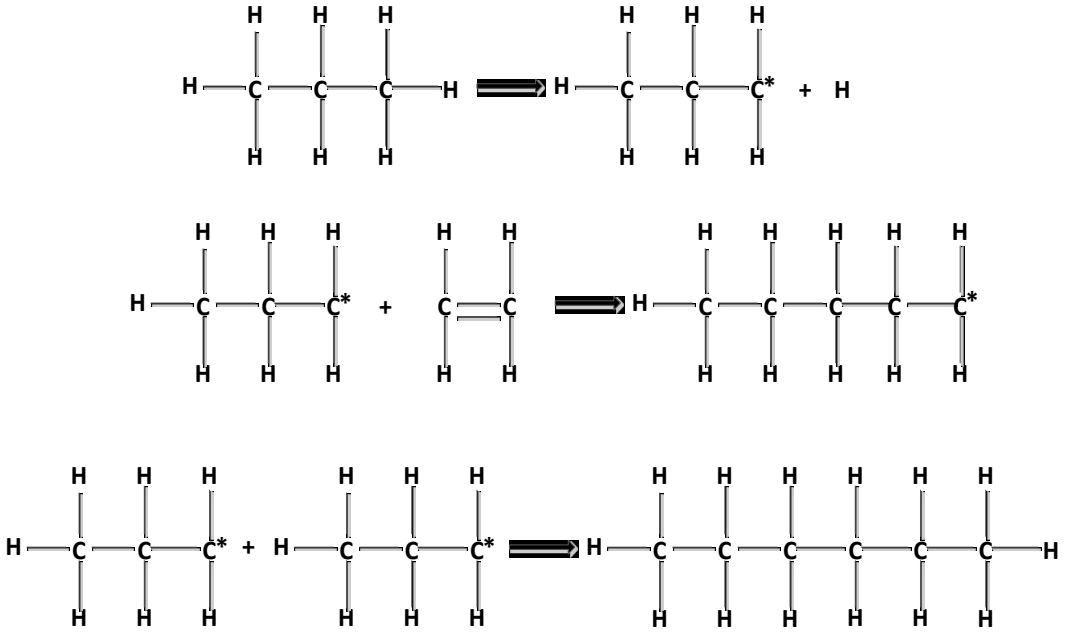

Figure 4: Polymerization reactions

Many experiments investigating irradiation of hydrocarbon compounds with electron beams have been reported. For example, electron beam radiation has been investigated as a way to upgrade heavy hydrocarbons [21]. In one experiment, 12 API heavy crude oil was irradiated using a 2 MeV beam with a 360kGy dose. The result was conversion of roughly 28% and 27% of >450^{o}C hydrocarbon residue (i.e. hydrocarbons that boil at 450^{o}C) to lighter fractions for dose rates of 20kGy/s and 37 kGy/s respectively [44]. This indicates a lack of dose rate dependence, and that electron beams can successfully degrade very heavy hydrocarbon compounds. Additionally, treatment of atmospheric residues using radiation thermal cracking (RTC) has been demonstrated to produce greater viscosity reductions and increases in distillable compounds than typical thermal cracking techniques [45, 46].

It is likely that electron beam irradiation would also produce these reactions in hydrocarbon compounds contained in soils, making them more amenable to other remediation techniques. This has been demonstrated for some light compounds. For example, 64% decomposition of formaldehyde in clay soil by irradiation with an 2 MeV electron beam was reported after a 70 ns treatment [47] . From equation 3, this corresponds to a dosage of roughly 28 Gy. Some of the resulting compounds were detected in the gas phase. Similar observations have been reported by Hilarides for 2,3,7,8-tetrachlorodibenzo-p-dioxin (dioxin), with destruction of up to 90% of contaminants reported using gamma irradiation [48].

Applications of these technologies to the remediation of soils have not been directly addressed in these experiments, and related concerns such as disposal and

transport of treated soils have not been researched. The goal of the present research is to begin to address these concerns

2.4 Surfactant Enhancement

Surfactants are often used to enhance the mobility of contaminants [49]. They enhance water solubility of hydrophobic contaminants and prevent adherence of contaminants to the soil. They consist of a hydrophilic head and a hydrophobic tail. The head bonds to water in an aqueous solution, while the tail is bonded with contaminants. This reduces surface tension and allows for easier phase separation, which could assist with separating hydrocarbon particles from soil. The effectiveness of a surfactant depends on concentration. Above the critical micellar concentration (CMC), the monomers of the surfactant form into a ball around oil particles, essentially achieving phase separation [50]. Figure 5 shows a micelle formed by a surfactant above CMC. Note that the contaminant is isolated from others in the system.

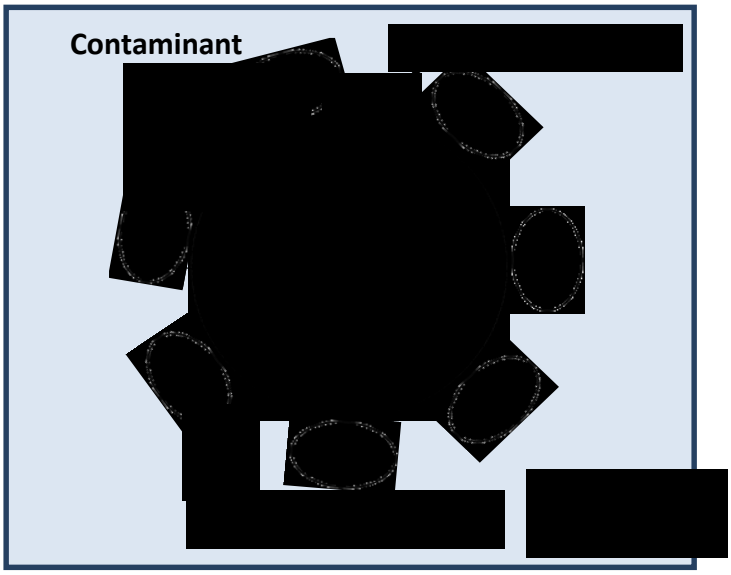

Figure 5: Micelle formed by a surfactant above CMC

This process occurs at lower concentrations for nonionic surfactants, making these ideal for electron beam testing.

Surfactants have been shown to elute 76-56% of DDT after 118 min. Also, extraction of oil adsorbed onto clay soil using Demsopan+2-propanol was attempted. 72% reduction of PAHs and a 97% reduction in n-alkanes was reported [51]. This shows high effectiveness for alcohols as solvents. Combined hydrocarbon and metal removal has also been observed, with removal efficiencies of 73% for phenanthrene and 82% for lead [5]. Biosurfactants can also be used. They are bio-degradeable substances that use microbes to decompose contaminants and increasing solubility. Previous experiments demonstrated styrene removal of 90% [52].

3. EXPERIMENTAL SETUP

3.1 Electron Beam System

The electron beam used for this research was located at the National Center for Electron Beam Research at Texas A&M University. The beam uses a single, vertically mounted 10 MeV, 15kW S-band microwave based Electron Beam Linear Accelerator (LINAC). The electron beam horn is located in a 2ft thick concrete bunker in the e-beam facility. The bunker provides room for a conveyor that moves samples below the electron beam and is shaped such that the conveyor must undergo three 90^{o} turns in order to scatter beam radiation and prevent it from entering areas where people may be exposed. The control room provides real-time monitoring of all e-beam system parameters to ensure safety and accurate testing. Figure 6 shows a diagram of the facility.

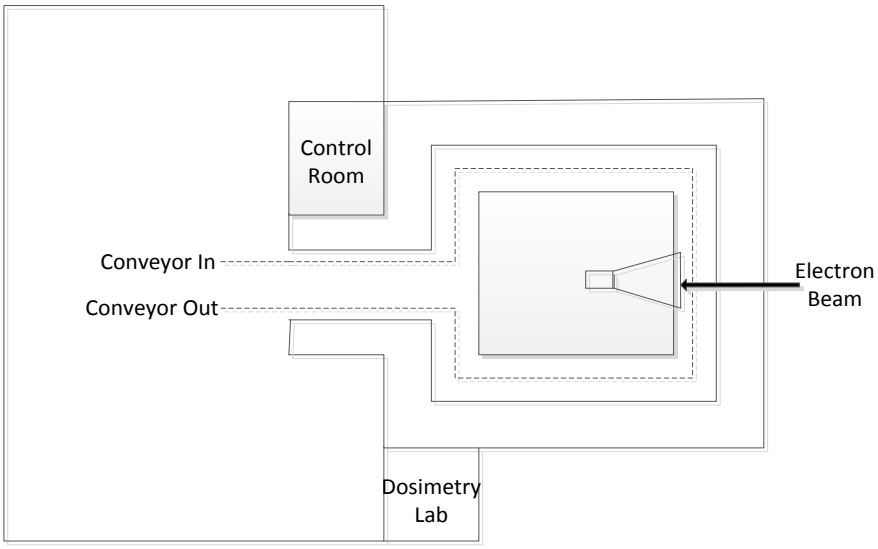

Figure 6: Electron beam facility

Key elements of the e-beam system include the accelerator, scanner, and material handling system [20, 24]. Figure 7 shows a diagram of the electron beam accelerator system [24].The accelerator uses alternating electric fields in evacuated (vacuum) electromagnetic cavities. Electrons are generated in an electron gun through thermionic emission from a cathode and formed into a beam using electric fields between the gun electrodes. The electron stream is focused into a narrow beam using magnetic deflection and formed into 20 μs clusters at a repetition rate of 256 Hz along the beam direction, resulting in a pulsed beam. This is done using alternating electric fields generated from coupling with microwave pulses supplied by the klysotron.

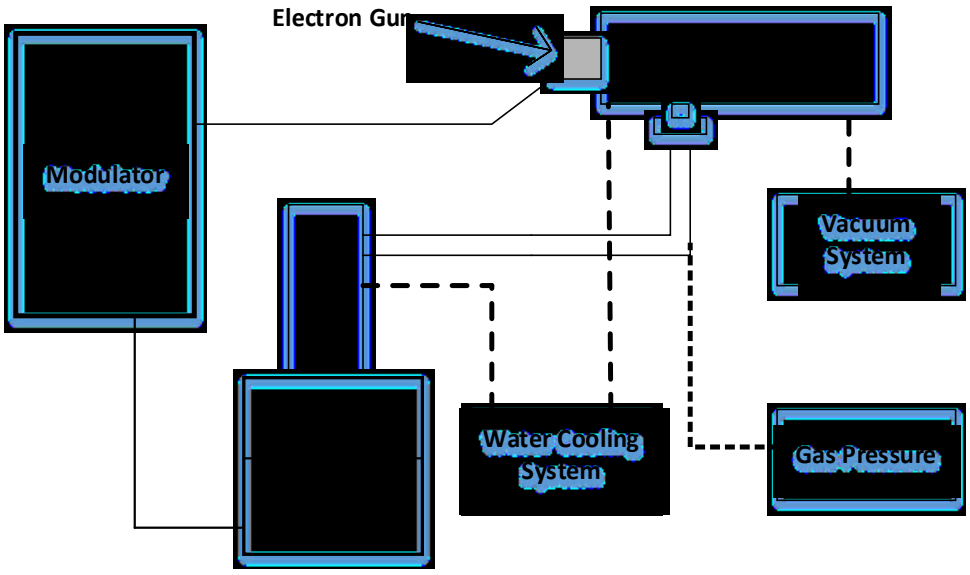

Figure 7: Diagram of an electron beam accelerator system

These systems are powered by the high-voltage modulator, which generates streams of electrical power pulses brought to high voltage with a pulse transformer that holds the

klysotron. The transformer uses a network of analog electrical components. Capacitors are charged and discharged into inductors to form a pulse.

Typical accelerators produce a beam that is too narrow to treat most products, so magnetic deflection with an alternating magnetic field is used to move the beam over the product width at a constant scanning rate of 315 Hz. This allows for scanning using a cone profile at constant deflection angle (~5^{o}) below the window [24]. The deflection angle may be controlled by varying the magnetic field between a maximum and minimum.

Typically, the accelerator and scanner systems operate at fixed parameters, and dose rate is controlled with the speed of the conveyor. The conveyor at the NCEBR uses a series of evenly spaced rollers, however, railings on each side of the conveyor allow for static placement of test reactors. Most experiments for this research were conducted with a static test setup. The beam intensity decreases logarithmically with distance below the beam due to electronic scattering and absorption by air. Water flows beneath the floor below the beam to absorb any radiation that passes through the air. Steady-state air flow occurs inside the bunker in order to prevent accumulation of dangerous gases, generated by the e-beam such as ozone and trace hydrocarbons released during processing.

3.2 Dose Measurement

Electrons enter a product and penetrate through formation of secondary and tertiary electrons until the kinetic energy of the primary electrons dissipates. The absorbed dose is dependent on depth and specific energy deposited per incident electron.

For this research, the soil sample was maintained at a small enough thickness to assume uniform dosage in the vertical direction. The dose rate was expected to decrease as a function of distance below the beam window due to a beam divergence of 5^{o}, so an initial experiment was run to quantify this dependence. Alanine tablets were placed 5", 10", 15", and 20" below the electron beam 1/2" behind 1/8" aluminum plates. The setup is shown in Figure 8.

Figure 8: Setup for dose-height dependence experiment

The beam was switched on for 2-5 seconds to ensure steady state beam current and avoid overdosing the tablets, which have a limit of 80 kGy. The dosage absorbed by the tablets is measured along with their distance from the e-beam window. Additionally, the instantaneous beam current is recorded (Figure 9). The beam current can be used to

obtain the time-dependent dose rate so that the integrated dose rate with respect to time is equivalent to the measured dose rate.

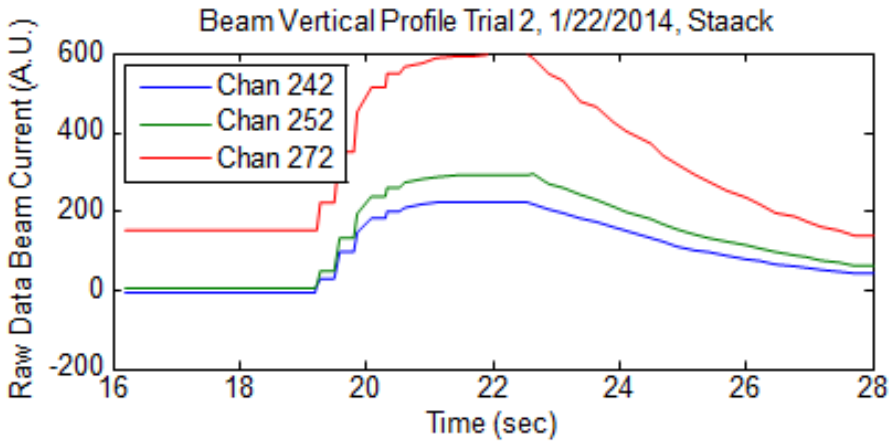

Figure 9: Instantaneous beam current from dose rate experiment.

To determine time dependent dose rate, beam current is normalized and transformed into a smooth function. The beam current is integrated to produce charge as a function of time and scaled such that the end value of charge is equivalent to the measured dosage at each distance. This is shown in Figure 10. The derivative of this produces time dependent dose rate, shown in Figure 11. Distances shown on the legend of both figures are in inches. Steady state dose rate is estimated as the maxima of the dose rate profile.

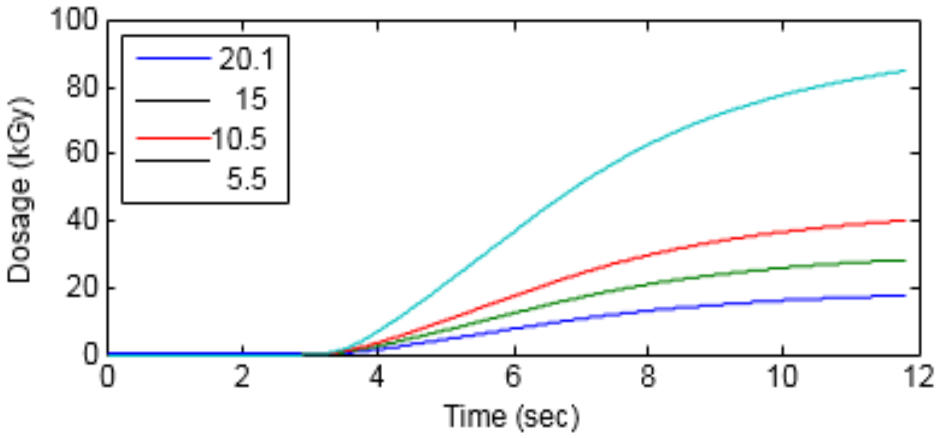

Figure 10: Accumulated dosage at each distance

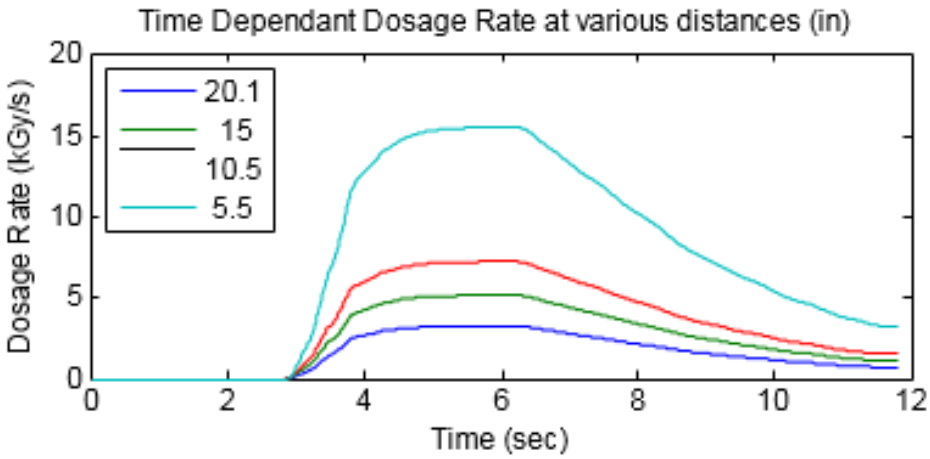

Figure 11: Time dependent dose rate at each distance

This analysis was used to produce measured dose and dose rate profiles as a function of distance. Predicted profiles were based on beam intensity decay resulting from divergence of the beam below the e-beam window. This is shown in the equation below, where x_o and w_o are the initial beam dimensions, z is distance from the window, and θ is the scattering angle, assumed to be 5^o.

$$I = \frac{I_o}{1 + 2\tan(\theta)\left(\frac{z}{w_o} + \frac{z}{x_o}\right) + 4\tan^2(\theta)\frac{z^2}{w_o x_o}} \tag{14}$$

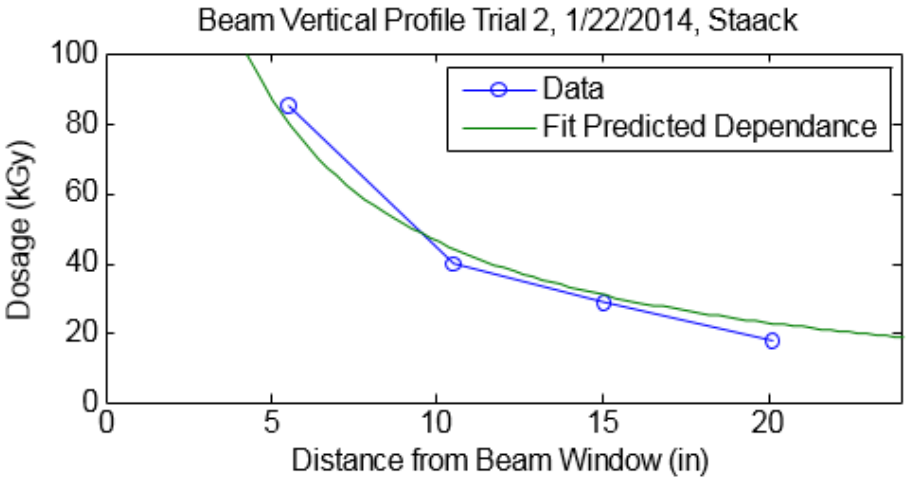

Figure 12: Measured and predicted vertical dosage profiles

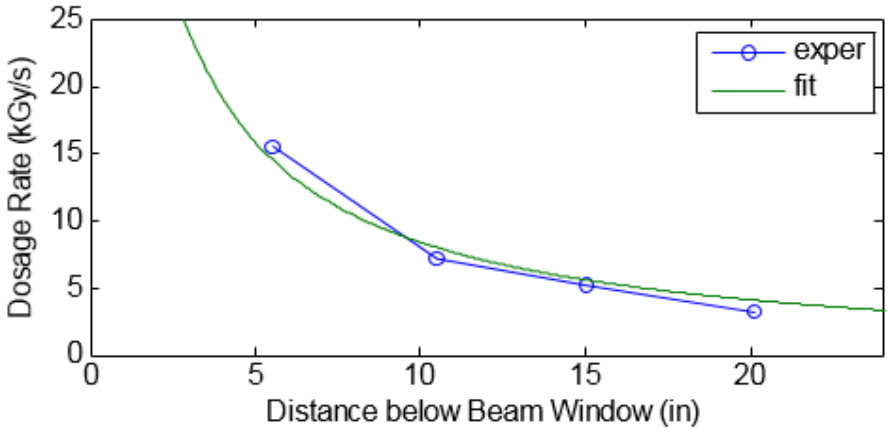

Figure 13: Measured and predicted vertical dose rate profiles

Accounting for height dependence lead to the construction of an adjustable height aluminum frame to support sample reactors below the beam. This allowed for reliable control of dose rate. Figure 13 was used to estimate dose rate for electron beam experiments by measuring the distance from the electron beam window to the sample and visually determining the dose rate corresponding to this distance.

Another experiment was run to determine beam size and uniformity. A piece of acrylic was placed below the beam for a five second run (Figure 14). The acrylic was placed 19” above the conveyor rails, corresponding to a dose rate of roughly 10 kGy/s. The beam discolored the acrylic, and the dimensions of this discoloration were assumed to be the beam dimensions, which was 1”x24”. Designs for soil sample holders were constrained to these dimensions.

Figure 14: Setup for beam profile experiment

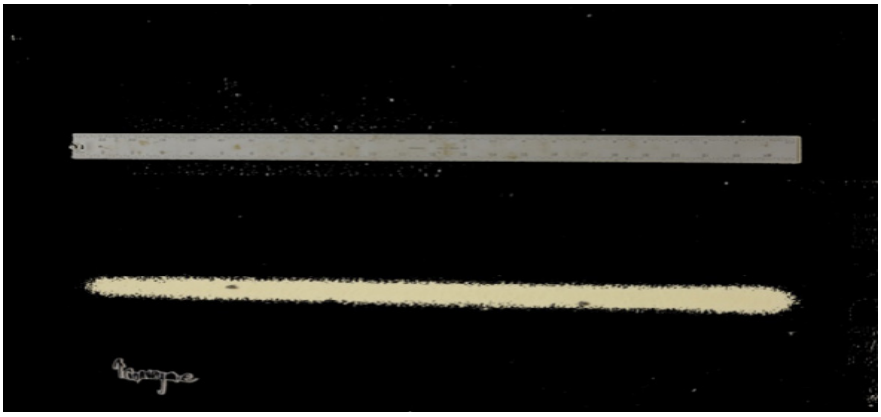

Figure 15: E-beam discolored acrylic after masking in photoshop

3.3 Setup and Procedure

3.3.1 Design of Soil Reactors

The basic reactor configuration for electron beam experiments is an aluminum sample pipe containing a soil sample and a ballast pipe that provides pressure reduction for the setup. Additionally, a box configuration and a single long pipe were tested. The configurations are shown in Table 1. Pipes are sealed using flanges and flourosilicone rubber gaskets.

Table 1: Electron beam reactor configurations

Config. #	Reactor Geometry	Reactor Dimensions	Ballast Pipe?
1	Pipe	1”	Yes
2	Pipe	2”	Yes
3	Pipe	2“	No
4	Box	8”x30”	No

Configurations 1 and 2 use a ballast pipe. The purpose of the ballast pipe is to reduce the pressure in the reactor during testing. During previous e-beam experiments with crude oil, the reactor reached a pressure of approximately 200 psi for the highest dosage using a single pipe, which created a limit on allowable dosage. It is expected that the additional volume will reduce the maximum pressure to about 20 psi. Another function of the pipe is to store gases that have evaporated from the sample, which are expected to condense once the pipe enters a room temperature environment. Ballast pipes consist of either a 4”ID PVC pipe or a 2”ID Aluminum pipe.

Configuration 1 was the first to be tested. The sample pipe consisted of a 1” diameter aluminum cylinder with 4” flanges welded to both ends. The flanges and end caps were milled flat along a 1.5” length to allow the pipe to rest flat without rotating, preventing soil mass losses from soil supports. The ballast pipe consisted of a 2” cylinder with a welded end cap and a three inch threaded flange. This setup had several drawbacks. The 1/8” wall thickness of the pipe meant the wall absorbed too much e-beam radiation. Also, the sample was not thermally isolated from the pipe wall, since the width of the sample was 1”. Configuration 2 uses a 3” OD, 1/16” thick pipe to isolate samples from the pipe wall.

Sample and ballast pipes are connected via compression fittings and copper tubing. To prevent breaking the seal from the compression fittings during handling, the ballast and sample pipes were connected using u-bolts attached to a mounting plate, as shown in Figure 16. This prevented the pipes from rotating independently.

Figure 16: Soil reactor configurations 1 (left) and 2 (right)

The inside of the sample pipe contains a support to elevate the soil above the pipe wall. This was done to (1) avoid contact between the soil and the pipe wall, (2) provide a place for physically separated oil to flow, and (3) to prevent re-condensing contaminants from flowing back into the soil. This allows for phase separation of liquid phase products produced by pyrolysis from the soil. Figure 17 shows the basic concept.

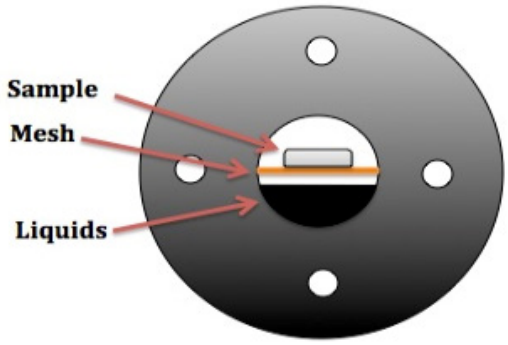

Figure 17: Soil sample reactor conceptual design

Configuration 3, shown in Figure 18, was designed to completely isolate soil samples from the pipe wall. It consisted of an 8”x30” box made of 1/16” aluminum sheets welded together. Soils were supported in an aluminum tray suspended in the center of the box with brass wires. This setup did not produce a good pressure seal, and alignment of soils below the electron beam was problematic.

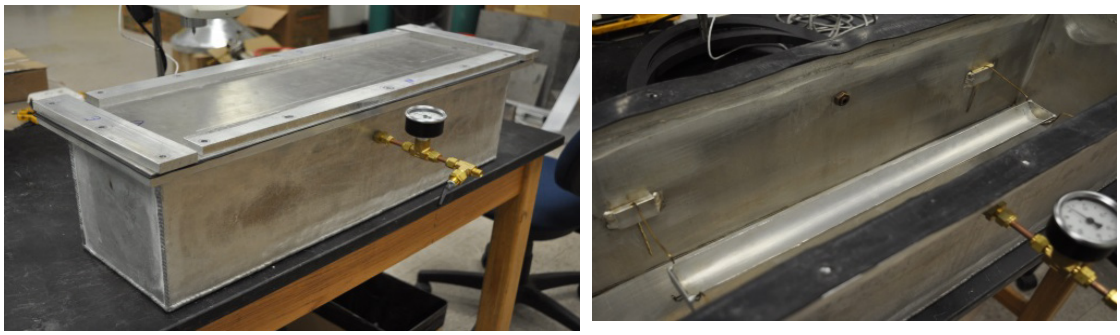

Figure 18: Soil reactor configuration 3

Configuration 4 consisted of a single, 4’ long aluminum pipe with a 3”OD and 1/16” wall thickness. This pipe accomplished the same objectives as configuration 2 while eliminating the ballast pipe. This significantly reduced the number of failure

modes of the pressure seal and simplified the setup. However, this setup was difficult to maneuver and maintain at a constant orientation.

3.3.2 Design of Soil Supports

Several designs for the soil support were used. Initially, dry soil samples were placed in an aluminum mesh tube. This tube consisted of a 3”x20” sheet of aluminum mesh wrapped into a tube shape and sealed on one end. The sample was filled in the other end, which is also then sealed. The mesh allowed for liquid phase separation from the soil. However, for wet soils, this setup was not practical. When wet samples are placed on the mesh, they tend to adhere to the mesh surface and inside the mesh holes. This made extraction of the soil with minimal mass loss problematic. Thus, for wet samples, an aluminum tray was used. This made phase separation less likely, but it was decided that obtaining an accurate mass balance was more important. Figure 19 shows these supports.

Figure 19: Aluminum mesh and tray soil supports

The final design incorporated the tray and mesh concepts into a single design suitable for all soil types. This setup is shown in Figure 20. A 250 micron stainless steel perforated sheet is used to hold soils and to induce phase separation while preventing loss of dry soil. The sheet is supported by an aluminum tray with the bottom drilled out to compensate for lack of structural strength in the sheet and to allow for separation of liquids. The new setup ensured that 99% of dry soil after testing was collected.

Figure 20: Final soil support design concept

For configuration 1, soil supports are simply pushed into sample pipes. For configurations 2 and 4, a frame was constructed to suspend the soil support in the center of the sample pipes. This is shown in the right picture of Figure 20. The frame has struts that rest on the pipe wall. Supports are secured with aluminum wires running through holes placed on the struts. To control position along the pipe length and prevent rotation of the soil supports, the frame is secured to a metal piece welded behind the pipe flange with small screws, shown in Figure 21.

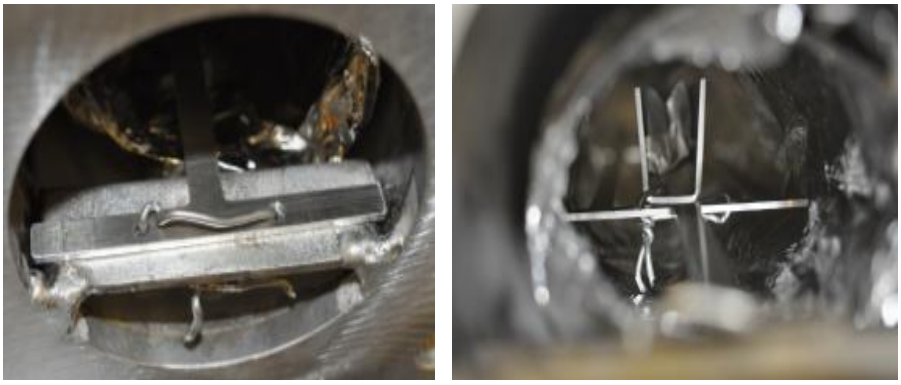

Figure 21: Soil support frame secured to the reactor pipe wall

3.3.3 Design of Reactor Support System and Diagnostics

An adjustable height aluminum frame was constructed to allow for control of dose rate. For the initial configuration, a tub was placed on the frame with hooks for supporting soil reactors (Figure 22). The height was set such that the dose rate was 8kGy/s. Initially, soil tests were conducted at low temperature by submerging half of the reactor in a water bath contained in the tub. It was found that maintaining low temperature adversely affected TPH reduction, so a high temperature test with the same tub but with the water bath just below the reactor was used.

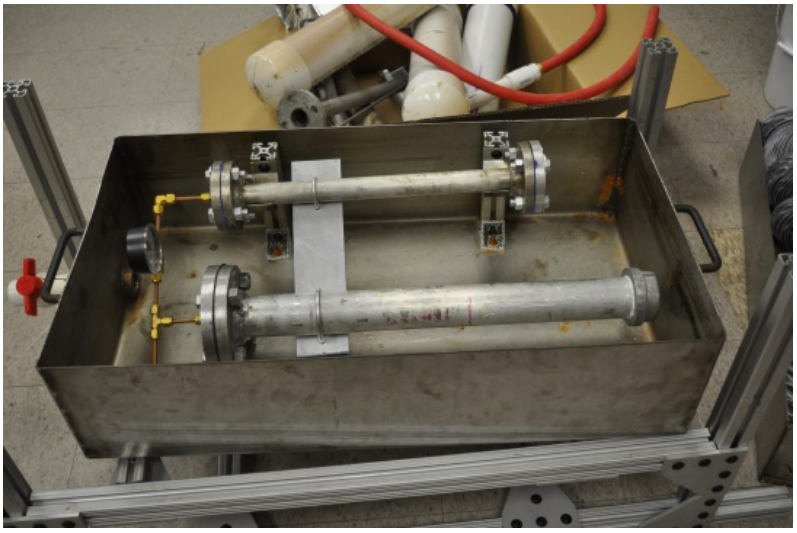

Figure 22: Electron beam reactor in the aluminum tub

The final design eliminated the tub and modified the frame so that it was the only structure supporting the reactors, as shown in Figure 23. Hooks are used to support sample pipes at an angle, which induced phase separation by allowing separated liquids to flow away from the soil sample. Rotation is prevented by a railing offset from the sample pipe on which the mounting plate is placed and held down with a c-clamp. This is shown in Figure 24.

Figure 23: Modified aluminum frame for high-temperature electron beam experiments

Figure 24: High-temperature electron beam setup with configuration 2

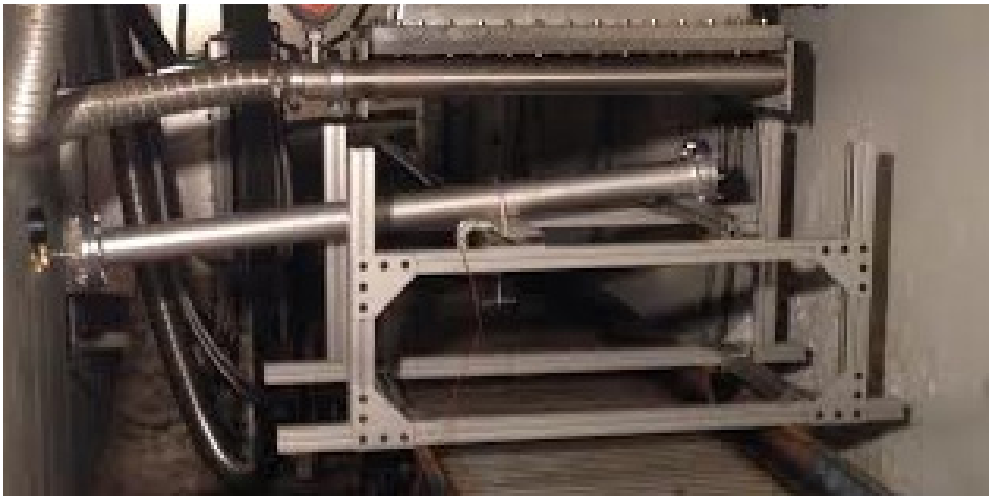

Figure 25: High-temperature electron beam setup with configuration 4

The railing is aligned such that the beam centerline is 15 3/8” away from the front edge of the railing. This is done so that the electron beam centerline is directly on the centerline of the reactor sample pipe.

Temperature and pressure diagnostics have been done using several methods. For initial experiments, a pressure gauge was used to record final pressure after testing, and a thermocouple was placed at various locations along the pipe to determine maximum temperature after treatment. For this approach, data was recorded roughly 2 minutes after testing ended, which did not provide an accurate picture of treatment conditions. To allow temperature measurements during testing, hose clamps were used to hold down a thermocouple between a piece of aluminum and the outer wall of sample pipes. This was initially used to record maximum temperature via a multi-meter. For the next approach, the multi-meter was placed near the control room and connected to the thermocouple via a BNC cable. The multi-meter screen was recorded during an e-beam run, and the data

was converted into a temperature time history. The setup is shown in the lower right picture in Figure 26.

Figure 26: Pressure and temperature diagnostics setup

A similar approach was used for pressure measurements. A pressure transducer was connected to the on/off flow control valve on the sample pipe and a multi-meter. This allowed for recording a pressure time history as well. Electrically sensitive components on the pressure transducer are covered with lead, as shown in the top of Figure 26.

A liquid nitrogen condenser, shown in Figure 27, was designed to allow for collection of more liquids without maintaining pressure. It consists of a collection vessel attached to the reactor flow control valve with an outlet pipe. The vessel is placed in a

can containing either ice, liquid nitrogen, or dry ice. The cool temperatures generated in the vessel cause evaporated gases to migrate to the vessel and condense before exiting the condenser through the outlet pipe. The condenser is tested without a ballast pipe.

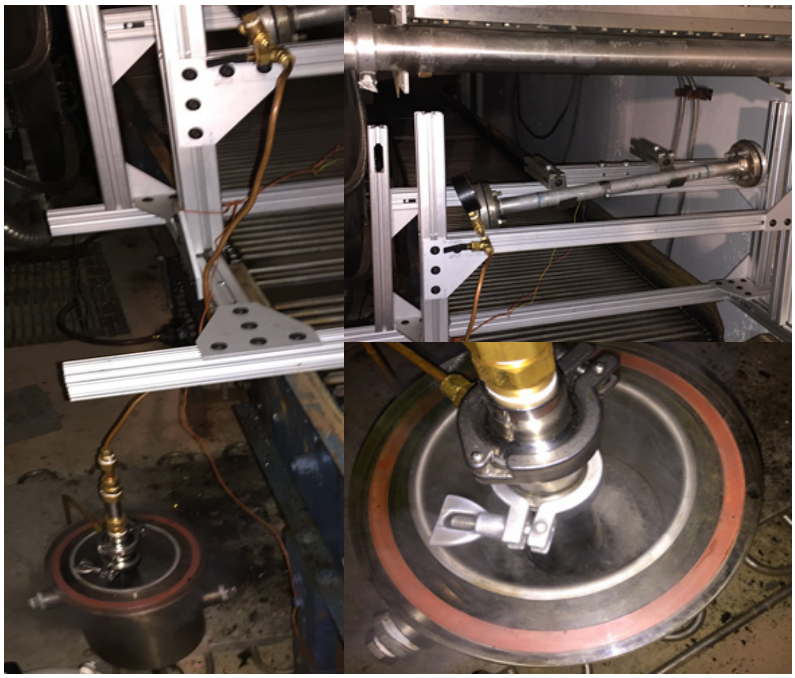

Figure 27: Liquid nitrogen condenser

3.3.4 Summary of Current Design

The current design for soil supports uses a 250 micron stainless steel mesh supported by an aluminum tray. For 1" pipes, this support is simply pushed into sample reactors. For 3" pipes, the support is attached to a frame secured behind the flange of the reactor. Sample reactors are connected to a ballast pipe and the pipes are secured with a bar. Reactors are placed on an adjustable aluminum frame and a thermocouple and a pressure transducer are connected to sample reactors.

3.3.5 Electron Beam Testing Procedure

Testing begins with placing the desired amount of soil sample into a soil support. The support is weighed with and without soil, and masses are recorded. The support is placed into the sample pipe. The sample pipe is connected to a ballast pipe if needed and the entire setup is pressure tested at 50 psi for 30 minutes to identify any leaks. The container is depressurized through the on/off flow control valve and the pressure after this process is recorded as the initial, or reference, pressure for that setup.

At the electron beam facility, the aluminum railing is placed on the conveyor and aligned with the beam. In initial experiments, the aluminum tub is placed on the railing, and the reactor is placed in the tub. For high-temperature experiments, water is filled to just below the reactor to prevent cooling through convection while allowing for absorption of the electron beam. For low-temperature experiments, the sample pipe is half submerged in water. In later experiments, the modified railing is placed on the conveyor and sample pipes are placed on this. If a ballast pipe is present, the mounting plate is clamped down with a c-clamp. For real-time diagnostics, a thermocouple and a pressure transducer are attached to the sample pipe.

After evacuating the electron beam bunker, the beam is switched on for the specified time to obtain the required dosage. Figure 28 shows the setup while the beam is turned on. 80 seconds after the beam switches off, personnel are allowed into the bunker to retrieve the sample reactor. The pressure and temperature of the reactor is recorded. The reactor is removed and taken outside to cool.

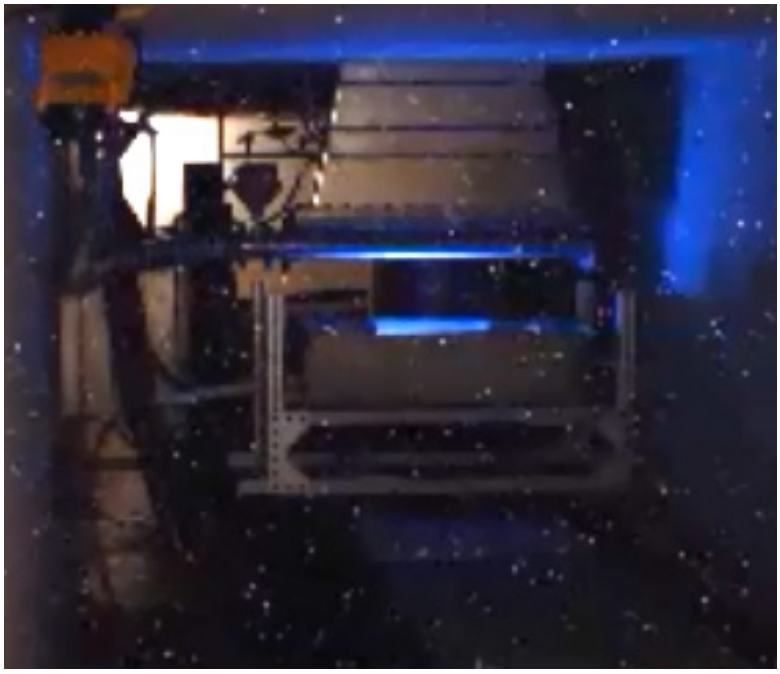

Figure 28: Experiment setup while the electron beam is on

After taking the reactor back to the lab, sample extraction begins. If the condenser is not present, a syringe is attached to the flow control valve and used to extract a sample of the produced gases. The syringe is saved for later analysis with a mass spectrometer. If a ballast pipe is present, ballast and sample pipes are disconnected and both are held over a jar to collect liquids. Otherwise, this is done only with the sample pipe. To extract solids, the sample support is removed from the reactor and solids are poured into another glass jar. The remaining soil adhering to the sample pipe walls is scraped into the same jar.

3.4 Analytical Methods

3.4.1 UV-Visible Absorbance Spectroscopy

3.4.1.1 Theory of Absorbance Spectroscopy

Absorbance spectroscopy compares the intensity of light that has traveled through a sample to the initial light intensity over a spectrum of wavelengths to determine the composition of the sample. In Ultraviolet-visible spectrometry, the light is in the wavelength spectrum between 100 and 800 nm. By capturing the light passing through the sample, transmission and absorbance spectra may be used to determine sample composition by comparing to the known spectra of pure substances.

Transmittance is defined as the ratio of the spectral intensity of the light that passes through a path length in a medium to the spectral intensity of the light through the same path length but without the medium present. When the spectral intensity is captured across a spectrum of wavelengths, a transmission spectrum may be obtained consisting of an array of transmittance values recorded with an array of wavelengths. When the spectral intensity is recorded without the medium present, the measurement is referred to as a reference. Spectral intensity is defined here as the total radiant power per wavelength. Absorbance is calculated by taking the logarithm of the inverse of transmittance, and may be assumed additive if the Beer-Lambert law holds over the wavelength range:

$$A = \log\left(\frac{1}{T}\right) = \alpha_\lambda bn \tag{15}$$

where α_λ is molar absorptivity, b is path length, and n is species concentration. If this condition is met, absorbance may be defined additively for mixtures with several components:

$$A_{mixture} = \alpha_{\lambda(1)} b n_1 + \alpha_{\lambda(2)} b n_2 + \cdots + \alpha_{\lambda(m)} b n_m \quad (16)$$

If we define the difference between successive wavelengths as fixed and reduce this difference to near zero, then the mixture absorptivity becomes the integral of spectral absorptivity with respect to wavelength. The validity of the Beer-Lambert law may be established by creating a calibration curve that shows the absorbance as a function of concentration at different wavelengths and determining the range in this curve where the absorbance changes linearly with concentration for these wavelengths.

3.4.1.2 Sample Preparation

Sample preparation involves two steps: (1) extraction of oils contained in a soil sample, and (2) dilution of these extracted oils. To begin the oil extraction process, a small amount of soil is crushed and diluted with dichloromethane (DCM) to produce a 1:10 mass ratio of soil to DCM. DCM was chosen as the solvent because it is a standard solvent for analyte extraction and is readily available. The mixture is sonicated for 1 hour at slightly elevated temperature (40^{o}C) and centrifuged for 15 minutes. After centrifuging, the liquid extract is removed and stored in an airtight container. Spiked soil samples (1.2 g) mixed with DCM (12g) are shown in Figure 29 before centrifuge (left) and after centrifuge (right). In the pictures the vial with the untreated soil is on the left

and the vial with the treated soil is on the right. Note the significantly higher opacity for the treated sample.

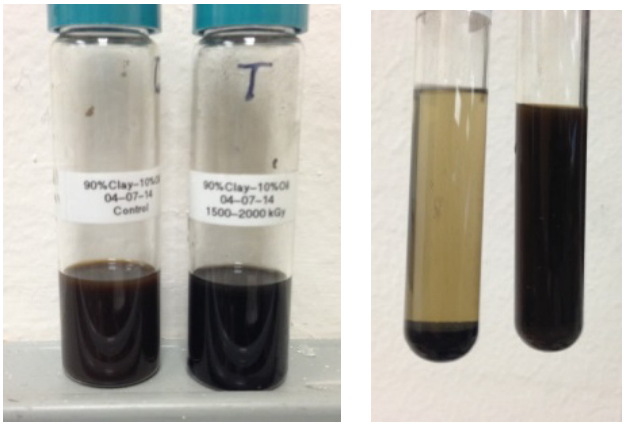

Figure 29: Extracted oils from treated and untreated soil samples before and after DCM dilution

For the absorption tests, the liquid solutions from the centrifuge were further diluted with DCM to facilitate ultraviolet-visible spectroscopy. The equations below represent the composition of a sample at different stages of preparation. The sample was assumed to consist of soil, DCM, oil fully soluble in DCM, and oil insoluble in DCM. Solution A is the mixture obtained after the clay soil is spiked with oil. Solution B is the solution extracted from Solution A using the method previously described.

3.4.1.3 UV-Visible Spectrometer Setup and Procedure

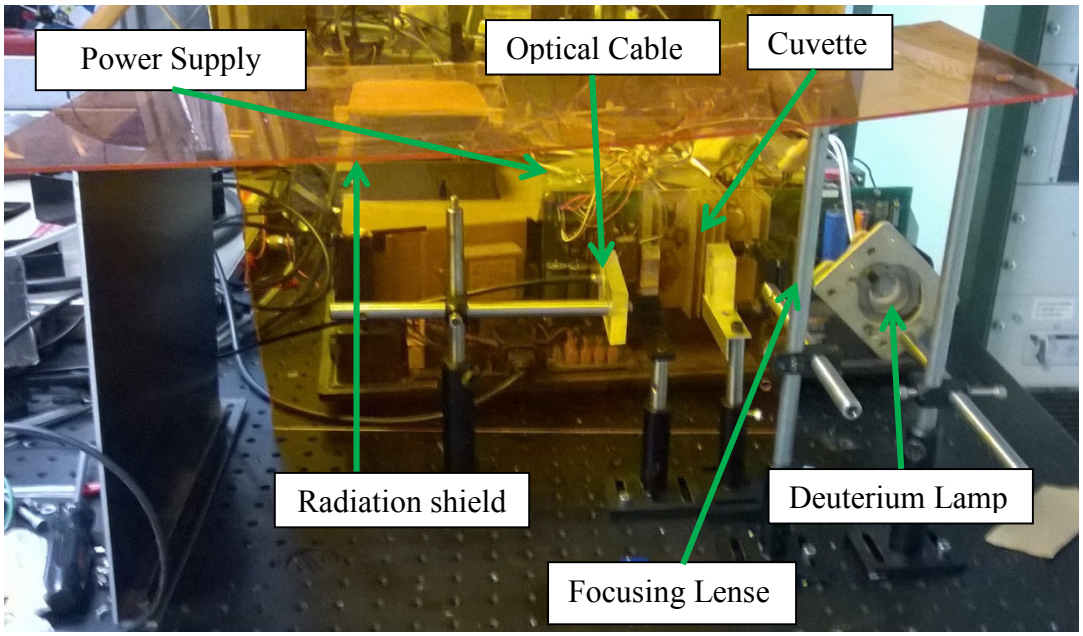

Figure 30: UV-Vis spectrometer setup

The spectrometer setup consists of a power unit, a data acquisition system, and a setup for securing the sample. The power unit contains the deuterium lamp and a high voltage power supply. The center of the emitted light from the lamp is aligned with an optical cable connected to the data acquisition system via a spectrometer. The spectrometer processes spectral intensity in the 200 nm to 800 nm wavelength range.

Samples are placed in a quartz cuvette with 0.5” path length that is aligned such hat the center of the light emitted from the lamp passes through the center of the t unobstructed portion of the cuvette. The lamp is also aligned with the center of a

focusing mirror located between the cuvette and the lamp. It directs most of the light passing through it into the optical cable.

For each set of measurements, a reference and a dark spectrum test must be performed. The reference is simply the spectrum obtained when the cuvette is empty. This accounts for the absorbance of the cuvette and the surrounding air. A "dark" measurement determines the intensity spectrum captured from the surrounding. This includes primarily the lights in the lab and also scattered portions of the light emitted by the tungsten bulb. This measurement is recorded by placing an obstruction between the lamp and the optical cable. After recording the dark and reference, each sample is placed in the cuvette and the transmitted intensity spectrum is recorded. Once the sample is removed, the cuvette is washed with DCM.

3.4.2 TPH Analysis

As-received soils were commercially analyzed for TPH using standard industry methods. In this case, TPH measurements accounted for gasoline (C5-C12), diesel (C12-C22), and oil range organics (C22-C40). Constituents detected in trace amounts, including aromatic and semi-volatile compounds, were excluded from analysis. Samples were analyzed using EPA method 8015B for the desired carbon ranges.

Method 8015B provides for gas chromatographic detection of certain organic compounds. Analyte extraction was accomplished using Method 3550C. The soil sample is mixed with anhydrous sodium sulfate to form a powder. Solvents are used with ultrasonic extraction and the extract is separated by vacuum filtration and centrifugation.

Separation and detection of organic compounds is done with a gas chromatograph and flame ionization detector respectively.

Gas chromatography is used to separate compounds that can evaporate without decomposition. The analytes are dissolved in a solvent if they are liquids or injected as is if they are gases. The analytes are then carried through the heated column of a gas chromatograph using a mobile, inert gas, typically helium. A syringe containing the analytes injects them into the carrier gas stream in a vaporization chamber typically heated 50°C above the lowest boiling point for all analytes. For small boiling ranges, the column is kept at constant temperature during vaporization. Temperature programming increases the temperature in steps, resolving the different boiling point compounds into separate phases.

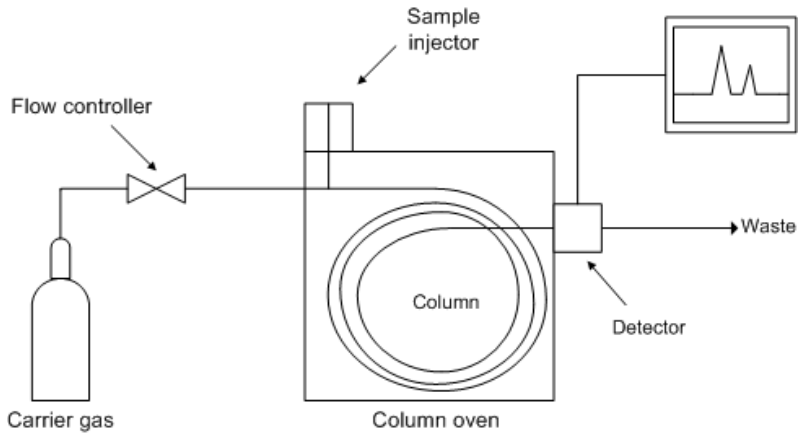

Figure 31: Diagram of a gas chromatograph

Separation is accomplished via adsorption to the column walls. Components with higher molecular weights will move more slowly through the column than faster components. After separation, the eluent enters the flame ionization detector (FID) oven

and is mixed with hydrogen fuel and oxidant. The mixture is then pulled through a flame nozzle. FID uses ions from burning organic substances with the hydrogen flame. Production of ions is a function of the concentration of organic components in the carrier gas stream. Ions generated at the positively charged flame are attracted to the negatively charged collector plate above the flame, and the ions generate a current upon hitting the collector plate. The current is proportional to the number of reduced carbon atoms produced by the flame. This can be used to calculate the concentration of each detected species in the original sample.

Untreated and treated samples were compared using histograms of dry results in mg/kg vs. carbon number range. The dry result of a compound refers to the portion of the soil mass consisting of the compound after all moisture is removed. Carbon concentrations were provided in ranges of 3 carbon numbers (C12-C14, C14-C16, etc…). Comparisons were done for each individual range as well as GRO, DRO, ORO, and total TPH. Data normalized for TPH was used to determine the change in composition of hydrocarbons between treated and untreated samples.

3.4.3 Mass Spectroscopy

30 mL gas samples were collected with a syringe via on/off flow control valves attached to electron beam reactors. A flow control valve connected to the syringe is used for controlling release of the collected sample once GCMS analysis begins. Analysis begins with pressurizing the GCMS system. A program called XTorr is opened to monitor pressure and record the mass spectrum. An air pump is run until the pressure reaches $2x10^{-2}$ torr. Then, a turbo pump is switched on to reduce pressure to $1.00x10^{-4}$

torr. The syringe containing the gas sample is connected to the turbo pump through a needle valve. To determine the ideal operating parameters for the mass analysis, scan speed and needle valve settings were adjusted while observing the resulting mass spectrum. This was done using only the surrounding air being pulled in by the pumps.

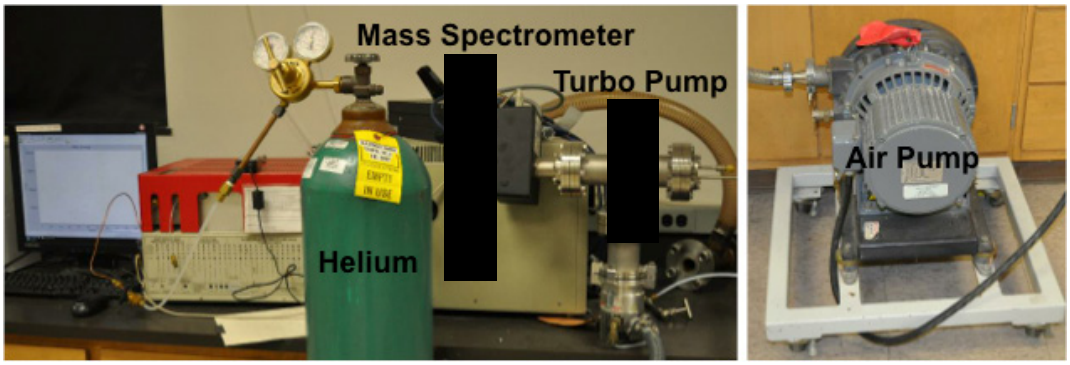

Figure 32: Mass spectrometry system

The valve had 25 unit markings around its circumference. A reference point was set such that the 7th marking aligned with the reference in the fully-closed position of the valve. After experimenting with the position of the valve, 6 units from closed was found to produce a good background scan. Higher valve openings produced excessive background noise while lower openings did not provide sufficient resolution due to low sample concentration.

4. RESULTS

4.1 Treated Soil Compositions

4.1.1 Manufactured Soils

Sand-based and clay-based soils were both mixed in the laboratory. Table 2 shows the manufactured soil compositions tested.

Table 2: Manufactured soil compositions

Mixture #	Sandy Soils (%mass)			Clay Soils (%mass)		
	Soil	Oil	Water	Soil	Oil	Water
1	80	10	10	80	10	10
2	90	10	0	90	10	0
3	100	0	0	60	10	30
4	80	0	20			

Sand-based spiked soils were very simple to make. The sand used was Quickrete All-Purpose sand obtained from Home Depot. The sand was mixed with Eocene crude and water (for wet soils) in plastic buckets with a stirring rod in various ratios of soil, oil, and water by mass. The notation for composition used here is %soil-%oil-%water. For example, a soil consisting of 10% oil and 10% water will be referred to as an 80-10-10 soil. No screening for soil particle size was done.

Determining a method for making spiked soils from Dublin clay provided by Chevron was more involved. Several methods were tested for soil drying. One method was mixing the soil with acetone and sonicating for 10 minutes. The acetone replaced the water in the soil, and then evaporated after being left under a ventilation hood for one

day. The resulting soil sample was extremely brittle and crumbled easily. The next method was baking in a firing oven at 110°C. The result was a dry soil that appeared to have undergone chemical changes; the soil turned a red-brown color and seemed very hard. Finally, a soil was simply left under a ventilation hood for two days. The result was a soil that seemed just as dry and brittle as the soil mixed with acetone. This method was used for all subsequent soil preparation. Soils prepared using these different methods are shown in Figure 33.

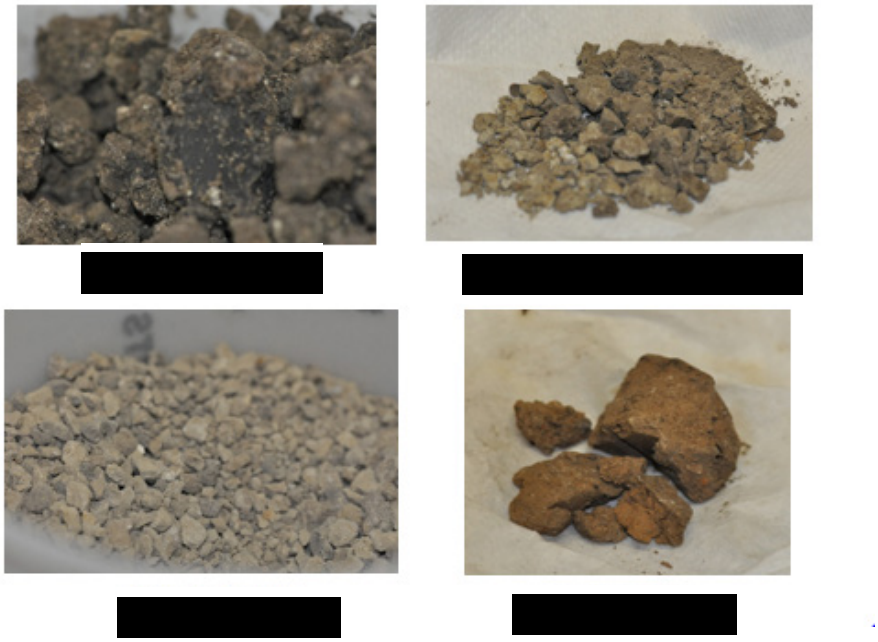

Figure 33: Dublin clay soil dried with different methods

To make the spiked soils, dry clay was crushed into a powder and mixed with oil (Eocene: API 14) It was noticed that simply pouring the oil in the dry sand does not result in a well-mixed product due to significant phase separation between the soil and oil. It was found that adding an amount of water approximately equal to the mass of the

oil increased the amount of oil absorbed by the soil, and the resulting mixture appeared uniform. For soils in which water is part of the treated mixture, the specified mass of water is poured and the soil is immediately placed in a sealed glass jar. Samples to be tested without water were left to dry in the ventilation hood. To determine the percent mass of water remaining in the soil, a 200g sample of a 90% sand-10% oil mixture was made (180g soil and 20g oil). After the water was poured and the sample dried, it was determined that 1.9 g of water remained in the sample, just under 1% of the total weight.

4.1.2 Real Impacted Soils

Real impacted soils from drilling sites were received from Chevron. Five types of soils were tested. The properties of these soils are shown in Table 3. The dry soils (GSC and GSI) were broken into pieces no larger than ¼" to allow for fitting in the electron beam setup. Other soils were tested as received. GSC1AOS and GSI14RD were dry clay soils that were highly weathered. BM1 and BM2 soils were mixed at Arizona State University and have high organic content. BM1 is a muddy soil while BM2 is powdery. BT Sludge was obtained from a surge pond and contained large amounts of organic matter. This soil has the highest TPH and water content. As-received soils are pictured in Figure 34.

Table 3: Properties of Real Impacted Soils

Soil Sample	GSC1AOS	GSI14RD	BM1	BM2	BT Sludge
GRO >C5-C12 (g/kg)	0.2	0.049	0.41	0.71	0.024
DRO >C12-C22 (g/kg)	23	10	6.8	8.3	10.9
ORO >C22-C40 (g/kg)	69	19	9	12	22.5
Total TPH (g/kg)	91	29	16	21	319
Total TPH (% mass)	9.1%	2.9%	1.6%	2.1%	31.9%
Moisture(% mass)	0.81%	1.4%	18.4%	2.1%	46.7%

Some BM1 soils were mixed with additives, which included ethanol, KCl, and citrus oil. The additives were used in 5wt% soil amounts. The resulting soil composition was 17.5% water and 1.52% oil. For solid additives (KCl), initial dry mass accounts for additive mass and is 81% of soil mass. Initial dry soil mass is 76% of soil mass if liquid additives are used. Soils with additives are pictured in Figure 35.

Figure 34: Untreated as-received soils

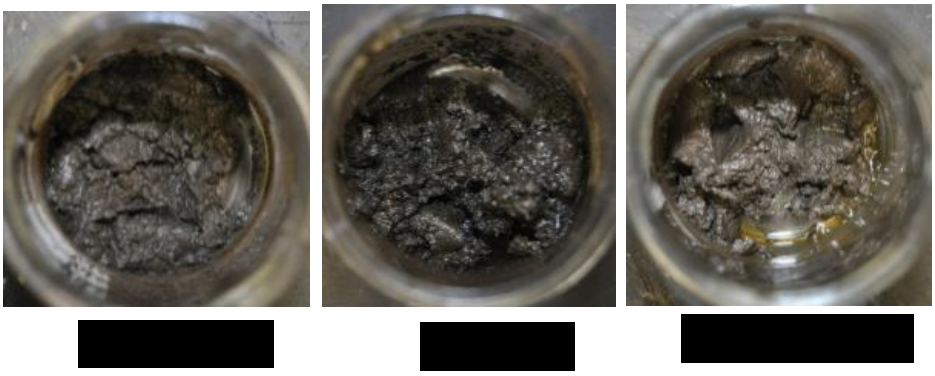

Figure 35: Untereated BM1 soils with additives

4.2 Contaminated Sand Experiments

Preliminary testing was conducted on soils with various levels of oil pollution in order to determine possible safety issues and evaluate the experimental setup. Four samples were made for each of the four compositions listed in Table 2. Roughly 1kg of each sample was placed in a heat-sealed mylar bag and transported under the electron

beam using the conveyor. For each composition, each sample received a dose of 0 kGy, 50 kGy, 150 kGy, and 250 kGy.

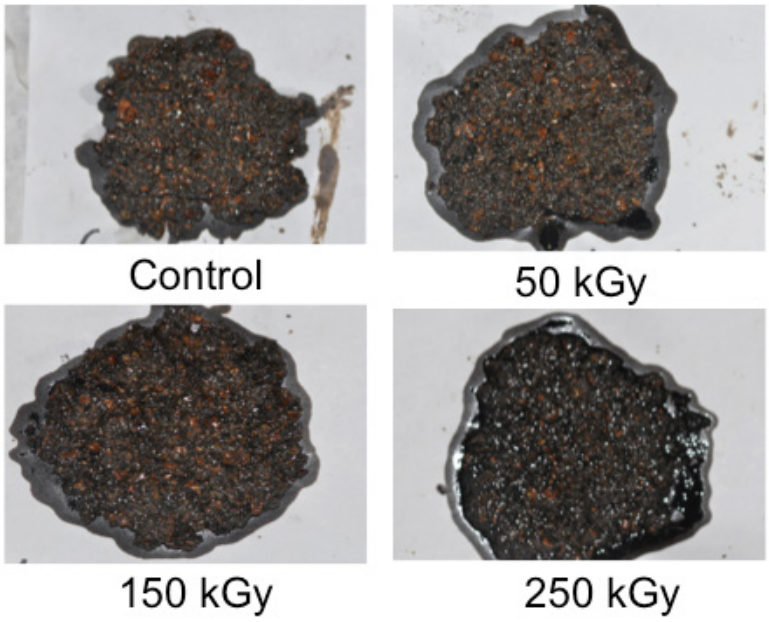

Figure 36: Treated 80-10-10 sand-based polluted soils

Soils were visually compared as shown in Figure 36. For higher doses (≈150 kGy and above) oily soils appeared to have a reduced viscosity. Also, oil flowed more easily for higher doses and appeared to flow out of the soil. This meant that the setup could be modified to induce phase separation between liquids and solids during treatment. Additionally, there was no noticeable gas production, which meant that pressure should not place a constraint on dosage.

Figure 37 shows the mass spectra in absolute signal level attained by GCMS analysis with MALDI ionization for DCM extracted oils for 500 kGy treated and untreated 90-10-0 sandy soils. Since peaks of 1600 and 200 were observed for the

untreated and treated samples respectively, a reduction in oil spiking by a factor of 8 for -the treated soil may be assumed. Later experiments showed that decreases of this magnitude were consistent. However, some inconsistencies in sample absorption into the matrix and the generally low signal level of the treated sample precluded further use of this analysis method.

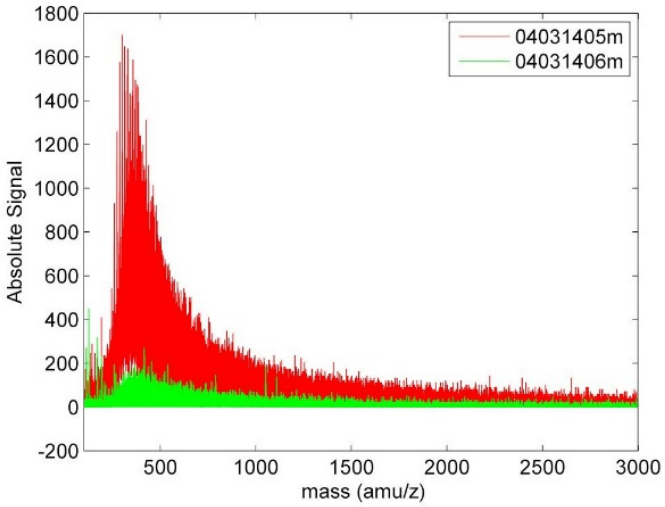

Figure 37: MALDI mass spectra for DCM extracted oils from a 90-10-0 sand based soil

4.3 Contaminated Clay Experiments

4.3.1 Calibration of UV-Absorbance Spectrometer

A systematic analysis procedure was developed to determine the effective spiking level of treated soil samples using results from clay soil experiments. First, a visual comparison of the solutions obtained from oils extracted from 2000 kGy treated and untreated 90-10-0 clay soils was done. Next, the range of DCM dilutions in which

the absorbance is a linear function of DCM dilution was determined for several wavelengths. Then, the dependence of absorbance on spiking level using 0% water controls with spiking levels of 1%, 2%, 5%, and 10% was determined for several wavelengths. Absorbance of treated samples at these same wavelengths was determined and visually compared to absorbance of the controls. Finally, the effective spiking level of the treated 90-10-0 sample at the same wavelengths was estimated using piecewise linear interpolation of the absorbance vs. spiking level data.

The absorbance of treated and control 90-10-0 clay soils were compared at dilutions of 8.62wt% Solution B. Figure 38 clearly shows that, on average, the treated soil absorbs less radiation in the UV-Visible spectrum than the untreated soil. This is prominent between 250 and 550 nm, which is the typical range of absorbing wavelengths for most alkanes. This indicates that the treated sample likely has a lower TPH. This trend is very dramatic at 350 nm, where the absorbance for the treated and untreated soils is 0.38 and 2.28 respectively, which corresponds to a percent reduction of 83.3%.

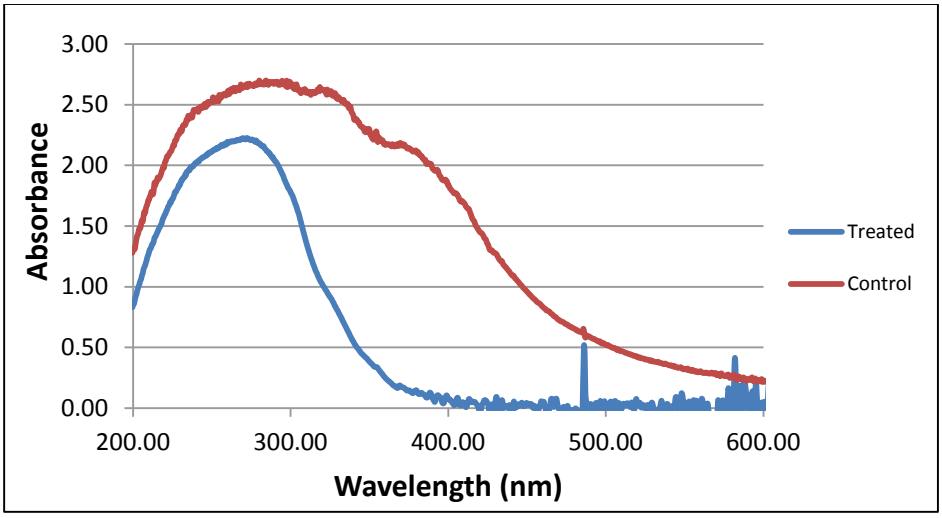

Figure 38: Absorbance spectrum for 8.62 wt% solution B in DCM

It was then desired to find the range over which absorbance is a linear function of dilution level. This was done by diluting the DCM/oil solutions previously made to wt% Solution B of 1, 0.5, and 0.25. The absorbance spectra in Figure 39 show a similar trend to Figure 38. Here, the spectra diverge from the peak absorbance at roughly 250 nm and converge near 500 nm. Absorbance in the higher wavelength range is very small, indicating a lack of absorbing species in this range (i.e. very heavy hydrocarbons).

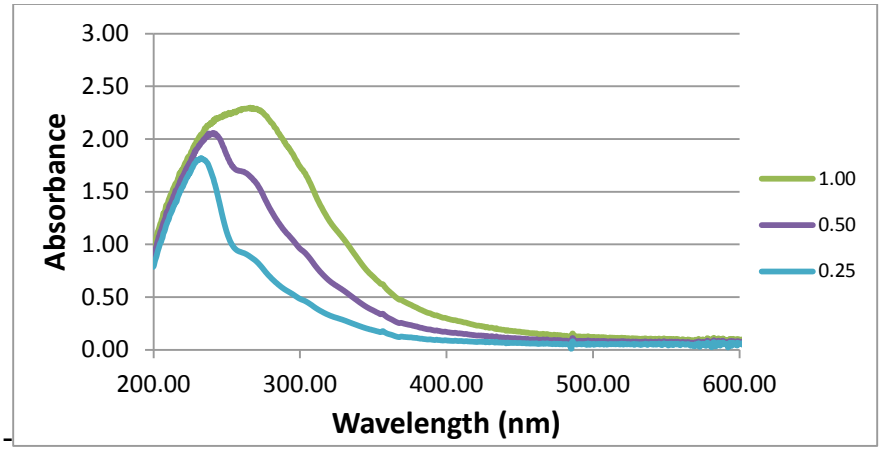

Figure 39: Absorbance spectrum of the control for 3 dilutions

Figure 40 shows absorbance spectra for all tests with the control. As expected, in the 250nm - 500 nm range absorbance is a function of dilution, with the least diluted sample having the highest absorbance.

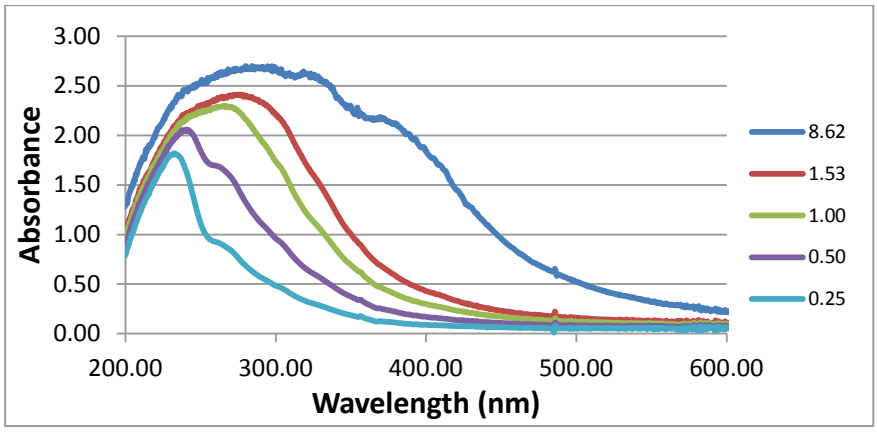

Figure 40: Absorbance spectrum of the control for all dilutions

Table 4 shows the exact absorbance at four wavelengths, which were those closest to 300, 350, 400, and 450 nm. These values are plotted as a function of dilution in Figure 41.

Table 4: Absorbance of a 90-10-10 clay soil for different wavelengths and DCM dilutions

Dilution	Wavelength			
	300.34	350.17	400.14	450.15
1.53	2.21	1	0.43	0.23
1	1.73	0.69	0.3	0.17
0.5	0.96	0.37	0.17	0.11
0.25	0.48	0.19	0.09	0.07

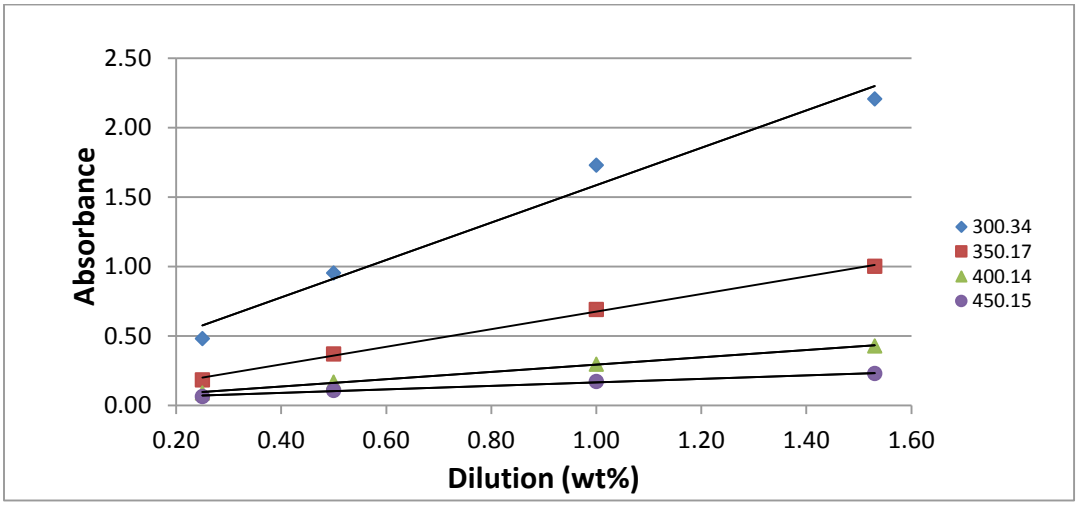

Figure 41: Absorbance vs. dilution for different wavelengths

When considering the dilutions in the range 0.25 %wt to 1 %wt, it can be seen that the relationship between concentration and absorbance is approximately linear. Since the goal was to find a dilution that allows for use of the Beer-Lambert law but also minimizes the amount of DCM used, a dilution of 1.0% appears adequate. Knowing an appropriate dilution, calibration curves that show absorbance as a function of oil spiking for the wavelengths in Table 4 at a fixed dilution (1.0wt% Solution B) were made for

each treated soil composition. The spiking percentages are 1%, 2%, 5%, and 10%. This data was used to quantify the reduction in the DCM soluble fraction of oil.

4.3.2 Analysis of Treated Clay Soils

Figure 42 shows that the absorption increases as spiking level increases. The 2000 kGy treated 90-10-0 soil appears to have the lowest absorption across all wavelengths for spiked soils. This indicates that the treated soil has a lower DCM soluble oil concentration than the control with 1% spiking, and has a significantly reduced DCM soluble oil concentration compared to its initial concentration.

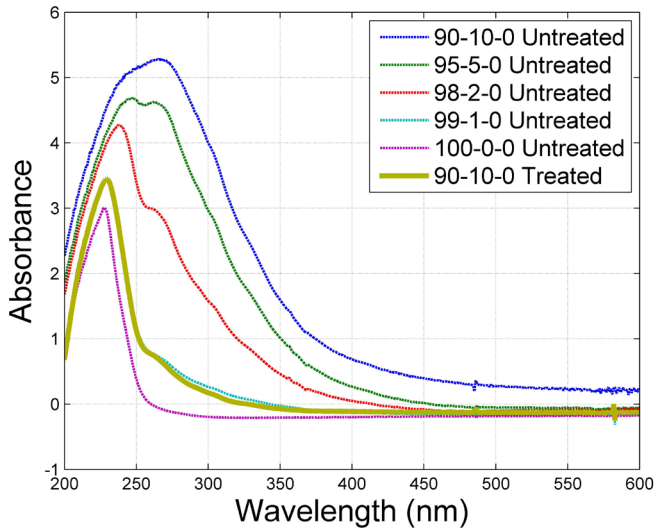

Figure 42: Absorbance of 2000 kGy e-beam treated 90-10-0 clay soil with 0% water controls

It was found that the relationship between absorbance and spiking percentage is approximately linear for wavelengths of 300nm, 350nm, 400nm, and 450nm. However, when spectra for DCM was added (i.e. 0% oil spiking), it was found that absorbance

increased between 1% and 0% spiking levels. This indicates that there is possibly a more complex functional dependence of absorbance on spiking level.

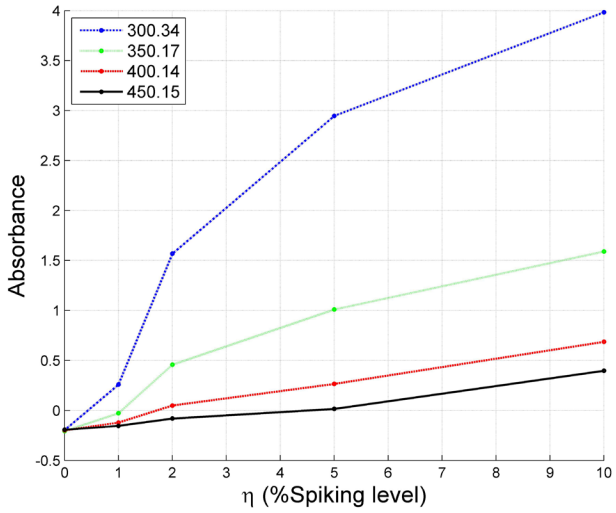

Figure 43: Absorbance vs. spiking for 0% water controls at 1.0wt% Solution B.

To avoid assumptions about the underlying functional dependence, piecewise linear interpolation was used to estimate effective oil spiking in the treated soil at the specified wavelengths. Table 5 shows the obtained values for effective oil spiking. The maximum effective spiking level is 1.69% at 450 nm. Figure 44 shows this data on the calibration plot with treated absorbance values plotted at the estimated spiking level. Reductions of TPH to less than 1% are seen at wavelengths of 300 nm and 350 nm. For consistency, the TPH at 300 nm was used for future evaluation.

Table 5: Estimated oil spiking percentage and absorbance reduction at different wavelengths for 2000 kGy treated 90-10-0 clay soil

Wavelength(nm)	Absorbance	Absorbance Reduction (%)	Effective Spiking (%)
300.34	0.17	95.73	0.80
350.17	-0.07	104.60	0.74
400.14	-0.11	116.48	1.04
450.15	-0.12	130.97	1.42

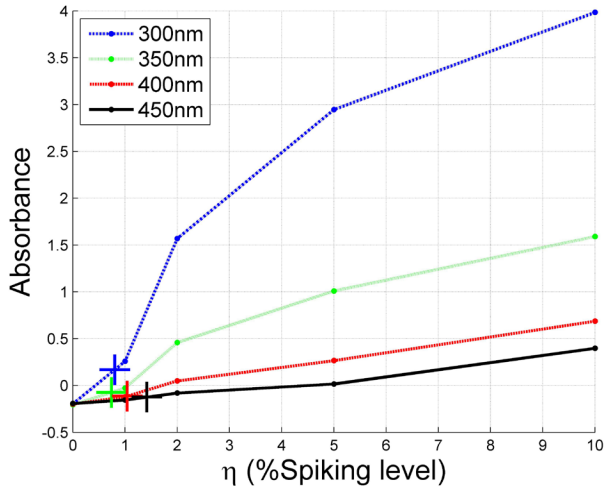

Figure 44: Effective spiking level estimation of 2000 kGy e-beam treated 90-10-0 clay soil with 0% water calibration

The calibration used for the dry soils was reevaluated to determine its applicability to soils with water. Spectra for un-spiked soil with 0% water and 10% water were compared, as shown in Figure 45. For wavelengths between 250nm and 350nm, the spectra converge. Since the 300nm-350nm range is used in our analysis, it would not be appropriate to use the same calibration for dry soil as in wet soil. It was

further concluded that any soils with different water concentrations would require a new calibration.

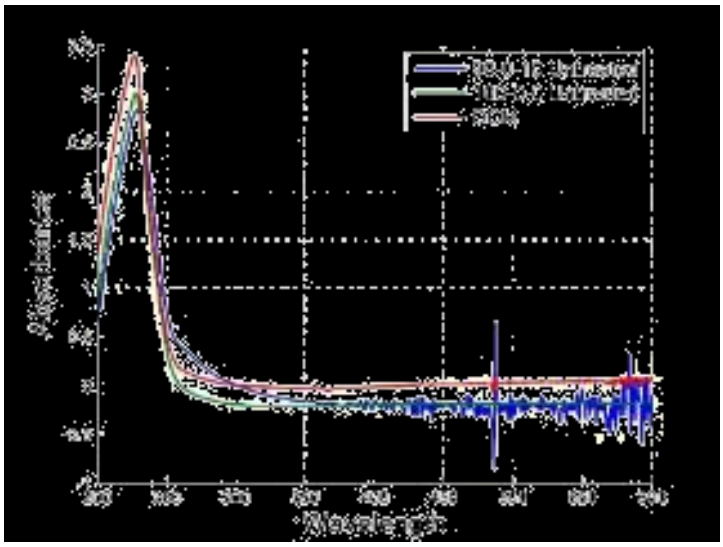

Figure 45: Spectra of DCM and unspiked 10% and 0% water clay soils

Four 80-10-10 soils were tested. Dosages of 1784 kGy and 496 kGy were applied to soils with reactors placed in a water bath (low temperature treatment), while doses of 960kGy and 480 kGy were applied without a water bath (high temperature treatment). From Figure 46, the absorbance spectrum of the higher dosage soil is between the 2% spiked and 1% spiked control spectra. These results are confirmed in Figure 47. The estimated spiking level at 300nm is 1.74%, which is the maximum spiking level for the considered wavelengths.

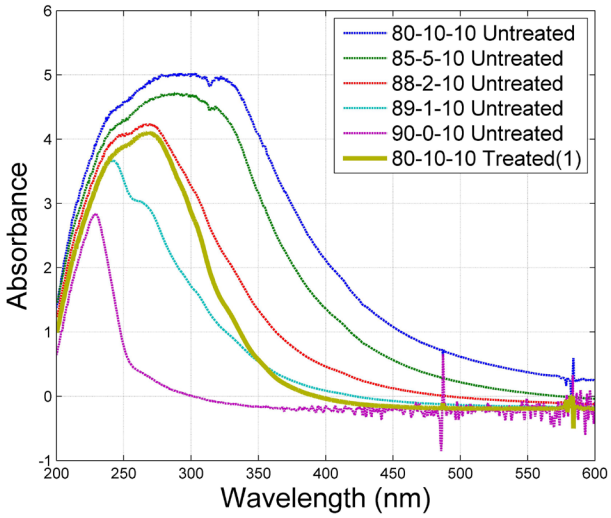

Figure 46: Absorbance of 1784 kGy e-beam treated 80-10-10 clay soil with absorbance of 10% water controls

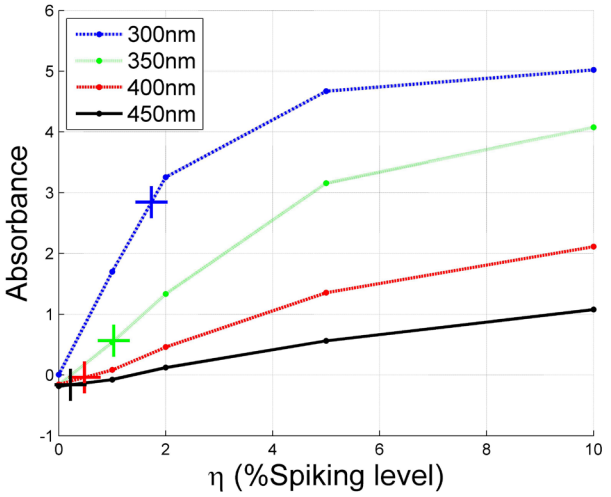

Figure 47: Effective spiking level estimation of 1784 kGy e-beam treated 80-10-10 clay soil with 10% water calibration

From Figure 48, the absorbance spectrum of the lower dosage soil lines up with the 5% spiked control spectrum. The spiking level of this soil at 300nm is 6.30%. Since the high

dose soil has 27% of the spiking level of the lower dose sample, TPH appears highly dose dependent.

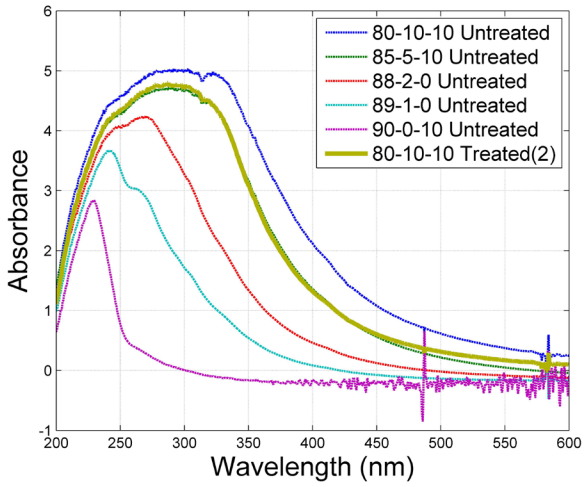

Figure 48: Absorbance of 496 kGy e-beam treated 80-10-10 clay soil with absorbance of 10% water controls

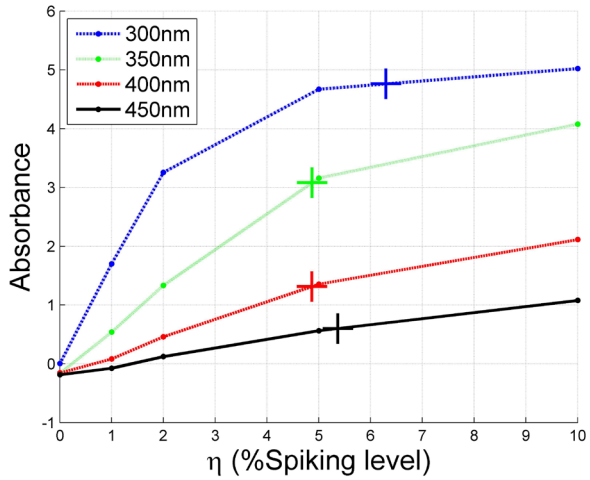

Figure 49: Effective spiking level estimation of 496 kGy e-beam treated 80-10-10 clay soil with 10% water calibration

Treating at high temperature appeared to significantly increase TPH reductions. From Figure 50, spiking levels appear to be less than 1% at all wavelengths. Specifically, spiking level at 300 nm is 0.52%, roughly three times less than the spiking level for the 1784 kGy treated soil. Estimated spiking levels in Figure 51 are less than those in Figure 49 for all wavelengths. At 300 nm, the spiking level is 4.56%. In both cases, large increases in TPH reduction are observed from treating at higher temperature. This indicated that use of a water bath was not only unnecessary, but detrimental for the performance of electron beam treatment.

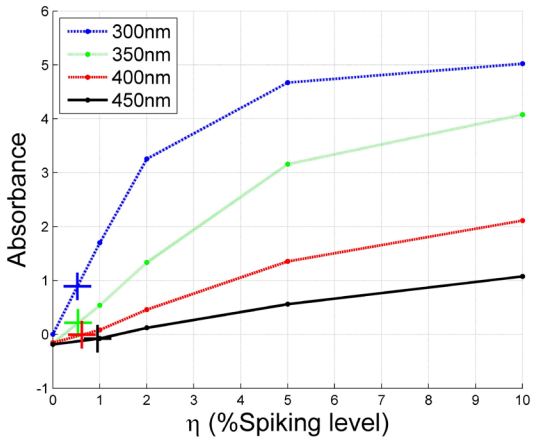

Figure 50: Effective spiking level estimation of 960 kGy e-beam treated 80-10-10 clay soil with 10% water calibration

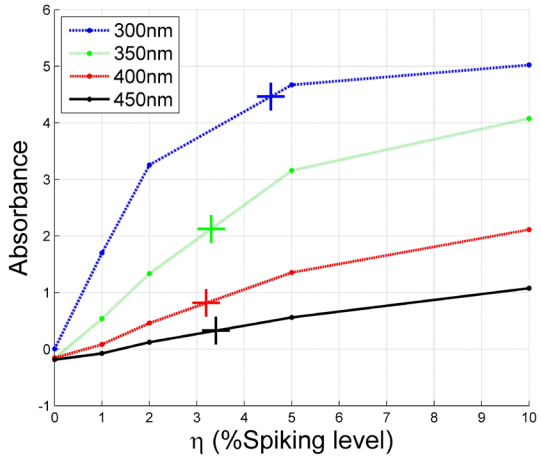

Figure 51: Effective spiking level estimation of 480 kGy e-beam treated 80-10-10 clay soil with 10% water calibration

One 60-10-30 soil was tested at low temperature with a dosage of 1920 kGy to evaluate the effects of water content. The treated soil has a spiking level between 5% and 10% in the visible range, which is much higher than for the 1784 kGy treated 80-10-10 soil. Estimated spiking level is greater than 6% for all wavelengths, and is 9.98% at 300 nm, meaning that no significant TPH reduction occurs. It is likely that the energy from electron beam treatment went to evaporating the water in the soil and little was absorbed by hydrocarbons. Thus, effectiveness of electron beam treatment appears to decrease with increasing water content.

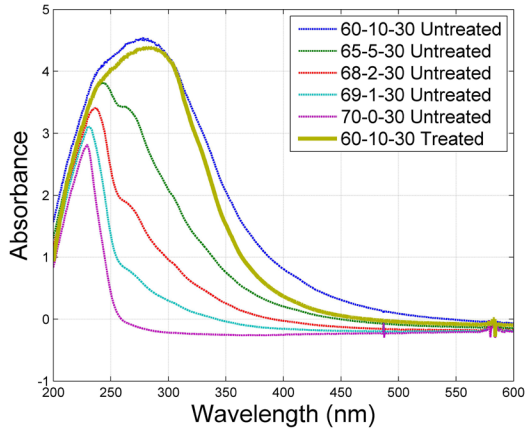

Figure 52: Absorbance of 1920 kGy e-beam treated 60-10-30 clay soil with absorbance of 30% water controls

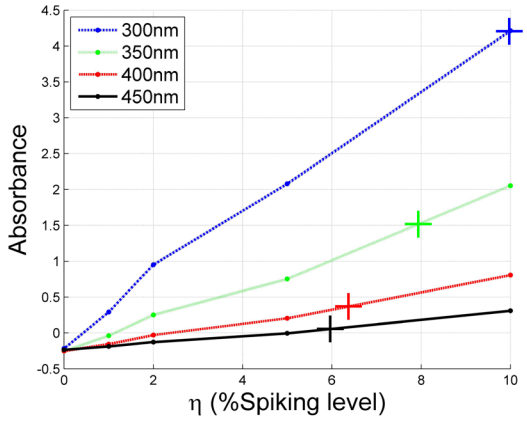

Figure 53: Effective spiking level estimation of 1920 kGy e-beam treated 60-10-30 clay soil with 30% water

Table 6 summarizes results from treatment and analysis of clay soils. A clear dose dependent reduction is observed for most treated soils with low water contents. Reductions in some cases to less than 1% were observed, strongly suggesting the viability of e-beam remediation. These results justified further testing with as-received soils and investment in standard commercial analysis.

Table 6: Summary of dosages and estimated TPH reduction for treated clay soils

Composition	Dose (kGy)	Configuration	Effective Spiking (300 nm)
90-10-0	2000	2	0.80
80-10-10	1784	2	1.74%
80-10-10	496	2	6.30%
80-10-10	960	3	0.52%
80-10-10	480	3	4.56%
60-10-30	1920	2	9.98%

4.4 As-Received Soil Experiments

4.4.1 TPH Results of Treated Soils

Figure 54 shows TPH reduction for real soils as a function of dosage. BM1 samples with additives are shown as a cluster at 720 kGy. E-beam treatment clearly produces a reduction in TPH. The percent reduction is shown in

Figure 55. BM1 and BM2 soils have both been reduced to less than 1% TPH by treatments of 960kGy and 820kGy respectively. GSC1AOS has been reduced to 0.15% TPH for an 1100 kGy dosage. GSI14RD soils have nearly reached this TPH level, with a reduction from 2.9% to 1.2% for a 720kGy dosage. The dry result TPH of BT Sludge reduces from 31.9% to 28% for an 1100 kGy dosage, indicating that most e-beam energy goes towards evaporating water (46.7% to 4.5% water by mass). TPH reductions for treated BM1 soils spiked with ethanol, KCl and citrus oil are 0.58%, 0.3%, and 0.42% respectively. These results are slightly better than the expected TPH value of a 720 kGy treated soil without additives, which was found to be 0.69% through linear interpolation.

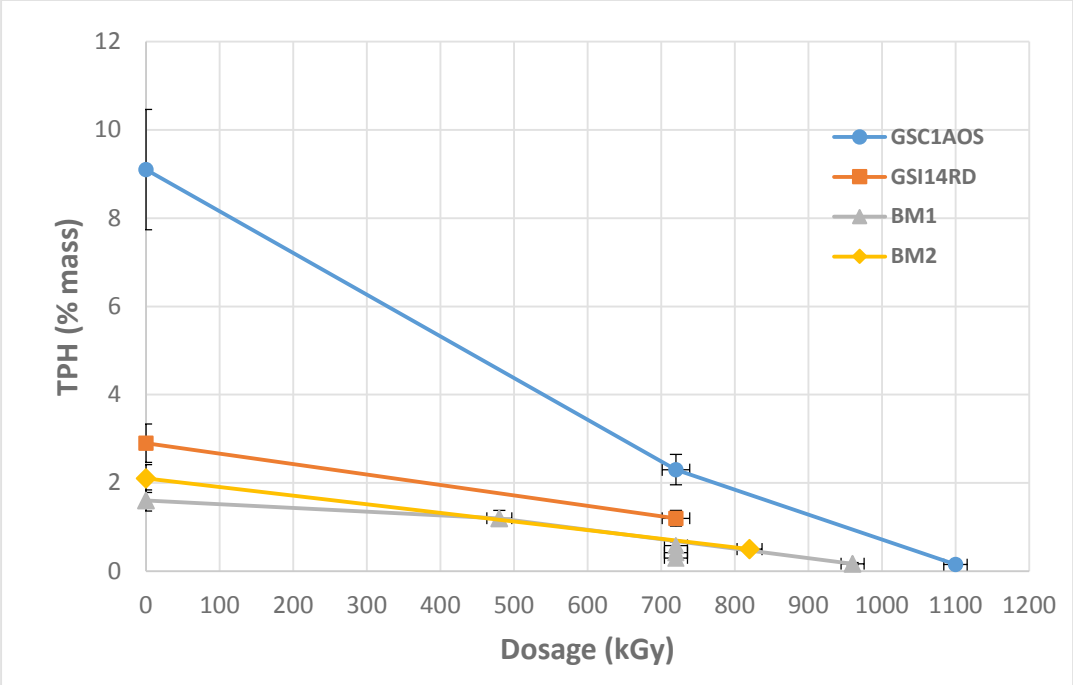

Figure 54: Dry result TPH vs. dosage for treated as-received soils

The maximum percent TPH reduction of 89.4% occurred for the BM1 soil at 960kGy, as shown in Figure 55. Except for BT sludge, oils treated above 700kGy appear to experience at least 60% TPH reductions, and those treated above 800kGy experience over 75% reductions. It appears that the initially dry soils (GSC1AOS, GSI14RD and BM2) have very similar TPH reduction trends. Those with water experience reductions much more slowly. However, the BM1 soil appears to experience TPH reductions more quickly after reaching a critical dosage. It is likely that this critical dosage is where most moisture has left the soil.

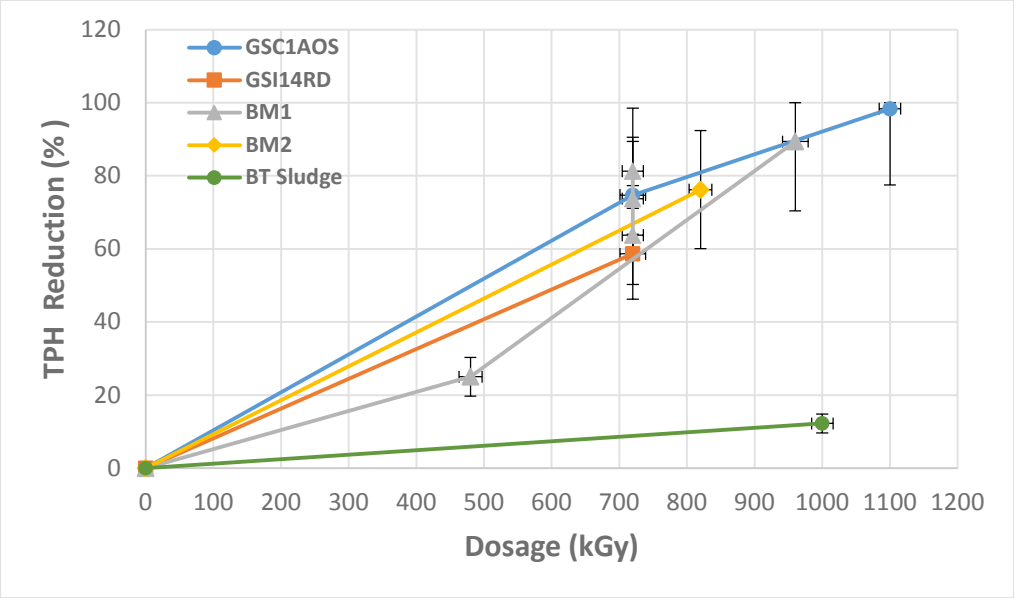

Figure 55: % Dry result TPH reduction vs. dosage for treated as-received soils

Table 7 shows the reactor configurations used for all real soil experiments. Setup 6 simply uses a 4', 3"OD pipe with no ballast volume.

Table 8 summarizes all electron beam tests that have been conducted on real soils. All TPH values are shown on a dry basis. The two results marked with asterisks next to the test date were not included in data analysis due to inconsistencies with previous results resulting from misalignment under the electron beam. Trends appeared to be independent of the setup used. For example, the TPH reduction trend for GSC1AOS in Figure 57 appears to be similar between data points, even though the 720 kGy and 1000 kGy dose samples were treated in 1" and 3" pipes respectively. The slope between the TPH levels for the treated soils is less steep than the rest of the trend, but this is consistent with decreasing removal efficiency as TPH is reduced. In fact, if the change in configuration affected TPH, a steeper slope would be expected for this portion

of the trend, since 3” pipes should reduce heat transfer from the soil. This indicates that heat transfer between the soil and pipe wall, an effect that was mitigated by using 3" OD rather than 1" ID pipes, is inconsequential.

Table 7: Reactor configurations for real soil experiments

Setup #	Config. #	Sample Pipe	Ballast Pipe	Volume (m^3)
1	1	1”ID x 20” Al	4”ID PVC	298.3
2	1	1”ID x 24” Al	4”ID PVC	310.4
3	2	3”OD x 24” Al	4”ID PVC	424.8
4	2	3”OD x 24” Al	2”ID Al	232.8
5	1	1”ID x 24” Al	2”ID Al	84.8
6	3	3”OD x 48” Al	N/A	318.1

Table 8: Summary of e-beam tests for all real soils

Soil	Dose (kGy)	TPH (% soil mass)	Setup #	Test Date	Additive
GSC1AOS	0	9.1	N/A	N/A	none
	720	2.3	5	8/22/2014	
	1000	2.1	3	10/21/2014*	
	1000	0.15	3	11/19/2014	
GSI14RD	0	2.9	N/A	N/A	none
	720	1.2	5	8/22/2014	
BM1	0	1.6	N/A	N/A	none
	480	1.2	2	10/22/2014	
	720	1.4	1	10/22/2014*	
	960	0.17	2	8/22/2014	
	720	0.58	1	11/19/2014	Ethanol
	720	0.42	5	11/19/2014	Citrus Oil
	720	0.3	2	11/19/2014	KCl
BM2	0	2.1	N/A	N/A	none
	820	0.5	6	10/22/2014	
BT Sludge	0	31.9	N/A	N/A	none
	1100	28	6	11/19/2014	

Figure 56 shows carbon number distributions for all BM1 soils. The 960kGy treated sample and the 720 kGy treated soils with additives show an increase in dry result with carbon number in heavy DRO and ORO ranges compared to the untreated soil, while the dry result in lighter ranges is nearly zero. This indicates that at higher doses, lighter carbons are preferentially removed. Additionally, the 960 kGy treated soil appears to have a higher TPH in the C15-C20 range than 720kGy treated soils with additives. Overall TPH appears to decrease as a function of dosage. From Figure 57, thermal effects are observed, since percent TPH is higher for heavy fractions in the treated soils than in the untreated soil. For the soil with citrus oil, an additional light component is seen at C12. Also, the soil with KCl appears to reach higher temperature, since it has the lowest TPH distribution. This is because the soil with KCl absorbs slightly more energy since the salt component does not evaporate like the other additives.

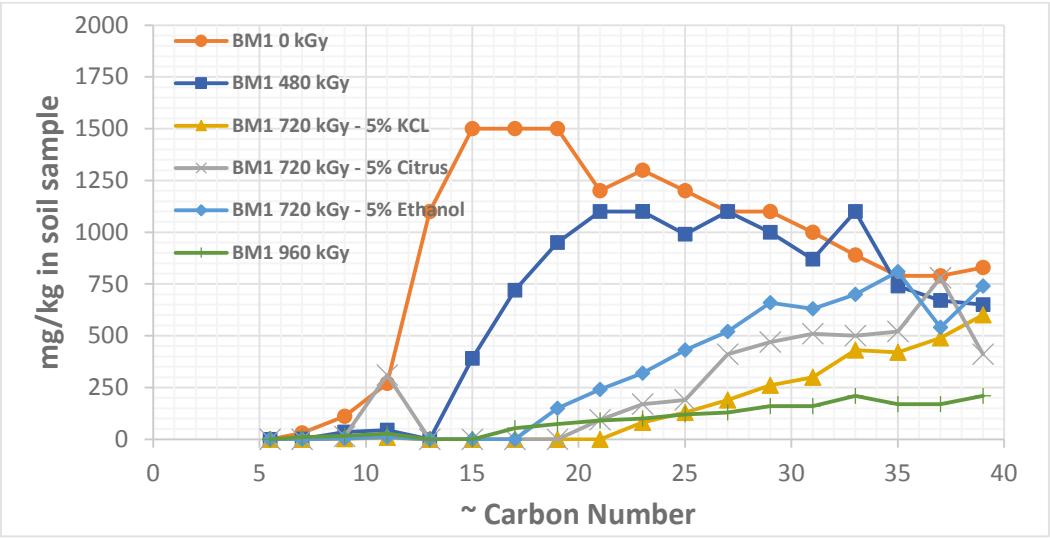

Figure 56: Dry result of TPH in BM1 for untreated and 960 kGy treated soils

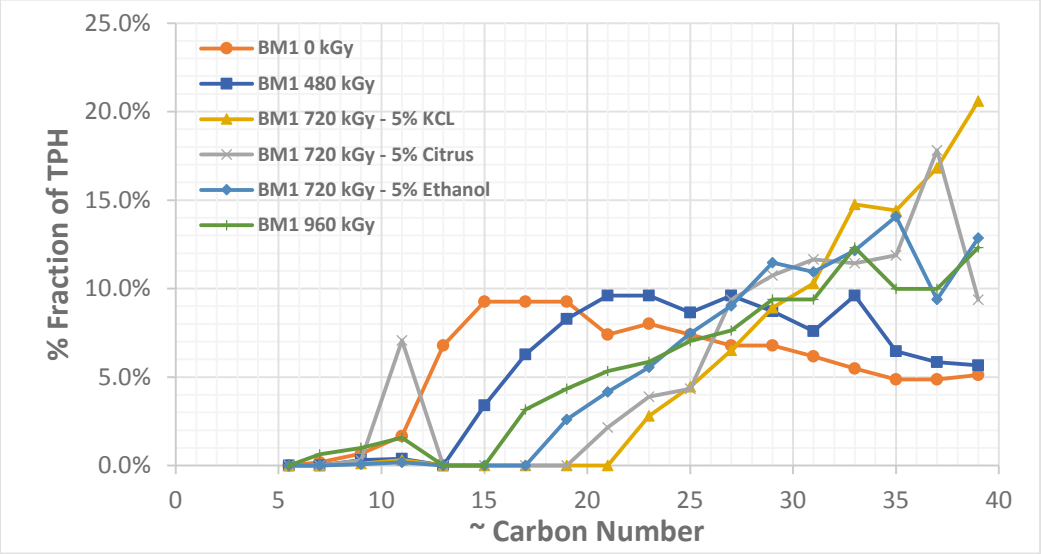

Figure 57: % TPH fraction for treated and untreated BM1 soils

BM2 TPH distributions appear to show significant non-thermal effects. A significant reduction in overall TPH from 2.1% to 0.5% is observed for the treated BM2 soil. However, this soil appears to have higher levels of light hydrocarbons, as seen in Figure 58. Additionally, the distributions above the GRO range in Figure 59 appear very similar, which means all fractions are being removed proportionately, including C40 alkanes. Since these heavy components would not thermally desorb, there must be non-thermal mechanisms present.

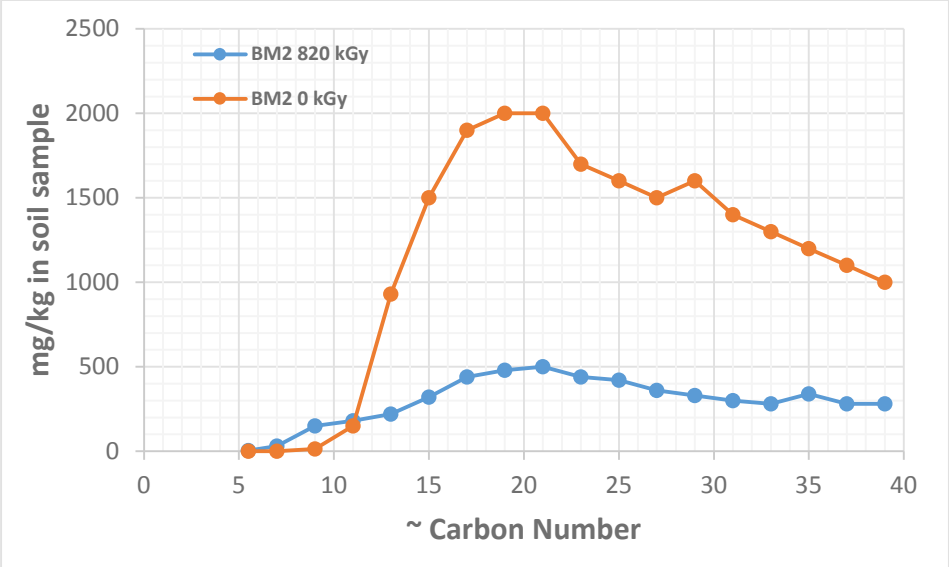

Figure 58: Dry result of TPH in BM2 soil for untreated, 720 kGy treated, and 1000 kGy treated soils.

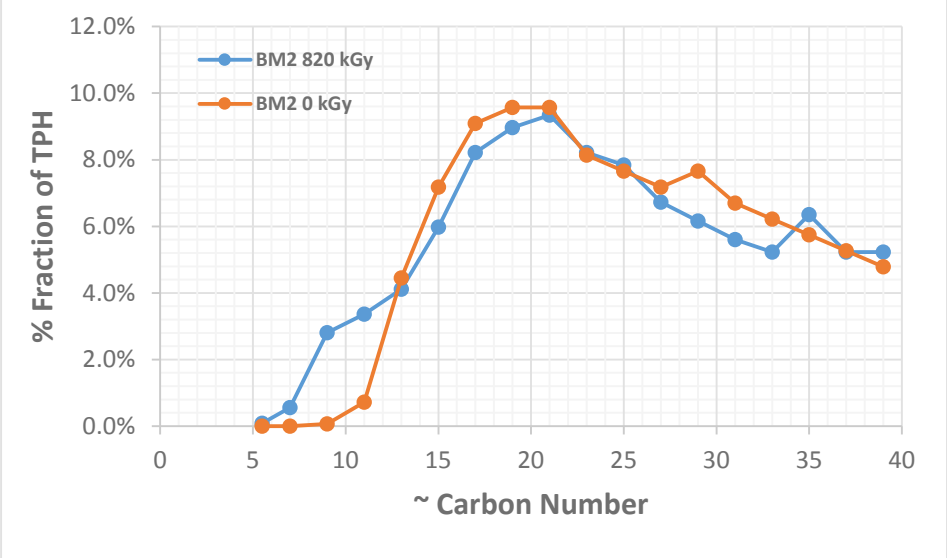

Figure 59: % TPH fractions for treated and untreated BM2 soils

Figure 60 shows a decrease in the dry result of DROs and OROs for the treated GSI14RD soils, but an increase in GROs. This again indicates significant contributions

from non-thermal processes. This is confirmed in Figure 61, which shows proportional reductions across GRO and ORO ranges and an increase in the GRO range for the treated soil. The most significant reduction again occurs in the DRO range. As with the BM1 soils, this means that most of the heavy TPH components either separated or could be removed by weathering. Overall TPH decreased from 2.9 % to 1.2% for this case. Thus, the treated sample has greater potential for use with other remediation methods.

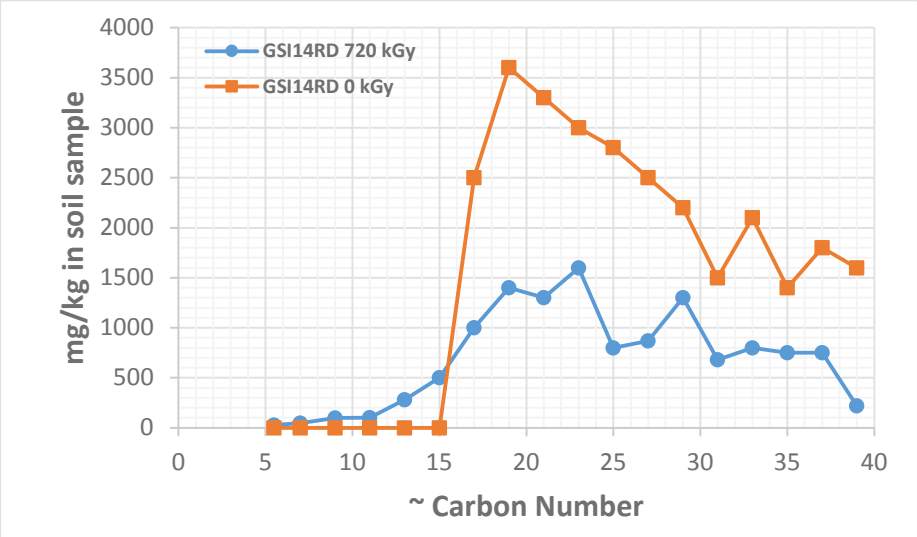

Figure 60: Dry result of TPH in GSI14RD soil for untreated and 720 kGy treated soils.

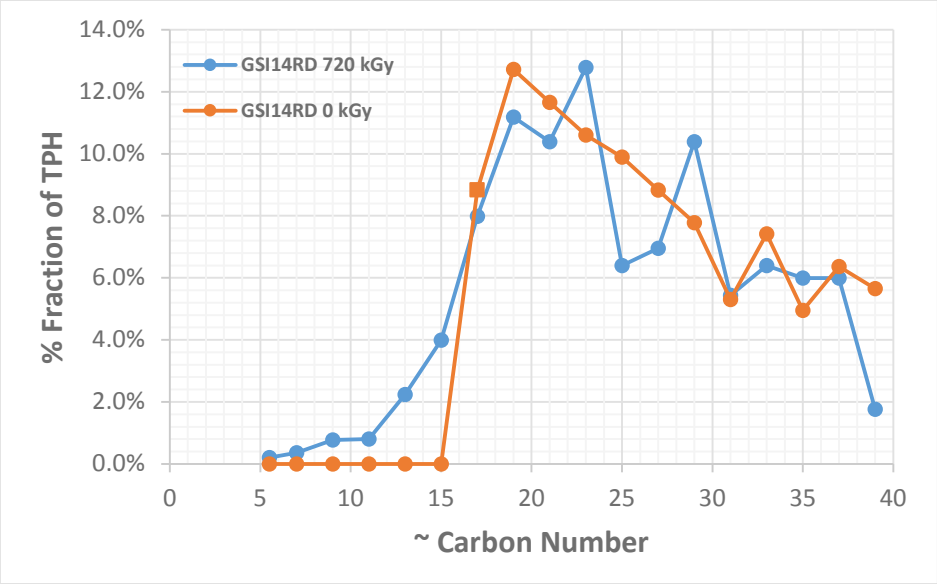

Figure 61: % TPH fraction for treated and untreated GSI14RD soils

Figure 62 shows the carbon number distribution for all treated GSC1AOS soils. TPH greatly decreases with dosage in the DRO and ORO ranges. A slight increase in GROs is seen in the 720 kGy treated soil, but this is overcome in the 1100 kGy treated soil to produce a reduction to less than 0.5% TPH across all carbon numbers. It appears that up to a certain dosage, non-thermal effects are predominant, producing increases in light hydrocarbon fractions and proportional reductions for others. At very high doses, thermal effects are more dominant and produce large reductions in TPH across all fractions. However, Figure 62 shows that the portion of TPH consisting of GROs increases significantly with dosage. Thus, whatever is not removed during treatment is easily removed with other methods such as bioremediation. By coupling e-beam treatment with other remediation methods, very high contaminant removal efficiencies could be achieved.

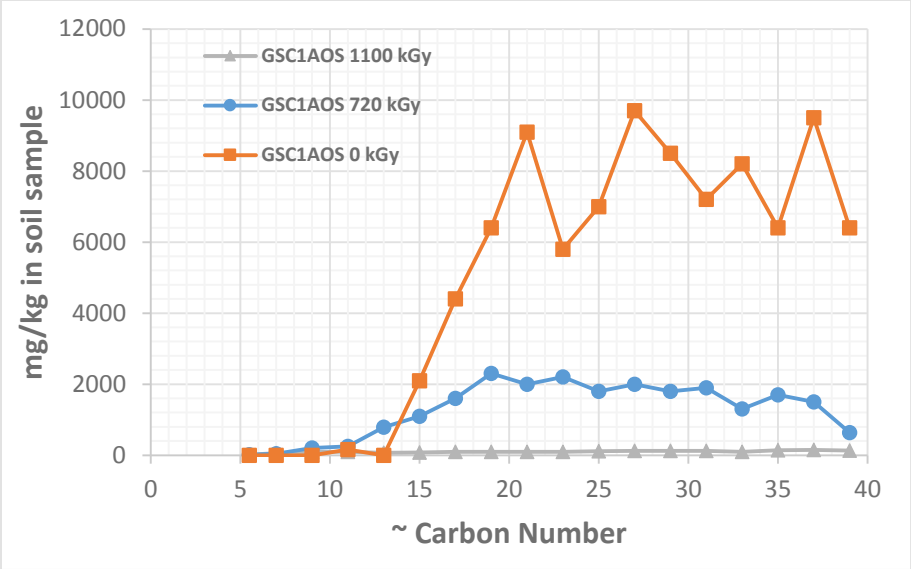

Figure 62: Dry result of TPH in GSC1AOS soil for untreated, 720 kGy treated, and 1000 kGy treated soils.

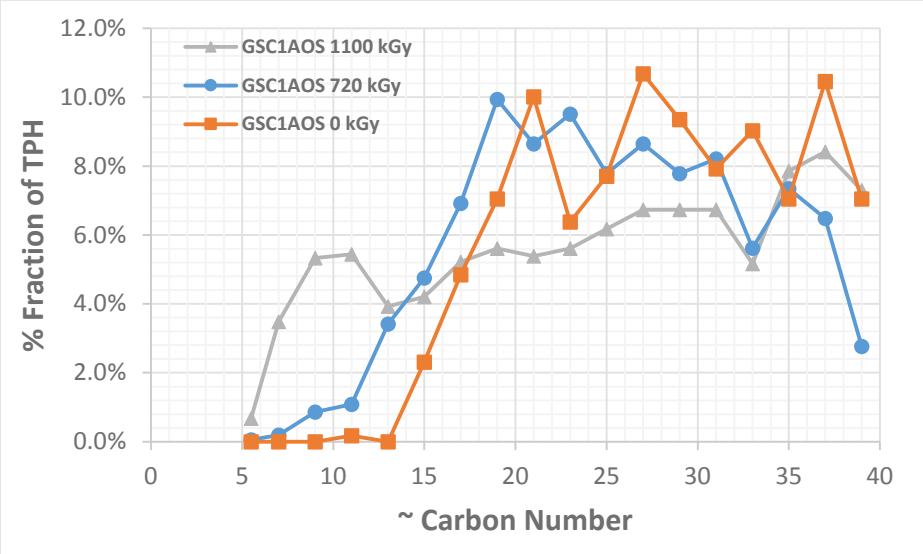

Figure 63: % TPH Fraction for treated and untreated GSC1AOS soils

Another important result is how electron beam treatment could possibly enhance other remediation methods such as bioremediation and produce hydrocarbon species

removable by environmental exposure (i.e. C16 alkanes and below). Figure 64 shows this for GSI14RD soil. This is a highly weathered soil initially, with no oils available for weathering. However, there appears to be some lighter hydrocarbons in the treated soil despite the overall decrease in TPH. This increase relative to soil mass was not observed for the other soils, but an increase relative to TPH was.

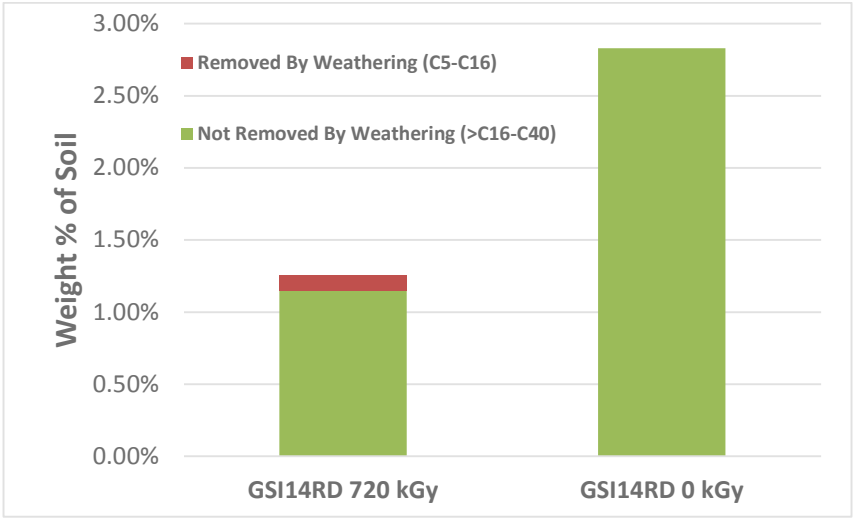

Figure 64: Amount of oil in GSI14RD soil that could be removed by weathering in % weight of soil

4.4.2 Measurement Uncertainty

Measurement uncertainty is graphically depicted as error bars in Figures 54 and 55. Error in dose measurements was ±10 kGy based on the dose measurement calibration in section 3.2. Dose rate error was estimated as 10 kGy divided by the run time of each experiment. Total dose error was calculated using the Kline McClintock uncertainty and accounted for the dose rate uncertainty and the time measurement uncertainty, which was 2 seconds. TPH measurement error was determined to be 15% of

EXPERIMENTAL SETUP AND PRELIMINARY RESULTS FOR ELECTRON BEAM REMEDIATION OF HEAVY HYDROCARBON CONTAMINATED SOILS

A Thesis

by

KENNETH WAYNE BRIGGS III

Submitted to the Office of Graduate and Professional Studies of
Texas A&M University
in partial fulfillment of the requirements for the degree of

MASTER OF SCIENCE

Chair of Committee,	David Staack
Committee Members,	Andrea Strzelec
	Suresh Pillai
Head of Department,	Andreas Polycarpou

May 2015

Major Subject: Mechanical Engineering

4.4.3 Mass Spectrometry

To prepare the spectrometer for analysis, a background measurement of air is taken before sample injection. This is done to account for the small amount of air incidentally pulled into the spectrometer. A needle valve attached to the sample injector is used to control the sample flow rate. After adjusting the needle valve to an ideal position, a mass scan of air is taken and used as a baseline. Background scans are done until the baseline reduces to zero. The background used for this experiment is shown in Figure 55.

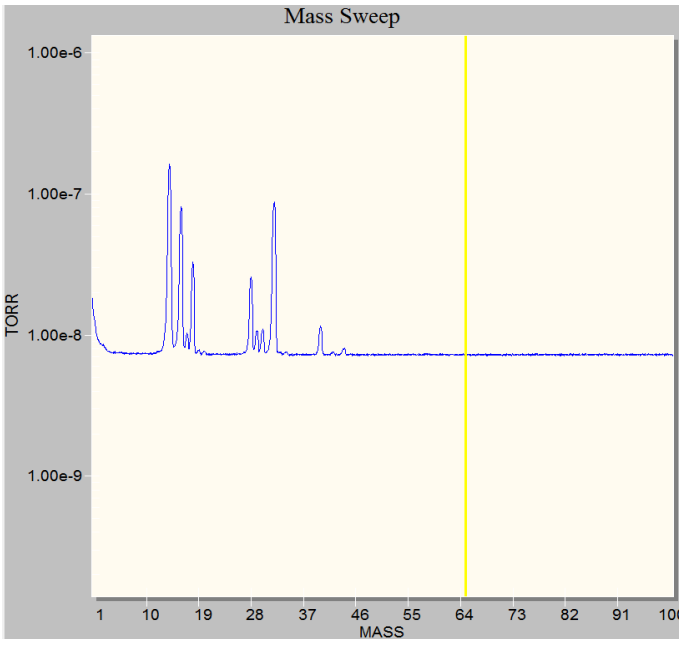

Figure 65: Background scan used for mass spectrometry

Then, using the same flow and scan settings, the gas sample in a syringe is injected into the system and analyzed. Screenshots and spreadsheets of the obtained data are saved

and analyzed for gas phase single chain alkanes. This is done by comparing recorded partial pressures of each constituent to the partial pressure of the baseline for the same mass. The partial pressures are assumed proportional to the concentration.

Figure 66 shows mass spectra obtained from gases produced from a 720 kGy treated GSC1AOS soil. Mainly air (from the system head gas) and hydrocarbons are noted in the spectra. Peaks at the molecular mass for H_2S are observed at a relative concentration of about 10 ppm. CO and CO_2 cannot be unambiguously identified. Among the hydrocarbons hydrogen is present, methane is the most abundant, and with decreasing concentration C_2 to C_7 are present.

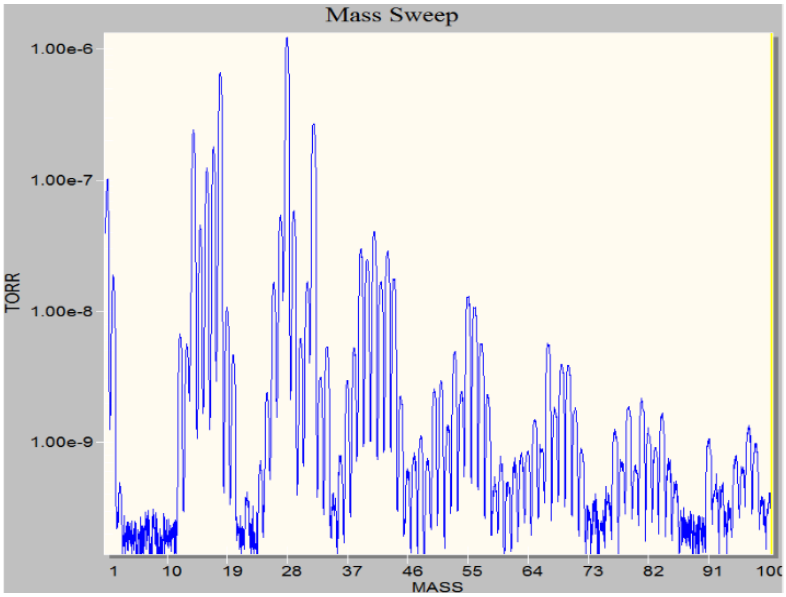

Figure 66: Mass spectra for gases obtained from a 720 kGy treated GSC1AOS soil

4.4.4 Temperature Diagnostics and Modeling

The real-time pressure diagnostic setup was used to obtain pressure time histories with 3 second intervals for 3 e-beam experiments. The setup containing 1100 kGy treated GSC1AOS appeared to maintain pressure, with a maximum pressure of 6.7 psi. Gaskets for setups 2 and 5, which contained BM1 soils, failed at 8.4 psi and 7.0 psi respectively. Failure is indicated by a sudden drop from peak pressure. These results indicate that the reactor configurations are not capable of maintaining pressure for wet soils. The plots have a much steeper slope than that of setup 3 due to water evaporation.

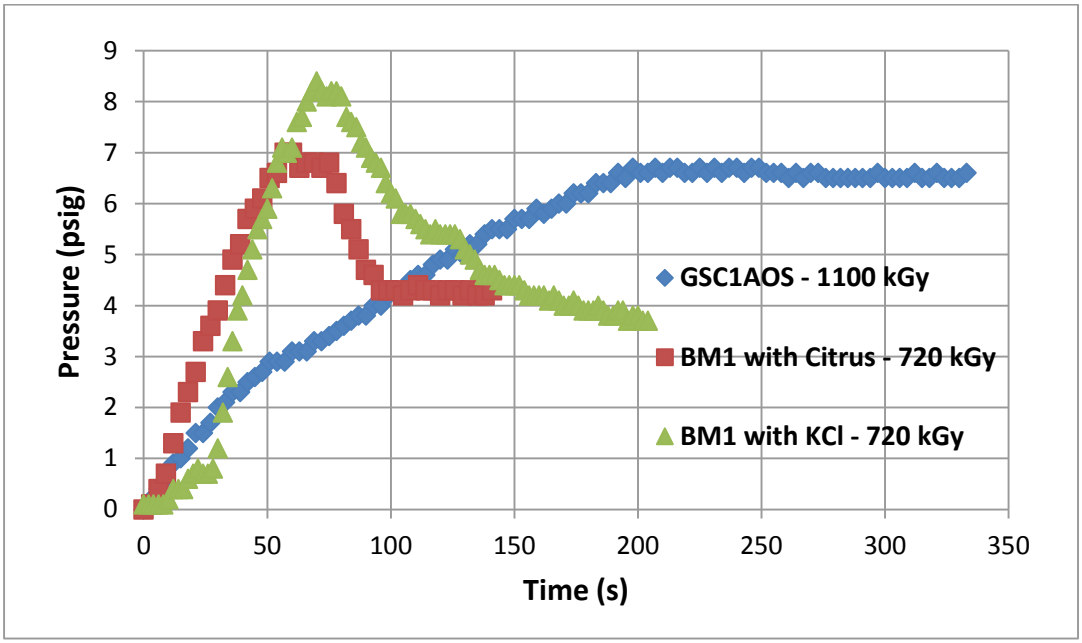

Figure 67: Pressure time history for setups 2, 3, and 5.

The temperature time history shown in Figure 68 shows a maximum temperature at 683°F occurring at the end of the e-beam run (123 sec). While the e-beam is on, the temperature increases at a decaying rate. After the e-beam is switched off, a gradual

decrease to 306°F (ΔT=377°F) after 380 sec is observed, corresponding to a cooling rate of roughly 7°F/s.

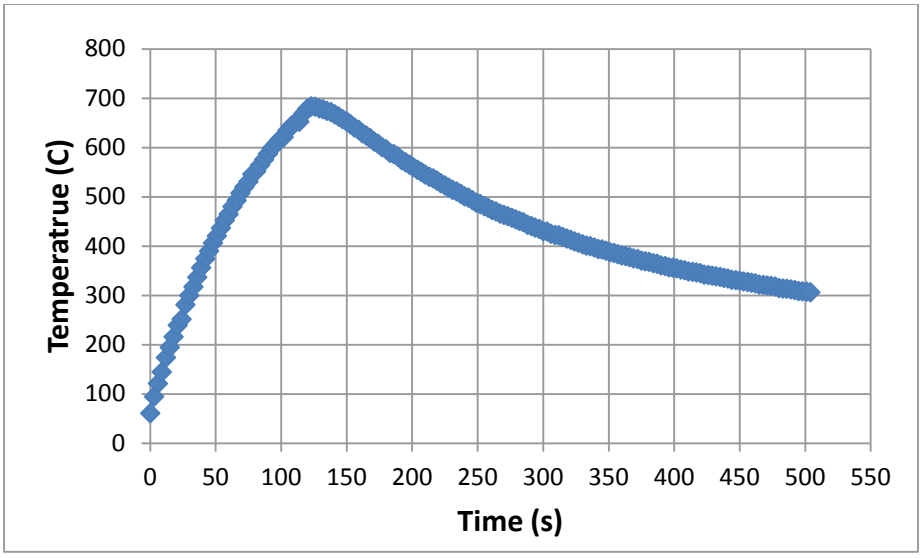

Figure 68: Temperature time history for 720 kGy treated BM1 with ethanol

Experimental temperature data in Figure 68 was fitted using an in-homogenous first order ODE as shown in equations 17 and 18.

$$mc\frac{dT}{dt} = h(T - T_\infty) \tag{17}$$

$$\frac{T - T_\infty}{T_o - T_\infty} = e^{-xt} \tag{18}$$

In these equations, T_o is the initial temperature, T_∞ is ambient temperature, and x is the inverse of the time constant. The model assumes no heat input and heat transfer by convection. These are accurate assumptions for the cooling profile but not the heating profile, since an external energy source (the electron beam) causes heating. These other

factors in the heating profile were lumped into the time constant, environmental temperature, and initial temperature using numerical non-linear curve fitting of the experimental temperature data. The same was done for the cooling temperature data. For heating, T_o is the maximum temperature during cooling and the initial temperature during heating. The curve fit, shown in Figure 69 allowed for estimation of heat transfer coefficient, dose rate, and cooling time constant.

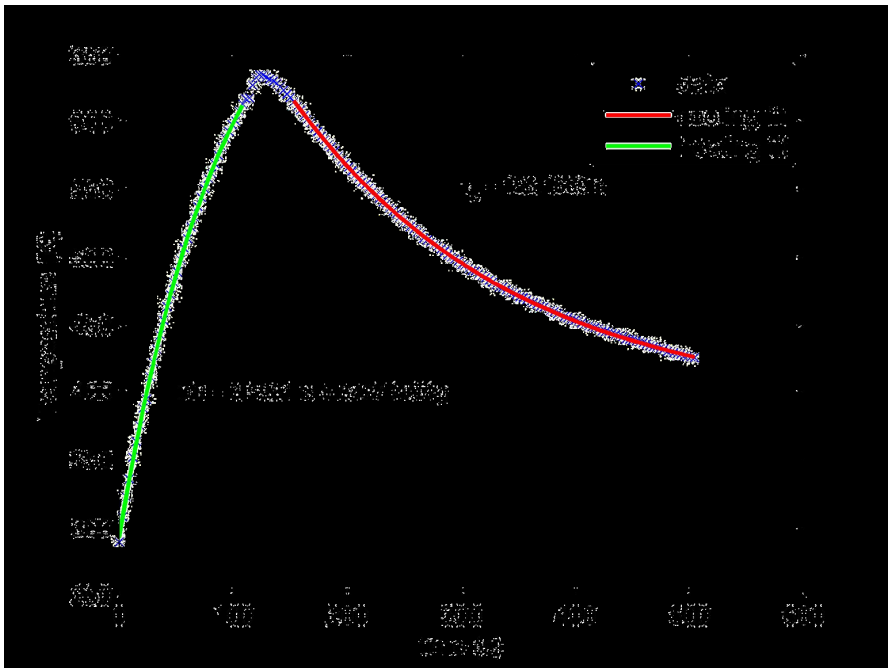

Figure 69: Curve fit of temperature history obtained from 720 kGy treated BM1 soilspiked with ethanol

4.4.5 Mass Balances

Mass balances were done for manufactured clay soils and as-received soil experiments. These are shown in Tables 10 and 11 respectively. Initial solids represents the expected dry soil content of the soil (i.e. the soil mass without the water and oil

masses). Expected liquid mass is the combined mass of oil and water in the untreated soil. The best mass balance achieved for clay soils was 96.17%. In many cases, liquids were not collected. In some cases, >100% of solids were collected. This is due to lack of phase separation, which causes oil and water to remain in the soil during collection. Additionally, the greatest percentage of liquid collected is 11.1%, indicating that liquid collection must be greatly improved. Overall, the mass balances are too inaccurate to learn anything meaningful about the composition of treated soils.

Table 10: Mass balance for experiments on manufactured clay soils

Clay Soils								
Soil	Dose (kGy)	Initial Soil Mass (g)	Initial Solids (g)	Collected Solids (g)	Collected Liquids (g)	% Collected Solids	% Collected Liquids	% Total Collected
90-10-0	2000	32.1	28.89	23.5	2.8	81.34	87.23	81.93
80-10-10	1784	67.1	53.68	53.5	11.1	99.66	82.71	96.27
80-10-10	496	67.7	54.16	59.7	2.1	110.23	15.51	91.29
80-10-10	480	60.8	48.64	53	0	108.96	0.00	87.17
80-10-10	960	61.4	49.12	51.3	3.1	104.44	25.24	88.60
60-10-30	1920	69.5	41.7	41.9	11.1	100.48	39.93	76.26

Mass balances were improved for real soils, with 95%-105% of solids collected. The best case for liquid collection was 17.1% with <1% liquid collection in many cases. This led to the design of a condenser setup to improve liquid collection to >95%.

Table 11: Mass balance for experiments on as-received soils

Real Soils								
Soil	Dose (kGy)	Initial Soil Mass (g)	Initial Solids (g)	Collected Solids (g)	Collected Liquids (g)	% Collected Solids	% Collected Liquids	% Total Collected
GSC1AOS	720	83.7	75.4	73.5	1	97.48	12.05	89.01
GSC1AOS	1100	99.74	89.86	86.42	1.09	96.17	11.03	87.74
GSI14RD	720	79.1	75.7	72.5	3	95.77	88.24	95.45
BM1-1	480	103.1	82.5	82.9	0.78	100.53	3.78	81.16
BM1-1	960	142.2	113.76	109.6	17.1	96.34	60.13	89.10
BM1 w/ ethanol	720	100.73	76.53	77.94	6.77	101.84	27.98	84.10
BM1 w/ KCL	720	104.36	84.51	85.14	2.84	100.75	14.31	84.30
BM1 w/ Citrus Oil	720	104.38	79.31	81.26	12.45	102.46	49.66	89.78
BM2	820	101.15	96.7	96.78	0	99.87	0.00	95.68

4.4.5 Condenser Experiments

The experiment with BT sludge was run in Configuration 6. Sample collection from the liquid nitrogen condenser was a new task and needed to be very carefully conducted. First, the condenser is disconnected from the reactor, and the collection vessel is removed from the liquid nitrogen bath and sealed with a flow control valve. Then, the vessel and tubing are weighed and compared to their original weight.

This experiment produced 3 distinct types of liquids, shown in the left picture of Figure 70: (1) a low viscosity water/oil mixture, (2) a slightly higher viscosity oil mixture obtained from the condenser, (3) and a heavy oil sludge. The sludge was

obtained from the end of the pipe opposite the soil. Light liquids were obtained by holding the open reactor over a jar.

Table 12: Breakdown of extracted BT Sludge components

Quantity	Thick Liquids	Thin Liquids	Condenser Liquids	Solids	Lost Mass
mass (g)	11.11	25.61	10.01	56.1	47.63
% soil mass	7.38	17.02	6.65	37.29	31.66

Table 12 shows a breakdown of the extracted BT Sludge components. Nearly one-third of the total initial mass was lost, a third was collected as liquids, and a third collected as solids. Roughly 7% of the total initial mass was collected by the condenser. An accurate mass balance was not obtained from this experiment.

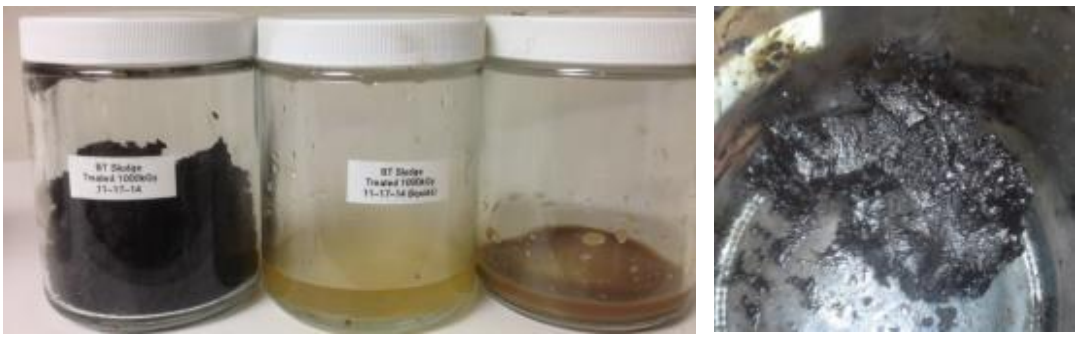

Figure 70: 1100 kGy treated BT Sludge with collected liquids. From left to right: dry soil, oil-water mixture, oil mixture, and heavy sludge.

A second experiment was run with a BM1 soil sample to verify the effectiveness of using liquid nitrogen in the condenser for obtaining a more accurate mass balance. Therefore, the experimental setup and parameters are almost identical to previous ones. BM1 soil was treated for 120 seconds for a total dose of 720 kGy.

Figure 71: Extracted components of treated BM1 soil

Extracted components from the condenser are shown in the right of Figure 71. Oils were extracted as ice, and trace amounts of water were condensed as liquids on the condenser wall. Additionally, it was estimated that 4.4 g of liquids were not collected. The majority of this was coating the walls of the piping connecting the condenser to the sample pipe.

Ideally, the mass difference accounting all components represents the sample quantity extracted from the soil, if there was no leaking and no water condensation on the condenser surface. The gas leak and water condensation are assumed to be negligible in our case considering the weight of condensed liquid. The mass balance was significantly improved by using the liquid nitrogen condenser. 92.9% of all initial mass was collected in jars. A total of 96.7% of the mass was contained in the setup.

Table 13: Mass balance calculation on extracted sample from BM1

Initial Soil	Initial Oil	Collected Soil	Condensed Liquids	Collected Liquids	Collected Solids (%)	Collected Liquids (%)	Total Collected (%)
116.89g	1.87g	92.43g	20.63g	16.17g	98.85	69.16	92.91

5. CONCLUSIONS

5.1 Summary

Work accomplished includes proof-of-concept of e-beam soil remediation through demonstration of TPH reduction to <1%. Non-thermal effects have been shown to play a role in thermal processing and effects from changing dose, treatment temperature, and water content have been distinguished. Additionally, a reactor design for e-beam treatment of soils was developed as well as an analysis method for screening TPH of treated soils.

Electron beam treatment appears to be an effective method for reducing TPH. Preliminary experiments with sand-oil mixtures appeared to show phase separation and TPH reduction by a factor of roughly 8. This was confirmed with UV-Spectroscopy of treated clay-oil mixtures, with a maximum reduction of 10% to 0.52% for a 1784kGy treated 80-10-10 soil. TPH reduction was shown to increase with dosage, increase with treatment temperature, and decrease with moisture. Further experiments with as received soils demonstrated significant dose dependent reductions in TPH. It was observed that higher temperatures produced greater TPH reductions and that for BM1 soil lighter hydrocarbons were preferentially removed, indicating thermal processing. For other soils, %TPH consisting of GROs and light DROs increased, indicating that non-thermal processing does occur and that electron beam treatment increases the viability of other remediation methods for these soils. Reduction of TPH to <1% was shown for BM1, BM2, and GSC1AOS soils. Maximum TPH reductions for real soils are 9.1% to 0.15% for GSC1AOS with an 1100kGy dosage, 2.9% to 1.2% for GSI14RD

with a 720kGy dosage, 1.6% to 0.17% for BM1 with a 960 kGy dosage, 2.1% to 0.5% for BM2 with an 820kGy dosage, and 31.9% to 28% for BT Sludge with an 1100kGy dosage. Three additives, ethanol, potassium chloride (KCl), and citrus oil were tested in 5wt% amounts with BM1. 720kGy treated soils with additives showed a TPH reduction to less than 0.5%, marginally better than results predicted by other BM1 experiments. It was shown that the addition of a condenser to the setup has the potential to produce an accurate mass balance of the system.

Electron beam treatment produces large TPH reductions within very short time frames compared to other methods. This allows for processing of large amounts of soil and continuous operation, greatly reducing operating costs compared to other methods. Additionally, it may be used to greatly increase efficiency of other methods that rely on the presence of lighter hydrocarbon fractions. With further characterization and implementation, this method could consistently produce TPH reductions that satisfy most government regulations and greatly assist with restoring polluted ecosystems.

5.2 Future Work

At this point, electron beam soil remediation has been demonstrated to be a viable concept. Further work must be done in characterizing the process. First, the contributions of thermal and non-thermal processes must be distinguished. This could be done with real-time temperature monitoring and comparison of this with experimental data from thermal treatment of soils with heating profiles that simulate soil heating in the e-beam. Further analysis of liquid and gas phase products will be necessary to determine a larger range of reaction mechanisms and the health risks posed by remediation by-

products. Collection of liquids produced must be improved. Low collection levels (roughly 60%) have precluded the use of mass balances as an analysis tool. Methods to improve this include the addition of a condenser. Finally, the applicability of this technology for field implementation will require transitioning from batch-scale experiments to continuous processing and providing a means for continuous removal of by-products.

REFERENCES

[1] B. Gargouri, F. Karray, N. Mhiri, F. Aloui, and S. Sayadi, "Bioremediation of Petroleum Hydrocarbons-Contaminated Soil by Bacterial Consortium Isolated from an Industrial Wastewater Treatment Plant," *Journal of Chemical Technology and Biotechnology,* vol. 89, pp. 978-987, 2014.

[2] V. Simanzhenkov and R. Idem, *Crude Oil Chemistry*. New York, NY: Marcel Dekker, 2003.

[3] "Alkane." Internet: <http://www.merriam-webster.com/dictionary/alkane>, [Feb. 04].

[4] "E&P Site Cleanup Levels Revisited: Opportunities for Risk-Based Decision Making," in *Sixth Annual International Petroleum Environmental Conference*, Houston, Texas, 1999.

[5] F. Khan, T. Husain, and R. Hejazi, "An Overview and Analysis of Site Remediation Technologies," *Journal of Environmental Management,* vol. 71, pp. 95-122, 2004.

[6] D. M. Hamby, "Site Remediation Techniques Supporting Environmental Restoration Activities: A Review," University of Michigan, Ann Arbor, MI 0048-9697, 1996.

[7] R. C. Sims, "Soil Remediation Techniques at Uncontrolled Hazardous Waste Sites," *Journal of the Air & Waste Management Association,* vol. 40, pp. 704-732, 1990.

[8] Y.-C. Chien, "Field Study of In Situ Remediation of Petroleum Hydrocarbon Contaminated Soil on Site Using Microwave Energy," *Journal of Hazardous Materials,* vol. 199–200, pp. 457-461, 2012.

[9] P. P. Falciglia, "Remediation of Hydrocarbon-Contaminated Soils by Ex Situ Microwave Treatment: Technical, Energy and Economic Considerations," *Environmental Technology,* vol. 35, pp. 2280-2288, 2014.

[10] P. P. Falciglia, M. G. Giustra, and F. G. A. Vagliasindi, "Low-Temperature Thermal Desorption of Diesel Polluted Soil: Influence of Temperature and Soil Texture on Contaminant Removal Kinetics," *Journal of Hazardous Materials,* vol. 185, pp. 392-400, 2011.

[11] M. R. Cleland, "Industrial Applications of Electron Accelerators," presented at the CAS-CERN Accelerator School, Zeegse, The Netherlands, 2005.

[12] A. J. Berejka, "Prospects and Challenges for the Industrial Use of Electron Beam Accelerators," in *International Topical Meeting on Nuclear Research Applications and Utilization of Accelerators*, Vienna, Austria, 2009, pp. 4-8.

[13] "Chemistry WebBook." Internet: http://webbook.nist.gov/chemistry/form-ser.html, [2011, Feb. 02].

[14] "ChemSpider." Internet: http://www.chemspider.com/Search.aspx, [2015, Feb. 02].

[15] K. Makuuchi and S. Cheng, "Basic Concepts of Radiation Processing," in *Radiation Processing of Polymer Materials and its Industrial Applications*, ed Hoboken, NJ: John Wiley & Sons, 2012.

[16] M. Faraday, "Experimental Researches in Electricity," *Philosophical Transactions of the Royal Society of London,* vol. 3, pp. 125-168, 1855.

[17] "Julius Plucker." Internet: http://chemed.chem.purdue.edu/genchem/history/plucker.html, [Jan. 8].

[18] "Johannes Hittorf." Internet: http://chemed.chem.purdue.edu/genchem/history/hittorf.html, [January 8].

[19] J. Thomson, "Cathode Rays," *The Electrician,* vol. 39, pp. 104-109, 1897.

[20] S. I. Molokovsky and A. D. Sushkov, *Intense Electron and Ion Beams*. Berlin, Germany: Springer Science + Business Media, Inc., 2005.

[21] D. Yang, "Heavy Oil Upgrading from Electron Beam (E-Beam) Irradiation," Master of Science, Petroleum Engineering, Texas A&M University, College Station, TX, 2009.

[22] Y. Zaikin and R. Zaikina, *Petroleum Radiation Processing*. Boca Raton, FL: CRC Press, 2014.

[23] A. H. W. Nias, "Ionizing Radiations," in *An Introduction to Radiobiology*, ed England: John Wiley & Sons, 1990, pp. 46-60.

[24] R. B. Miller, *Electronic Irradiation of Foods: An Introduction to the Technology*. New York, NY: Springer Science + Business Media, Inc., 2005.

[25] K. Semple, K. Doick, P. Burauel, A. Craven, H. Harms, and K. Jones, "Defining Bioavailibility and Bioaccessibility of Contaminated Soil and Sediment is Complicated," *Environmental Science and Technology,* vol. 38, pp. 228-231, 2004.

[26] M. D. MacRae and T. J. Anderson, "Persistant Organic Wastes," in *Environmental and Ecological Chemistry*. vol. 2, A. Sabljic, Ed., ed Croatia: Rudjer Boskovic Institute, 2009.

[27] "Introduction Technology Watch Report: Contaminated Soil Remediation Techniques."

[28] Y. Yang, D. Ratté, B. F. Smets, J. J. Pignatello, and D. Grasso, "Mobilization of Soil Organic Matter by Complexing Agents and Implications for Polycyclic Aromatic Hydrocarbon Desorption," *Chemosphere,* vol. 43, pp. 1013-1021, 2001.

[29] M. J. Mann et al., *Soil Washing/Soil Flushing*. Annapolis, MD: American Academy of Envronmental Engineers, 1993.

[30] R. A. Brouns, J. L. Buelt, and W. F. Bonner, "In-Situ Vitrification of Soil," U.S. Patent 4 376 598, 1983.

[31] J. L. Buelt and R. K. Farnsworth, "In Situ Vitrification of Soils Containing Various Metals," Pacific Northwest Laboratory, Richland, WA

[32] S. Gan, E. V. Lau, and H. K. Ng, "Remediation of Soils Contaminated with Polycyclic Aromatic Hydrocarbons (PAHs)," *Journal of Hazardous Materials,* vol. 172, pp. 532-549, 2009.

[33] G. L. Stegemeier and H. J. Vinegar, "Thermal Conduction Heating for In Situ Thermal Desorption of Soils," *Chapter,* vol. 4, pp. 1-37, 2001.

[34] J. S. Lighty, D. W. Pershing, V. A. Cundy, and D. G. Linz, "Characterization of Thermal Desorption Phenomena for the Cleanup of Contaminated Soil," *Nuclear and Chemical Waste Management,* vol. 8, pp. 225-237, 1988.

[35] D. Sarkar, M. Ferguson, R. Datta, and S. Birnbaum, "Bioremediation of Petroleum Hydrocarbons in Contaminated Soils: Comparison of Biosolids Addition, Carbon Supplementation, and Monitored Natural Attenuation," *Environmental Pollution,* vol. 136, pp. 187-195, 2005.

[36] G. J. Smith, "Coupled Electrokinetic–Thermal Desorption," in *Electrochemical Remediation Technologies for Polluted Soils, Sediments and Groundwater*, K. R. Reddy and C. Cameselle, Eds., ed Hoboken, NJ: John Wiley & Sons, 2009, pp. 505-535.

[37] E. Méndez, M. Pérez, O. Romero, E. D. Beltrán, S. Castro, J. L. Corona, A. Corona, M. C. Cuevas, and E. Bustos, "Effects of Electrode Material on the Efficiency of Hydrocarbon Removal by an Electrokinetic Remediation Process," *Electrochimica Acta,* vol. 86, pp. 148-156, 2012.

[38] H. I. Chung and M. Kamon, "Ultrasonically Enhanced Electrokinetic Remediation for Removal of Pb and Phenanthrene in Contaminated Soils," *Engineering Geology,* vol. 77, pp. 233-242, 2005.

[39] S. Guo, R. Fan, T. Li, N. Hartog, F. Li, and X. Yang, "Synergistic Effects of Bioremediation and Electrokinetics in the Remediation of Petroleum-Contaminated Soil," *Chemosphere,* vol. 109, pp. 226-233, 2014.

[40] G. Wu, Y. Katsumura, C. Matsuura, K. Ishigure, and J. Kubo, "Radiation Effect on the Thermal Cracking of n-Hexadecane. 1. Products from Radiation-Thermal Cracking," *Industrial & Engineering Chemistry Research,* vol. 36, pp. 1973-1978, 1997.

[41] G. Wu, Y. Katsumura, C. Matsuura, K. Ishigure, and J. Kubo, "Radiation Effect on the Thermal Cracking of n-Hexadecane. 2. A Kinetic Approach to Chain Reaction," *Industrial & Engineering Chemistry Research,* vol. 36, pp. 3498-3504, 1997.

[42] R. Salovey and W. E. Falconer, "Radiation-Induced Reactions in n-Hexadecane," *Journal of Physical Chemistry,* vol. 69, pp. 2345-2350, 1965.

[43] L. V. Zhigilei, MSE 2090. Class Lecture, Topic: "Polymer Structures." University of Virginia, Charlottesville, VA, 2010.

[44] Y. A. Zaikin and R. F. Zaikina, "Self-Sustain Cracking of Hydrocarbons," U.S. Patent 8 192 591, 2012.

[45] M. Alfi, P. F. D. Silva, M. A. Barrufet, and R. G. Moreira, "Electron-Induced Chain Reactions of Heavy Petroleum Fluids-Dominant Process Variables," presented at the SPE Heavy Oil Conference Canada, Calgary, Alberta, Canada, 2012.

[46] M. Alfi, P. F. D. Silva, M. A. Barrufet, and R. G. Moreira, "Utilization of Charged Particles as an Efficient Way to Improve Rheological Properties of Heavy Asphaltic Petroleum Fluids," presented at the SPE Latin America and Caribbean Petroleum Engineering Conference, Mexico City, Mexico, 2012.

[47] G. Imada, "Treatment of Volatile Organic Compounds Contained in Soil by Pulsed Intense Relativistic Electron Beam Irradiation," *IEEJ Transactions on Electrical and Electronic Engineering,* vol. 6, pp. 88-90, 2011.

[48] R. Hilarides, K. A. Gray, J. Guzzetta, N. Cortellucci, and C. Sommer, "Radiolytic Degradation of Dioxin on Soil: Optimal Conditions and Economic Considerations," *Environmental Progress,* vol. 13, pp. 263-268, 1994.

[49] X. Mao, R. Jiang, W. Xiao, and J. Yu, "Use of Surfactants for the Remediation of Contaminated Soils: A Review," *Journal of Hazardous Materials,* vol. 285, pp. 419-435, 2015.

[50] E. Ruckenstein and R. Nagarajan, "Critical Micelle Concentration. Transition Point for Micellar Size Distribution," *The Journal of Physical Chemistry,* vol. 79, pp. 2622-2626, 1975.

[51] M. Peyda, A. Fakhru'l-Razi, M. Zakaria, and Z. Abidin, "Polymer Partitioning Approach for Petroleum Hydrocarbon Reduction in a Clay Soil," *Water, Air, and Soil Pollution,* vol. 224, pp. 1-12, 2013.

[52] C. N. Mulligan, "Recent Advances in the Environmental Applications of Biosurfactants," *Current Opinion in Colloid & Interface Science,* vol. 14, pp. 372-378, 2009.

APPENDIX

The appendix contains screenshots of analysis reports provided by Lancaster Laboratories for TPH analysis of treated as-received soils

eurofins | Lancaster Laboratories Environmental

2425 New Holland Pike, Lancaster, PA 17601 • 717-656-2300 • Fax: 717-656-2681 • www.LancasterLabs.com

Analysis Report

Sample Description: GSI14RD-1-041714 1650 14-0016-01 Soil
HHSRG

LL Sample # SW 7441136
LL Group # 1469535
Account # 10863

Project Name: HHSRG

Collected: 04/22/2014 10:40

Submitted: 04/24/2014 09:30
Reported: 05/13/2014 12:54

Chevron Energy Technology Co.
100 Chevron Way
50-1263
Richmond CA 94802

HHSR1

CAT No.	Analysis Name	CAS Number	Dry Result		Dry Method Detection Limit*	Dry Limit of Quantitation	Dilution Factor
GC/MS	Semivolatiles SW-846 8270C SIM		ug/kg		ug/kg	ug/kg	
10242	17a(H)-diahopane	n.a.	320		10	250	10
10242	A1-C20TAS	n.a.	1,400		10	250	10
10242	A2-C21TAS	n.a.	1,500		10	250	10
10242	A3-C26TAS(20S)	n.a.	3,700		10	250	10
10242	A4-C26/C27TAS	n.a.	13,000		10	250	10
10242	A5-C27TAS(20R)	n.a.	8,000		10	250	10
10242	A6-TAS(20S)	n.a.	3,300		10	250	10
10242	A7-TAS(20R)	n.a.	3,100		10	250	10
10242	Acenaphthene	83-32-9	N.D.		100	250	10
10242	Acenaphthylene	208-96-8	N.D.		100	250	10
10242	Anthracene	120-12-7	120	J	100	250	10
10242	Benzo(a)anthracene	56-55-3	150	J	100	250	10
10242	Benzo(a)pyrene	50-32-8	N.D.		100	250	10
10242	Benzo(b)fluoranthene	205-99-2	120	J	100	250	10
10242	Benzo(e)pyrene	192-97-2	200	J	100	250	10
10242	Benzo(g,h,i)perylene	191-24-2	N.D.		100	250	10
10242	Benzo(k)fluoranthene	207-08-9	N.D.		100	250	10
10242	C1-Benzanthrene/chrysenes	n.a.	1,400		100	250	10
10242	C1-Dibenzothiophene	n.a.	4,400		100	250	10
10242	C1-Fluoranthrenes/pyrenes	n.a.	2,600		100	250	10
10242	C1-Fluorenes	n.a.	N.D.		100	250	10
10242	C1-Naphthalenes	n.a.	N.D.		100	250	10
10242	C1-Phenanthrenes/anthracenes	n.a.	2,600		100	250	10
10242	C2-Benzanthrene/chrysenes	n.a.	3,900		100	250	10
10242	C2-Dibenzothiophene	n.a.	11,000		100	250	10
10242	C2-Fluoranthrenes/pyrenes	n.a.	2,800		100	250	10
10242	C2-Fluorenes	n.a.	N.D.		100	250	10
10242	C2-Naphthalenes	n.a.	440		100	250	10
10242	C2-Phenanthrenes/anthracenes	n.a.	8,100		100	250	10
10242	C3-Benzanthrene/chrysenes	n.a.	2,100		100	250	10
10242	C3-Dibenzothiophene	n.a.	16,000		100	250	10
10242	C3-Fluoranthrenes/pyrenes	n.a.	3,800		100	250	10
10242	C3-Fluorenes	n.a.	7,400		100	250	10
10242	C3-Naphthalenes	n.a.	5,200		100	250	10
10242	C3-Phenanthrenes/anthracenes	n.a.	13,000		100	250	10
10242	C4-Benzanthrene/chrysenes	n.a.	1,400		100	250	10
10242	C4-Dibenzothiophene	n.a.	11,000		100	250	10
10242	C4-Fluoranthrenes/pyrenes	n.a.	4,200		100	250	10
10242	C4-Naphthalenes	n.a.	11,000		100	250	10
10242	C4-Phenanthrenes/anthracenes	n.a.	7,400		100	250	10
10242	Cholestane	n.a.	14,000		10	250	10
10242	Chrysene	218-01-9	560		100	250	10
10242	Dibenz(a,h)anthracene	53-70-3	N.D.		100	250	10
10242	Dibenzothiophene	132-65-0	720		100	250	10
10242	Fluoranthene	206-44-0	110	J	100	250	10
10242	Fluorene	86-73-7	N.D.		100	250	10
10242	Indeno(1,2,3-cd)pyrene	193-39-5	N.D.		100	250	10
10242	Naphthalene	91-20-3	N.D.		100	250	10
10242	Perylene	198-55-0	930		100	250	10
10242	Phenanthrene	85-01-8	460		100	250	10
10242	Pyrene	129-00-0	650		100	250	10

*=This limit was used in the evaluation of the final result

Sample Description: GSI14RD-1-041714 1650 14-0016-01 Soil
HHSRG

LL Sample # SW 7441136
LL Group # 1469535
Account # 10863

Project Name: HHSRG

Collected: 04/22/2014 10:40

Submitted: 04/24/2014 09:30
Reported: 05/13/2014 12:54

Chevron Energy Technology Co.
100 Chevron Way
50-1263
Richmond CA 94802

HHSR1

CAT No.	Analysis Name	CAS Number	Dry Result		Dry Method Detection Limit*	Dry Limit of Quantitation	Dilution Factor
GC/MS Semivolatiles	SW-846 8270C SIM		ug/kg		ug/kg	ug/kg	
10242	S10-Methyldiacholestane	n.a.	N.D.		10	250	10
10242	S11-Methyldiacholestane	n.a.	2,200		10	250	10
10242	S12-Cholestane	n.a.	6,600		10	250	10
10242	S14-Cholestane(20R)	n.a.	7,800		10	250	10
10242	S15-Cholestane(20S)	n.a.	7,600		10	250	10
10242	S18-Ethyldiacholestane	n.a.	1,300		10	250	10
10242	S19-Ethyldiacholestane	n.a.	N.D.		10	250	10
10242	S20-Methylcholestane	n.a.	2,500		10	250	10
10242	S22-Methylcholestane(20R)	n.a.	8,900		10	250	10
10242	S23-Methylcholestane(20S)	n.a.	7,600		10	250	10
10242	S24-MethylCholestane	n.a.	7,800		10	250	10
10242	S25-EthylCholestane	n.a.	4,800		10	250	10
10242	S26-Ethylcholestane(20R)	n.a.	6,000		10	250	10
10242	S27-Ethylcholestane(20S)	n.a.	5,200		10	250	10
10242	S28-Ethylcholestane	n.a.	6,300		10	250	10
10242	S4-Diacholestane	n.a.	3,600		10	250	10
10242	S5-Diacholestane	n.a.	950		10	250	10
10242	S6-Diacholestane	n.a.	N.D.		10	250	10
10242	S7-Diacholestane	n.a.	920		10	250	10
10242	S8-Methyldiacholestane	n.a.	940		10	250	10
10242	T10-C29Tricyclictriterpane(R)	n.a.	1,700		10	250	10
10242	T11-Trisnorhopane(TS)	n.a.	370		10	250	10
10242	T12-Trisnorhopane(TM)	n.a.	1,400		10	250	10
10242	T13a-29,30-Bisnorhopane	n.a.	N.D.		10	250	10
10242	T13-Trisnorhopane	n.a.	380		10	250	10
10242	T14a-C28,C30Bisnorhopane	n.a.	460		10	250	10
10242	T14b-C29,C25Norhopane	n.a.	1,100		10	250	10
10242	T14-Bisnorhopane	n.a.	460		10	250	10
10242	T15-C29Norhopane	n.a.	4,200		10	250	10
10242	T16-Norneohopane	n.a.	520		10	250	10
10242	T17-C30 Normoretane	n.a.	370		10	250	10
10242	T18-C30 Oleanane	n.a.	N.D.		10	250	10
10242	T19-C30 Hopane	n.a.	6,500		10	250	10
10242	T20-Moretane	n.a.	1,100		10	250	10
10242	T21-C31 Homohopane(S)	n.a.	2,600		10	250	10
10242	T22a-Gammacerane	559-65-9	N.D.		10	250	10
10242	T22-C31 Homohopane(R)	n.a.	2,900		10	250	10
10242	T23-Homohopane	471-62-5	2,000		10	250	10
10242	T24-Homomoretane	n.a.	370		10	250	10
10242	T25-Diploptene	n.a.	110	J	10	250	10
10242	T26-C32-Bishomohopane(S)	n.a.	2,300		10	250	10
10242	T27-C32-Bishomohopane(R)	n.a.	1,700		10	250	10
10242	T28-Bishomomoretane	n.a.	1,000		10	250	10
10242	T29-Homohopane	n.a.	800		10	250	10
10242	T30-C33-Trishomohopane(S)	n.a.	1,900		10	250	10
10242	T31-C33-Trishomohopane(R)	n.a.	1,200		10	250	10
10242	T32-Tetrakishomohopane(S)	n.a.	1,300		10	250	10
10242	T33-Tetrakishomohopane(R)	n.a.	790		10	250	10
10242	T34-Pentakishomohopane(S)	n.a.	2,500		10	250	10
10242	T35-Pentakishomohopane(R)	n.a.	2,400		10	250	10
10242	T4-C23 Diterpane	n.a.	5,200		10	250	10

*=This limit was used in the evaluation of the final result

Sample Description: GSI14RD-1-041714 1650 14-0016-01 Soil
HHSRG

LL Sample # SW 7441136
LL Group # 1469535
Account # 10863

Project Name: HHSRG

Collected: 04/22/2014 10:40

Submitted: 04/24/2014 09:30
Reported: 05/13/2014 12:54

Chevron Energy Technology Co.
100 Chevron Way
50-1263
Richmond CA 94802

HHSR1

CAT No.	Analysis Name	CAS Number	Dry Result		Dry Method Detection Limit*	Dry Limit of Quantitation	Dilution Factor
GC/MS Semivolatiles	**SW-846 8270C SIM**		**ug/kg**		**ug/kg**	**ug/kg**	
10242	T5-C24Diterpane	n.a.	3,100		10	250	10
10242	T6a-C24TetracyclicTerpane	n.a.	N.D.		10	250	10
10242	T6b-C26Tricyclic[S]	n.a.	1,100		10	250	10
10242	T6-C25Diterpane	n.a.	2,900		10	250	10
10242	T6c-C26Tricyclic[R]	n.a.	1,500		10	250	10
10242	T7-C28Tricyclictriterpane[S]	n.a.	1,200		10	250	10
10242	T8-C28Tricyclictriterpane[R]	n.a.	1,600		10	250	10
10242	T9-C29 Tricyclictriterpane(S)	n.a.	1,600		10	250	10

Reporting limits were raised due to interference from the sample matrix.

The LCS and/or LCSD recoveries are outside the stated QC window but within the marginal exceedance allowance of +/- 4 standard deviations as defined in the NELAC Standards. The following analytes are accepted based on this allowance:
chrysene

GC Volatiles	**SW-846 8015B modified**		**mg/kg**		**mg/kg**	**mg/kg**	
12989	C10-C12	n.a.	N.D.		42	210	5181.35
12989	C5-C6	n.a.	N.D.		42	210	5181.35
12989	C6-C8	n.a.	N.D.		42	210	5181.35
12989	C8-C10	n.a.	N.D.		42	210	5181.35
12989	Total GRO (C5-C12)	n.a.	49	J	42	210	5181.35

Reporting limits were raised due to sample foaming.

GC Petroleum Hydrocarbons	**MA DEP EPH 5/04**		**mg/kg**		**mg/kg**	**mg/kg**	
07062	Aliphatics >C10 - C12	n.a.	N.D.		580	580	5
07062	Aliphatics >C12 - C16	n.a.	N.D.		580	580	5
07062	Aliphatics >C16 - C35	n.a.	8,100		580	580	5
07062	Aromatics >C10 - C12	n.a.	N.D.		230	230	2
07062	Aromatics >C12 - C16	n.a.	N.D.		230	230	2
07062	Aromatics >C16 - C21	n.a.	2,300		230	230	2
07062	Aromatics >C21 - C35	n.a.	4,000		230	230	2

GC Petroleum Hydrocarbons	**SW-846 8015B**		**mg/kg**		**mg/kg**	**mg/kg**	
02729	>C12-C14	n.a.	N.D.		810	2,400	100
02729	>C14-C16	n.a.	N.D.		810	2,400	100
02729	>C16-C18	n.a.	2,500		810	2,400	100
02729	>C18-C20	n.a.	3,600		810	2,400	100
02729	>C20-C22	n.a.	3,300		810	2,400	100
02729	>C22-C24	n.a.	3,000		810	2,400	100
02729	>C24-C26	n.a.	2,800		810	2,400	100
02729	>C26-C28	n.a.	2,500		810	2,400	100
02729	>C28-C30	n.a.	2,200	J	810	2,400	100
02729	>C30-C32	n.a.	1,500	J	810	2,400	100
02729	>C32-C34	n.a.	2,100	J	810	2,400	100
02729	>C34-C36	n.a.	1,400	J	810	2,400	100
02729	>C36-C38	n.a.	1,800	J	810	2,400	100

*=This limit was used in the evaluation of the final result

Sample Description: GSI14RD-1-041714 1650 14-0016-01 Soil
HHSRG

LL Sample # SW 7441136
LL Group # 1469535
Account # 10863

Project Name: HHSRG

Collected: 04/22/2014 10:40

Submitted: 04/24/2014 09:30
Reported: 05/13/2014 12:54

Chevron Energy Technology Co.
100 Chevron Way
50-1263
Richmond CA 94802

HHSR1

CAT No.	Analysis Name	CAS Number	Dry Result		Dry Method Detection Limit*	Dry Limit of Quantitation	Dilution Factor
GC Petroleum Hydrocarbons	**SW-846 8015B**		**mg/kg**		**mg/kg**	**mg/kg**	
02729	>C38-C40	n.a.	1,600	J	810	2,400	100
02729	DRO >C12-C22	n.a.	10,000		810	2,400	100
02729	ORO >C22-C40	n.a.	19,000		810	2,400	100
02729	Total TPH	n.a.	29,000		810	2,400	100
Wet Chemistry	**SM 2540 G-1997**		**%**		**%**	**%**	
00111	Moisture	n.a.	1.4		0.50	0.50	1

Moisture represents the loss in weight of the sample after oven drying at 103 - 105 degrees Celsius. The moisture result reported is on an as-received basis.

General Sample Comments

CA ELAP Lab Certification No. 2792; CA NELAP Lab Certification No. 10276CA

All QC is compliant unless otherwise noted. Please refer to the Quality Control Summary for overall QC performance data and associated samples.

Laboratory Sample Analysis Record

CAT No.	Analysis Name	Method	Trial#	Batch#	Analysis Date and Time	Analyst	Dilution Factor
10242	Alkyl PAHs in Soil by GC/MS	SW-846 8270C SIM	1	14120SLA026	05/06/2014 16:55	Joseph M Gambler	10
10481	Alkyl PAH Microwave Soils	SW-846 3546	1	14120SLA026	05/01/2014 10:00	David S Schrum	1
12989	Custom TPH-GRO soil C5-C12	SW-846 8015B modified	1	14119A16A	04/29/2014 21:00	Marie D Beamenderfer	5181.35
01150	GC - Bulk Soil Prep	SW-846 5035A Modified	1	201411534329	04/25/2014 20:56	Scott W Freisher	n.a.
07062	TPH-CWG	MA DEP EPH 5/04	1	14119O023A	05/02/2014 16:49	Heather E Williams	2
07062	TPH-CWG	MA DEP EPH 5/04	1	14119O023A	05/02/2014 17:29	Heather E Williams	5
02729	Custom TPH with Ranges (soil)	SW-846 8015B	1	141160014A	04/28/2014 19:58	Heather E Williams	100
11235	LA EPH Soils Extraction	SW-846 3546	1	14119O023A	04/30/2014 06:20	Roman Kuropatkin	1
11219	Custom TPH w/Ranges Ext (S)	SW-846 3550C	1	141160014A	04/28/2014 10:00	Katheryne V Sponheimer	1
00497	Silica Gel Fractionation	SW-846 3630C modified	1	14119O023A	04/30/2014 16:30	Edwin Ortiz	1
00111	Moisture	SM 2540 G-1997	1	14115820003B	04/25/2014 18:50	Scott W Freisher	1

*=This limit was used in the evaluation of the final result

Sample Description: GSC1AOS-1-041714 1700 14-0016-02 Soil
HHSRG

LL Sample # SW 7441137
LL Group # 1469535
Account # 10863

Project Name: HHSRG

Collected: 04/22/2014 10:40

Submitted: 04/24/2014 09:30
Reported: 05/13/2014 12:54

Chevron Energy Technology Co.
100 Chevron Way
50-1263
Richmond CA 94802

HHSR2

CAT No.	Analysis Name	CAS Number	Dry Result		Dry Method Detection Limit*	Dry Limit of Quantitation	Dilution Factor
GC/MS	Semivolatiles SW-846 8270C SIM		ug/kg		ug/kg	ug/kg	
10242	17a(H)-diahopane	n.a.	870		20	500	10
10242	A1-C20TAS	n.a.	3,400		20	500	10
10242	A2-C21TAS	n.a.	3,600		20	500	10
10242	A3-C26TAS(20S)	n.a.	11,000		20	500	10
10242	A4-C26/C27TAS	n.a.	42,000		20	500	10
10242	A5-C27TAS(20R)	n.a.	27,000		20	500	10
10242	A6-TAS(20S)	n.a.	9,600		20	500	10
10242	A7-TAS(20R)	n.a.	10,000		20	500	10
10242	Acenaphthene	83-32-9	N.D.		200	500	10
10242	Acenaphthylene	208-96-8	N.D.		200	500	10
10242	Anthracene	120-12-7	N.D.		200	500	10
10242	Benzo(a)anthracene	56-55-3	400	J	200	500	10
10242	Benzo(a)pyrene	50-32-8	N.D.		200	500	10
10242	Benzo(b)fluoranthene	205-99-2	350	J	200	500	10
10242	Benzo(e)pyrene	192-97-2	530		200	500	10
10242	Benzo(g,h,i)perylene	191-24-2	320	J	200	500	10
10242	Benzo(k)fluoranthene	207-08-9	N.D.		200	500	10
10242	C1-Benzanthrene/chrysenes	n.a.	2,500		200	500	10
10242	C1-Dibenzothiophene	n.a.	14,000		200	500	10
10242	C1-Fluoranthrenes/pyrenes	n.a.	4,200		200	500	10
10242	C1-Fluorenes	n.a.	1,700		200	500	10
10242	C1-Naphthalenes	n.a.	1,600		200	500	10
10242	C1-Phenanthrenes/anthracenes	n.a.	7,600		200	500	10
10242	C2-Benzanthrene/chrysenes	n.a.	7,500		200	500	10
10242	C2-Dibenzothiophene	n.a.	33,000		200	500	10
10242	C2-Fluoranthrenes/pyrenes	n.a.	5,000		200	500	10
10242	C2-Fluorenes	n.a.	6,200		200	500	10
10242	C2-Naphthalenes	n.a.	7,600		200	500	10
10242	C2-Phenanthrenes/anthracenes	n.a.	17,000		200	500	10
10242	C3-Benzanthrene/chrysenes	n.a.	3,800		200	500	10
10242	C3-Dibenzothiophene	n.a.	41,000		200	500	10
10242	C3-Fluoranthrenes/pyrenes	n.a.	6,600		200	500	10
10242	C3-Fluorenes	n.a.	14,000		200	500	10
10242	C3-Naphthalenes	n.a.	24,000		200	500	10
10242	C3-Phenanthrenes/anthracenes	n.a.	15,000		200	500	10
10242	C4-Benzanthrene/chrysenes	n.a.	4,500		200	500	10
10242	C4-Dibenzothiophene	n.a.	19,000		200	500	10
10242	C4-Fluoranthrenes/pyrenes	n.a.	7,400		200	500	10
10242	C4-Naphthalenes	n.a.	28,000		200	500	10
10242	C4-Phenanthrenes/anthracenes	n.a.	10,000		200	500	10
10242	Cholestane	n.a.	44,000		20	500	10
10242	Chrysene	218-01-9	1,400		200	500	10
10242	Dibenz(a,h)anthracene	53-70-3	N.D.		200	500	10
10242	Dibenzothiophene	132-65-0	4,100		200	500	10
10242	Fluoranthene	206-44-0	340	J	200	500	10
10242	Fluorene	86-73-7	240	J	200	500	10
10242	Indeno(1,2,3-cd)pyrene	193-39-5	N.D.		200	500	10
10242	Naphthalene	91-20-3	N.D.		200	500	10
10242	Perylene	198-55-0	2,500		200	500	10
10242	Phenanthrene	85-01-8	1,500		200	500	10
10242	Pyrene	129-00-0	1,100		200	500	10

*=This limit was used in the evaluation of the final result

Sample Description: GSC1AOS-1-041714 1700 14-0016-02 Soil
HHSRG

LL Sample # SW 7441137
LL Group # 1469535
Account # 10863

Project Name: HHSRG

Collected: 04/22/2014 10:40

Submitted: 04/24/2014 09:30
Reported: 05/13/2014 12:54

Chevron Energy Technology Co.
100 Chevron Way
50-1263
Richmond CA 94802

HHSR2

CAT No.	Analysis Name	CAS Number	Dry Result		Dry Method Detection Limit*	Dry Limit of Quantitation	Dilution Factor
GC/MS Semivolatiles	SW-846 8270C SIM		ug/kg		ug/kg	ug/kg	
10242	S10-Methyldiacholestane	n.a.	N.D.		20	500	10
10242	S11-Methyldiacholestane	n.a.	6,500		20	500	10
10242	S12-Cholestane	n.a.	24,000		20	500	10
10242	S14-Cholestane(20R)	n.a.	31,000		20	500	10
10242	S15-Cholestane(20S)	n.a.	27,000		20	500	10
10242	S18-Ethyldiacholestane	n.a.	4,500		20	500	10
10242	S19-Ethyldiacholestane	n.a.	N.D.		20	500	10
10242	S20-Methylcholestane	n.a.	22,000		20	500	10
10242	S22-Methylcholestane(20R)	n.a.	32,000		20	500	10
10242	S23-Methylcholestane(20S)	n.a.	8,000		20	500	10
10242	S24-MethylCholestane	n.a.	31,000		20	500	10
10242	S25-EthylCholestane	n.a.	18,000		20	500	10
10242	S26-Ethylcholestane(20R)	n.a.	23,000		20	500	10
10242	S27-Ethylcholestane(20S)	n.a.	19,000		20	500	10
10242	S28-Ethylcholestane	n.a.	27,000		20	500	10
10242	S4-Diacholestane	n.a.	9,000		20	500	10
10242	S5-Diacholestane	n.a.	2,000		20	500	10
10242	S6-Diacholestane	n.a.	N.D.		20	500	10
10242	S7-Diacholestane	n.a.	2,000		20	500	10
10242	S8-Methyldiacholestane	n.a.	9,900		20	500	10
10242	T10-C29Tricyclictriterpane(R)	n.a.	4,700		20	500	10
10242	T11-Trisnorhopane(TS)	n.a.	1,100		20	500	10
10242	T12-Trisnorhopane(TM)	n.a.	5,000		20	500	10
10242	T13a-29,30-Bisnorhopane	n.a.	N.D.		20	500	10
10242	T13-Trisnorhopane	n.a.	1,300		20	500	10
10242	T14a-C28,C30Bisnorhopane	n.a.	1,900		20	500	10
10242	T14b-C29,C25Norhopane	n.a.	N.D.		20	500	10
10242	T14-Bisnorhopane	n.a.	N.D.		20	500	10
10242	T15-C29Norhopane	n.a.	16,000		20	500	10
10242	T16-Norneohopane	n.a.	2,000		20	500	10
10242	T17-C30 Normoretane	n.a.	1,800		20	500	10
10242	T18-C30 Oleanane	n.a.	2,500		20	500	10
10242	T19-C30 Hopane	n.a.	26,000		20	500	10
10242	T20-Moretane	n.a.	3,200		20	500	10
10242	T21-C31 Homohopane(S)	n.a.	11,000		20	500	10
10242	T22a-Gammacerane	559-65-9	N.D.		20	500	10
10242	T22-C31 Homohopane(R)	n.a.	12,000		20	500	10
10242	T23-Homohopane	471-62-5	9,300		20	500	10
10242	T24-Homomoretane	n.a.	1,500		20	500	10
10242	T25-Diploptene	n.a.	360	J	20	500	10
10242	T26-C32-Bishomohopane(S)	n.a.	9,300		20	500	10
10242	T27-C32-Bishomohopane(R)	n.a.	7,400		20	500	10
10242	T28-Bishomomoretane	n.a.	1,200		20	500	10
10242	T29-Homohopane	n.a.	3,100		20	500	10
10242	T30-C33-Trishomohopane(S)	n.a.	8,100		20	500	10
10242	T31-C33-Trishomohopane(R)	n.a.	5,300		20	500	10
10242	T32-Tetrakishomohopane(S)	n.a.	4,800		20	500	10
10242	T33-Tetrakishomohopane(R)	n.a.	3,900		20	500	10
10242	T34-Pentakishomohopane(S)	n.a.	11,000		20	500	10
10242	T35-Pentakishomohopane(R)	n.a.	11,000		20	500	10
10242	T4-C23 Diterpane	n.a.	13,000		20	500	10

*=This limit was used in the evaluation of the final result

Sample Description: GSC1AOS-1-041714 1700 14-0016-02 Soil
HHSRG

LL Sample # SW 7441137
LL Group # 1469535
Account # 10863

Project Name: HHSRG

Collected: 04/22/2014 10:40

Submitted: 04/24/2014 09:30
Reported: 05/13/2014 12:54

Chevron Energy Technology Co.
100 Chevron Way
50-1263
Richmond CA 94802

HHSR2

CAT No.	Analysis Name	CAS Number	Dry Result		Dry Method Detection Limit*	Dry Limit of Quantitation	Dilution Factor
GC/MS Semivolatiles	**SW-846 8270C SIM**		**ug/kg**		**ug/kg**	**ug/kg**	
10242	T5-C24Diterpane	n.a.	8,100		20	500	10
10242	T6a-C24TetracyclicTerpane	n.a.	N.D.		20	500	10
10242	T6b-C26Tricyclic[S]	n.a.	2,700		20	500	10
10242	T6-C25Diterpane	n.a.	8,000		20	500	10
10242	T6c-C26Tricyclic[R]	n.a.	3,300		20	500	10
10242	T7-C28Tricyclictriterpane[S]	n.a.	3,300		20	500	10
10242	T8-C28Tricyclictriterpane[R]	n.a.	4,200		20	500	10
10242	T9-C29 Tricyclictriterpane(S)	n.a.	4,600		20	500	10

Reporting limits were raised due to interference from the sample matrix.

The LCS and/or LCSD recoveries are outside the stated QC window but within the marginal exceedance allowance of +/- 4 standard deviations as defined in the NELAC Standards. The following analytes are accepted based on this allowance:
chrysene

GC Volatiles	**SW-846 8015B modified**		**mg/kg**		**mg/kg**	**mg/kg**	
12989	C10-C12	n.a.	160	J	41	210	5107.25
12989	C5-C6	n.a.	N.D.		41	210	5107.25
12989	C6-C8	n.a.	N.D.		41	210	5107.25
12989	C8-C10	n.a.	N.D.		41	210	5107.25
12989	Total GRO (C5-C12)	n.a.	200	J	41	210	5107.25

Reporting limits were raised due to sample foaming.

GC Petroleum Hydrocarbons	**MA DEP EPH 5/04**		**mg/kg**		**mg/kg**	**mg/kg**	
07062	Aliphatics >C10 - C12	n.a.	N.D.		6,000	6,000	5
07062	Aliphatics >C12 - C16	n.a.	N.D.		6,000	6,000	5
07062	Aliphatics >C16 - C35	n.a.	44,000		6,000	6,000	5
07062	Aromatics >C10 - C12	n.a.	N.D.		2,400	2,400	2
07062	Aromatics >C12 - C16	n.a.	N.D.		2,400	2,400	2
07062	Aromatics >C16 - C21	n.a.	7,400		2,400	2,400	2
07062	Aromatics >C21 - C35	n.a.	27,000		2,400	2,400	2

GC Petroleum Hydrocarbons	**SW-846 8015B**		**mg/kg**		**mg/kg**	**mg/kg**	
02729	>C12-C14	n.a.	N.D.		2,000	6,000	50
02729	>C14-C16	n.a.	2,100	J	2,000	6,000	50
02729	>C16-C18	n.a.	4,400	J	2,000	6,000	50
02729	>C18-C20	n.a.	6,400		2,000	6,000	50
02729	>C20-C22	n.a.	9,100		2,000	6,000	50
02729	>C22-C24	n.a.	5,800	J	2,000	6,000	50
02729	>C24-C26	n.a.	7,000		2,000	6,000	50
02729	>C26-C28	n.a.	9,700		2,000	6,000	50
02729	>C28-C30	n.a.	8,500		2,000	6,000	50
02729	>C30-C32	n.a.	7,200		2,000	6,000	50
02729	>C32-C34	n.a.	8,200		2,000	6,000	50
02729	>C34-C36	n.a.	6,400		2,000	6,000	50
02729	>C36-C38	n.a.	9,500		2,000	6,000	50

*=This limit was used in the evaluation of the final result

Sample Description: GSC1AOS-1-041714 1700 14-0016-02 Soil
HHSRG

LL Sample # SW 7441137
LL Group # 1469535
Account # 10863

Project Name: HHSRG

Collected: 04/22/2014 10:40

Submitted: 04/24/2014 09:30
Reported: 05/13/2014 12:54

Chevron Energy Technology Co.
100 Chevron Way
50-1263
Richmond CA 94802

HHSR2

CAT No.	Analysis Name	CAS Number	Dry Result	Dry Method Detection Limit*	Dry Limit of Quantitation	Dilution Factor
GC Petroleum Hydrocarbons	**SW-846 8015B**		**mg/kg**	**mg/kg**	**mg/kg**	
02729	>C38-C40	n.a.	6,400	2,000	6,000	50
02729	DRO >C12-C22	n.a.	23,000	2,000	6,000	50
02729	ORO >C22-C40	n.a.	69,000	2,000	6,000	50
02729	Total TPH	n.a.	91,000	2,000	6,000	50
Wet Chemistry	**SM 2540 G-1997**		**%**	**%**	**%**	
00111	Moisture	n.a.	0.81	0.50	0.50	1

Moisture represents the loss in weight of the sample after oven drying at 103 - 105 degrees Celsius. The moisture result reported is on an as-received basis.

General Sample Comments

CA ELAP Lab Certification No. 2792; CA NELAP Lab Certification No. 10276CA

All QC is compliant unless otherwise noted. Please refer to the Quality Control Summary for overall QC performance data and associated samples.

Laboratory Sample Analysis Record

CAT No.	Analysis Name	Method	Trial#	Batch#	Analysis Date and Time	Analyst	Dilution Factor
10242	Alkyl PAHs in Soil by GC/MS	SW-846 8270C SIM	1	14120SLA026	05/07/2014 05:56	Joseph M Gambler	10
10481	Alkyl PAH Microwave Soils	SW-846 3546	1	14120SLA026	05/01/2014 10:00	David S Schrum	1
12989	Custom TPH-GRO soil C5-C12	SW-846 8015B modified	1	14118A16A	04/29/2014 06:19	Laura M Krieger	5107.25
01150	GC - Bulk Soil Prep	SW-846 5035A Modified	1	201411534329	04/25/2014 20:58	Scott W Freisher	n.a.
07062	TPH-CWG	MA DEP EPH 5/04	1	14119002 3A	05/02/2014 19:29	Heather E Williams	2
07062	TPH-CWG	MA DEP EPH 5/04	1	14119002 3A	05/02/2014 20:09	Heather E Williams	5
02729	Custom TPH with Ranges (soil)	SW-846 8015B	1	141160014A	04/29/2014 20:39	Heather E Williams	50
11235	LA EPH Soils Extraction	SW-846 3546	1	14119002 3A	04/30/2014 06:20	Roman Kuropatkin	1
11219	Custom TPH w/Ranges Ext (S)	SW-846 3550C	1	141160014A	04/28/2014 10:00	Katheryne V Sponheimer	1
00497	Silica Gel Fractionation	SW-846 3630C modified	1	14119002 3A	04/30/2014 16:30	Edwin Ortiz	1
00111	Moisture	SM 2540 G-1997	1	14115820003B	04/25/2014 18:50	Scott W Freisher	1

*=This limit was used in the evaluation of the final result

Sample Description: BM1-1-06042014 Composite Soil Sample
Chevron HHSRG

LL Sample # SW 7488435
LL Group # 1479651
Account # 14783

Project Name: Chevron HHSRG

Collected: 06/04/2014 10:00 by PD

Submitted: 06/05/2014 09:15
Reported: 06/19/2014 16:09

Arizona State University
PO Box 875912
Tempe AZ 85287-5912

BM1-1

CAT No.	Analysis Name	CAS Number	As Received Result	As Received Method Detection Limit*	As Received Limit of Quantitation	Dilution Factor
GC Volatiles	**SW-846 8015B modified**		**mg/kg**	**mg/kg**	**mg/kg**	
12989	C10-C12	n.a.	270	3.8	19	478.01
12989	C5-C6	n.a.	N.D.	3.8	19	478.01
12989	C6-C8	n.a.	30	3.8	19	478.01
12989	C8-C10	n.a.	110	3.8	19	478.01
12989	Total GRO (C5-C12)	n.a.	410	3.8	19	478.01
GC Petroleum Hydrocarbons	**MA DEP EPH 5/04**		**mg/kg**	**mg/kg**	**mg/kg**	
07062	Aliphatics >C10 - C12	n.a.	460	300	300	25
07062	Aliphatics >C12 - C16	n.a.	1,800	300	300	25
07062	Aliphatics >C16 - C35	n.a.	6,800	300	300	25
07062	Aromatics >C10 - C12	n.a.	N.D.	120	120	10
07062	Aromatics >C12 - C16	n.a.	500	120	120	10
07062	Aromatics >C16 - C21	n.a.	840	120	120	10
07062	Aromatics >C21 - C35	n.a.	1,700	120	120	10
GC Petroleum Hydrocarbons	**SW-846 8015B**		**mg/kg**	**mg/kg**	**mg/kg**	
02729	>C12-C14	n.a.	1,100	120	360	10
02729	>C14-C16	n.a.	1,500	120	360	10
02729	>C16-C18	n.a.	1,500	120	360	10
02729	>C18-C20	n.a.	1,500	120	360	10
02729	>C20-C22	n.a.	1,200	120	360	10
02729	>C22-C24	n.a.	1,300	120	360	10
02729	>C24-C26	n.a.	1,200	120	360	10
02729	>C26-C28	n.a.	1,100	120	360	10
02729	>C28-C30	n.a.	1,100	120	360	10
02729	>C30-C32	n.a.	1,000	120	360	10
02729	>C32-C34	n.a.	890	120	360	10
02729	>C34-C36	n.a.	790	120	360	10
02729	>C36-C38	n.a.	790	120	360	10
02729	>C38-C40	n.a.	830	120	360	10
02729	DRO >C12-C22	n.a.	6,900	120	360	10
02729	ORO >C22-C40	n.a.	9,000	120	360	10
02729	Total TPH	n.a.	16,000	120	360	10
Wet Chemistry	**SM 2540 G-1997**		**%**	**%**	**%**	
00111	Moisture	n.a.	18.4	0.50	0.50	1

Moisture represents the loss in weight of the sample after oven drying at 103 - 105 degrees Celsius. The moisture result reported is on an as-received basis.

*=This limit was used in the evaluation of the final result

Sample Description: GSI14RD Treated 720kGy Solid

Project Name: Chevron

LL Sample # SW 7591210
LL Group # 1501656
Account # 19947

Collected: 08/22/2014

Submitted: 09/08/2014 12:50
Reported: 09/19/2014 12:08

Texas A & M University
Mechanical Engineering
3123 TAMU
College Station TX 77843

I14RD

CAT No.	Analysis Name	CAS Number	Dry Result		Dry Method Detection Limit	Dilution Factor
GC Volatiles	**SW-846 8015B modified**		**mg/kg**		**mg/kg**	
12989	C10-C12	n.a.	100		4.2	520.29
12989	C5-C6	n.a.	26		4.2	520.29
12989	C6-C8	n.a.	45		4.2	520.29
12989	C8-C10	n.a.	97		4.2	520.29
12989	Total GRO (C5-C12)	n.a.	270		4.2	520.29
GC Petroleum Hydrocarbons	**MA DEP EPH 5/04**		**mg/kg**		**mg/kg**	
07062	Aliphatics >C10 - C12	n.a.	N.D.		120	10
07062	Aliphatics >C12 - C16	n.a.	260		120	10
07062	Aliphatics >C16 - C35	n.a.	3,100		120	10
07062	Aromatics >C10 - C12	n.a.	N.D.		120	10
07062	Aromatics >C12 - C16	n.a.	210		120	10
07062	Aromatics >C16 - C21	n.a.	1,000		120	10
07062	Aromatics >C21 - C35	n.a.	2,400		120	10
	The holding time was not met. The sample was submitted to the laboratory outside of the holding time.					
GC Petroleum Hydrocarbons	**SW-846 8015B**		**mg/kg**		**mg/kg**	
02729	>C12-C14	n.a.	280		80	20
02729	>C14-C16	n.a.	500		80	20
02729	>C16-C18	n.a.	1,000		80	20
02729	>C18-C20	n.a.	1,400		80	20
02729	>C20-C22	n.a.	1,300		80	20
02729	>C22-C24	n.a.	1,600		80	20
02729	>C24-C26	n.a.	800		80	20
02729	>C26-C28	n.a.	870		80	20
02729	>C28-C30	n.a.	1,300		80	20
02729	>C30-C32	n.a.	680		80	20
02729	>C32-C34	n.a.	800		80	20
02729	>C34-C36	n.a.	750		80	20
02729	>C36-C38	n.a.	750		80	20
02729	>C38-C40	n.a.	220	J	80	20
02729	DRO >C12-C22	n.a.	4,600		80	20
02729	ORO >C22-C40	n.a.	7,800		80	20
02729	Total TPH	n.a.	12,000		80	20
	The holding time was not met. The sample was submitted to the laboratory outside of the holding time.					
Wet Chemistry	**SM 2540 G-1997**		**%**		**%**	
00111	Moisture	n.a.	0.52		0.50	1
	Moisture represents the loss in weight of the sample after oven drying at 103 - 105 degrees Celsius. The moisture result reported is on an as-received basis.					

Sample Description: Benchmark 1 Treated 960kGy Solid

Project Name: Chevron

LL Sample # SW 7591211
LL Group # 1501656
Account # 19947

Collected: 08/22/2014

Submitted: 09/08/2014 12:50
Reported: 09/19/2014 12:08

Texas A & M University
Mechanical Engineering
3123 TAMU
College Station TX 77843

BNHMK

CAT No.	Analysis Name	CAS Number	Dry Result		Dry Method Detection Limit	Dilution Factor
GC Volatiles	**SW-846 8015B modified**		**mg/kg**		**mg/kg**	
12989	C10-C12	n.a.	27		3.8	480.77
12989	C5-C6	n.a.	N.D.		3.8	480.77
12989	C6-C8	n.a.	11	J	3.8	480.77
12989	C8-C10	n.a.	17	J	3.8	480.77
12989	Total GRO (C5-C12)	n.a.	57		3.8	480.77
GC Petroleum Hydrocarbons	**MA DEP EPH 5/04**		**mg/kg**		**mg/kg**	
07062	Aliphatics >C10 - C12	n.a.	N.D.		60	5
07062	Aliphatics >C12 - C16	n.a.	N.D.		60	5
07062	Aliphatics >C16 - C35	n.a.	650		60	5
07062	Aromatics >C10 - C12	n.a.	N.D.		12	1
07062	Aromatics >C12 - C16	n.a.	15		12	1
07062	Aromatics >C16 - C21	n.a.	51		12	1
07062	Aromatics >C21 - C35	n.a.	250		12	1
	The holding time was not met. The sample was submitted to the laboratory outside of the holding time.					
GC Petroleum Hydrocarbons	**SW-846 8015B**		**mg/kg**		**mg/kg**	
02729	>C12-C14	n.a.	N.D.		40	10
02729	>C14-C16	n.a.	N.D.		40	10
02729	>C16-C18	n.a.	54	J	40	10
02729	>C18-C20	n.a.	74	J	40	10
02729	>C20-C22	n.a.	91	J	40	10
02729	>C22-C24	n.a.	100	J	40	10
02729	>C24-C26	n.a.	120		40	10
02729	>C26-C28	n.a.	130		40	10
02729	>C28-C30	n.a.	160		40	10
02729	>C30-C32	n.a.	160		40	10
02729	>C32-C34	n.a.	210		40	10
02729	>C34-C36	n.a.	170		40	10
02729	>C36-C38	n.a.	170		40	10
02729	>C38-C40	n.a.	210		40	10
02729	DRO >C12-C22	n.a.	260		40	10
02729	ORO >C22-C40	n.a.	1,400		40	10
02729	Total TPH	n.a.	1,700		40	10
	The holding time was not met. The sample was submitted to the laboratory outside of the holding time.					
Wet Chemistry	**SM 2540 G-1997**		**%**		**%**	
00111	Moisture	n.a.	N.D.		0.50	1
	Moisture represents the loss in weight of the sample after oven drying at 103 - 105 degrees Celsius. The moisture result reported is on an as-received basis.					

Sample Description: GSC1AOS Treated 720kGy Solid

Project Name: Chevron

LL Sample # SW 7591212
LL Group # 1501656
Account # 19947

Collected: 08/22/2014

Submitted: 09/08/2014 12:50
Reported: 09/19/2014 12:08

Texas A & M University
Mechanical Engineering
3123 TAMU
College Station TX 77843

C1AOS

CAT No.	Analysis Name	CAS Number	Dry Result		Dry Method Detection Limit	Dilution Factor
GC Volatiles	**SW-846 8015B modified**		**mg/kg**		**mg/kg**	
12989	C10-C12	n.a.	250		3.8	471.7
12989	C5-C6	n.a.	13	J	3.8	471.7
12989	C6-C8	n.a.	44		3.8	471.7
12989	C8-C10	n.a.	200		3.8	471.7
12989	Total GRO (C5-C12)	n.a.	500		3.8	471.7
GC Petroleum Hydrocarbons	**MA DEP EPH 5/04**		**mg/kg**		**mg/kg**	
07062	Aliphatics >C10 - C12	n.a.	N.D.		580	5
07062	Aliphatics >C12 - C16	n.a.	730		580	5
07062	Aliphatics >C16 - C35	n.a.	5,200		580	5
07062	Aromatics >C10 - C12	n.a.	N.D.		580	5
07062	Aromatics >C12 - C16	n.a.	720		580	5
07062	Aromatics >C16 - C21	n.a.	2,300		580	5
07062	Aromatics >C21 - C35	n.a.	5,700		580	5
	The holding time was not met. The sample was submitted to the laboratory outside of the holding time.					
GC Petroleum Hydrocarbons	**SW-846 8015B**		**mg/kg**		**mg/kg**	
02729	>C12-C14	n.a.	790		200	50
02729	>C14-C16	n.a.	1,100		200	50
02729	>C16-C18	n.a.	1,600		200	50
02729	>C18-C20	n.a.	2,300		200	50
02729	>C20-C22	n.a.	2,000		200	50
02729	>C22-C24	n.a.	2,200		200	50
02729	>C24-C26	n.a.	1,800		200	50
02729	>C26-C28	n.a.	2,000		200	50
02729	>C28-C30	n.a.	1,800		200	50
02729	>C30-C32	n.a.	1,900		200	50
02729	>C32-C34	n.a.	1,300		200	50
02729	>C34-C36	n.a.	1,700		200	50
02729	>C36-C38	n.a.	1,500		200	50
02729	>C38-C40	n.a.	640		200	50
02729	DRO >C12-C22	n.a.	7,700		200	50
02729	ORO >C22-C40	n.a.	15,000		200	50
02729	Total TPH	n.a.	23,000		200	50
	The holding time was not met. The sample was submitted to the laboratory outside of the holding time.					
Wet Chemistry	**SM 2540 G-1997**		**%**		**%**	
00111	Moisture	n.a.	0.75		0.50	1
	Moisture represents the loss in weight of the sample after oven drying at 103 - 105 degrees Celsius. The moisture result reported is on an as-received basis.					

Sample Description: BM2-1-09172014 Composite Soil Sample
Chevron HHSRG

LL Sample # SW 7608418
LL Group # 1505076
Account # 14783

Project Name: Chevron HHSRG

Collected: 09/17/2014 18:00 by PD

Submitted: 09/22/2014 09:05
Reported: 10/06/2014 12:11

Arizona State University
PO Box 875912
Tempe AZ 85287-5912

BM2-1

CAT No.	Analysis Name	CAS Number	As Received Result		As Received Method Detection Limit*	As Received Limit of Quantitation	Dilution Factor
GC Volatiles	**SW-846 8015B modified**		**mg/kg**		**mg/kg**	**mg/kg**	
12989	C10-C12	n.a.	150		3.9	20	489.24
12989	C5-C6	n.a.	N.D.		3.9	20	489.24
12989	C6-C8	n.a.	N.D.		3.9	20	489.24
12989	C8-C10	n.a.	14	J	3.9	20	489.24
12989	Total GRO (C5-C12)	n.a.	170		3.9	20	489.24
GC Petroleum Hydrocarbons	**MA DEP EPH 5/04**		**mg/kg**		**mg/kg**	**mg/kg**	
07062	Aliphatics >C10 - C12	n.a.	N.D.		580	580	5
07062	Aliphatics >C12 - C16	n.a.	1,200		580	580	5
07062	Aliphatics >C16 - C35	n.a.	5,700		580	580	5
07062	Aromatics >C10 - C12	n.a.	N.D.		120	120	1
07062	Aromatics >C12 - C16	n.a.	460		120	120	1
07062	Aromatics >C16 - C21	n.a.	1,200		120	120	1
07062	Aromatics >C21 - C35	n.a.	2,900		120	120	1
GC Petroleum Hydrocarbons	**SW-846 8015B**		**mg/kg**		**mg/kg**	**mg/kg**	
02729	>C12-C14	n.a.	930		100	300	25
02729	>C14-C16	n.a.	1,500		100	300	25
02729	>C16-C18	n.a.	1,900		100	300	25
02729	>C18-C20	n.a.	2,000		100	300	25
02729	>C20-C22	n.a.	2,000		100	300	25
02729	>C22-C24	n.a.	1,700		100	300	25
02729	>C24-C26	n.a.	1,600		100	300	25
02729	>C26-C28	n.a.	1,500		100	300	25
02729	>C28-C30	n.a.	1,600		100	300	25
02729	>C30-C32	n.a.	1,400		100	300	25
02729	>C32-C34	n.a.	1,300		100	300	25
02729	>C34-C36	n.a.	1,200		100	300	25
02729	>C36-C38	n.a.	1,100		100	300	25
02729	>C38-C40	n.a.	1,000		100	300	25
02729	DRO >C12-C22	n.a.	8,300		100	300	25
02729	ORO >C22-C40	n.a.	12,000		100	300	25
02729	Total TPH	n.a.	21,000		100	300	25
Wet Chemistry	**SM 2540 G-1997**		**%**		**%**	**%**	
00111	Moisture	n.a.	2.1		0.50	0.50	1

Moisture represents the loss in weight of the sample after oven drying at 103 - 105 degrees Celsius. The moisture result reported is on an as-received basis.

General Sample Comments

All QC is compliant unless otherwise noted. Please refer to the Quality Control Summary for overall QC performance data and associated samples.

*=This limit was used in the evaluation of the final result

Sample Description: BM1-1 Soil Sample
Treated 480 kGy

LL Sample # SW 7656281
LL Group # 1514922
Account # 19947

Project Name: Chevron

Collected: n.a.

Submitted: 10/30/2014 10:30
Reported: 11/11/2014 14:32

Texas A & M University
Mechanical Engineering
3123 TAMU
College Station TX 77843

CBM11

CAT No.	Analysis Name	CAS Number	Dry Result		Dry Method Detection Limit	Dilution Factor
GC Volatiles	**SW-846 8015B modified**		**mg/kg**		**mg/kg**	
12989	C10-C12	n.a.	44		0.81	100.1
12989	C5-C6	n.a.	N.D.		0.81	100.1
12989	C6-C8	n.a.	1.0	J	0.81	100.1
12989	C8-C10	n.a.	35		0.81	100.1
12989	Total GRO (C5-C12)	n.a.	80		0.81	100.1
GC Petroleum Hydrocarbons	**MA DEP EPH 5/04**		**mg/kg**		**mg/kg**	
07062	Aliphatics >C10 - C12	n.a.	N.D.		240	20
07062	Aliphatics >C12 - C16	n.a.	290		240	20
07062	Aliphatics >C16 - C35	n.a.	4,400		240	20
07062	Aromatics >C10 - C12	n.a.	N.D.		120	10
07062	Aromatics >C12 - C16	n.a.	N.D.		120	10
07062	Aromatics >C16 - C21	n.a.	450		120	10
07062	Aromatics >C21 - C35	n.a.	1,500		120	10
GC Petroleum Hydrocarbons	**SW-846 8015B**		**mg/kg**		**mg/kg**	
02729	>C12-C14	n.a.	N.D.		150	20
02729	>C14-C16	n.a.	390	J	150	20
02729	>C16-C18	n.a.	720		150	20
02729	>C18-C20	n.a.	950		150	20
02729	>C20-C22	n.a.	1,100		150	20
02729	>C22-C24	n.a.	1,100		150	20
02729	>C24-C26	n.a.	990		150	20
02729	>C26-C28	n.a.	1,100		150	20
02729	>C28-C30	n.a.	1,000		150	20
02729	>C30-C32	n.a.	870		150	20
02729	>C32-C34	n.a.	1,100		150	20
02729	>C34-C36	n.a.	740		150	20
02729	>C36-C38	n.a.	670		150	20
02729	>C38-C40	n.a.	650		150	20
02729	DRO >C12-C22	n.a.	3,300		150	20
02729	ORO >C22-C40	n.a.	8,300		150	20
02729	Total TPH	n.a.	12,000		150	20
Wet Chemistry	**SM 2540 G-1997**		**%**		**%**	
00111	Moisture	n.a.	0.57		0.50	1

Moisture represents the loss in weight of the sample after oven drying at 103 - 105 degrees Celsius. The moisture result reported is on an as-received basis.

General Sample Comments

State of Texas Lab Certification No. T104704194-13-10

All QC is compliant unless otherwise noted. Please refer to the Quality Control Summary for overall QC performance data and associated samples.

Sample Description: BM2-2 Soil Sample
Treated 783 kGy

LL Sample # SW 7656283
LL Group # 1514922
Account # 19947

Project Name: Chevron

Collected: n.a.

Submitted: 10/30/2014 10:30
Reported: 11/11/2014 14:32

Texas A & M University
Mechanical Engineering
3123 TAMU
College Station TX 77843

CBM22

CAT No.	Analysis Name	CAS Number	Dry Result		Dry Method Detection Limit	Dilution Factor
GC Volatiles	**SW-846 8015B modified**		**mg/kg**		**mg/kg**	
12989	C10-C12	n.a.	180		4.1	503.52
12989	C5-C6	n.a.	4.6	J	4.1	503.52
12989	C6-C8	n.a.	30		4.1	503.52
12989	C8-C10	n.a.	150		4.1	503.52
12989	Total GRO (C5-C12)	n.a.	360		4.1	503.52
GC Petroleum Hydrocarbons	**MA DEP EPH 5/04**		**mg/kg**		**mg/kg**	
07062	Aliphatics >C10 - C12	n.a.	N.D.		59	5
07062	Aliphatics >C12 - C16	n.a.	180		59	5
07062	Aliphatics >C16 - C35	n.a.	1,100		59	5
07062	Aromatics >C10 - C12	n.a.	65		59	5
07062	Aromatics >C12 - C16	n.a.	210		59	5
07062	Aromatics >C16 - C21	n.a.	670		59	5
07062	Aromatics >C21 - C35	n.a.	1,200		59	5
GC Petroleum Hydrocarbons	**SW-846 8015B**		**mg/kg**		**mg/kg**	
02729	>C12-C14	n.a.	220		40	10
02729	>C14-C16	n.a.	320		40	10
02729	>C16-C18	n.a.	440		40	10
02729	>C18-C20	n.a.	480		40	10
02729	>C20-C22	n.a.	500		40	10
02729	>C22-C24	n.a.	440		40	10
02729	>C24-C26	n.a.	420		40	10
02729	>C26-C28	n.a.	360		40	10
02729	>C28-C30	n.a.	330		40	10
02729	>C30-C32	n.a.	300		40	10
02729	>C32-C34	n.a.	280		40	10
02729	>C34-C36	n.a.	340		40	10
02729	>C36-C38	n.a.	280		40	10
02729	>C38-C40	n.a.	280		40	10
02729	DRO >C12-C22	n.a.	2,000		40	10
02729	ORO >C22-C40	n.a.	3,000		40	10
02729	Total TPH	n.a.	5,000		40	10
Wet Chemistry	**SM 2540 G-1997**		**%**		**%**	
00111	Moisture	n.a.	1.3		0.50	1

Moisture represents the loss in weight of the sample after oven drying at 103 - 105 degrees Celsius. The moisture result reported is on an as-received basis.

General Sample Comments

State of Texas Lab Certification No. T104704194-13-10

All QC is compliant unless otherwise noted. Please refer to the Quality Control Summary for overall QC performance data and associated samples.

Sample Description: GSC1AOS Treated 1000kGy Soil
Chevron

LL Sample # SW 7684755
LL Group # 1520439
Account # 19947

Project Name: Chevron

Collected: n.a.

Submitted: 11/21/2014 09:30
Reported: 11/26/2014 14:53

Texas A & M University
Mechanical Engineering
3123 TAMU
College Station TX 77843

GSC1A

CAT No.	Analysis Name	CAS Number	Dry Result		Dry Method Detection Limit	Dilution Factor
GC Volatiles	**SW-846 8015B modified**		**mg/kg**		**mg/kg**	
12989	C10-C12	n.a.	97		2.0	246.55
12989	C5-C6	n.a.	12		2.0	246.55
12989	C6-C8	n.a.	62		2.0	246.55
12989	C8-C10	n.a.	95		2.0	246.55
12989	Total GRO (C5-C12)	n.a.	270		2.0	246.55
	Reporting limits were raised due to sample foaming.					
GC Petroleum Hydrocarbons	**MA DEP EPH 5/04**		**mg/kg**		**mg/kg**	
07062	Aliphatics >C10 - C12	n.a.	N.D.		120	1
07062	Aliphatics >C12 - C16	n.a.	N.D.		120	1
07062	Aliphatics >C16 - C35	n.a.	280		120	1
07062	Aromatics >C10 - C12	n.a.	N.D.		120	1
07062	Aromatics >C12 - C16	n.a.	N.D.		120	1
07062	Aromatics >C16 - C21	n.a.	160		120	1
07062	Aromatics >C21 - C35	n.a.	470		120	1
GC Petroleum Hydrocarbons	**SW-846 8015B**		**mg/kg**		**mg/kg**	
02729	>C12-C14	n.a.	70	J	25	2
02729	>C14-C16	n.a.	75		25	2
02729	>C16-C18	n.a.	93		25	2
02729	>C18-C20	n.a.	100		25	2
02729	>C20-C22	n.a.	96		25	2
02729	>C22-C24	n.a.	100		25	2
02729	>C24-C26	n.a.	110		25	2
02729	>C26-C28	n.a.	120		25	2
02729	>C28-C30	n.a.	120		25	2
02729	>C30-C32	n.a.	120		25	2
02729	>C32-C34	n.a.	92		25	2
02729	>C34-C36	n.a.	140		25	2
02729	>C36-C38	n.a.	150		25	2
02729	>C38-C40	n.a.	130		25	2
02729	DRO >C12-C22	n.a.	440		25	2
02729	ORO >C22-C40	n.a.	1,100		25	2
02729	Total TPH	n.a.	1,500		25	2
Wet Chemistry	**SM 2540 G-1997**		**%**		**%**	
00111	Moisture	n.a.	N.D.		0.50	1
	Moisture represents the loss in weight of the sample after oven drying at 103 - 105 degrees Celsius. The moisture result reported is on an as-received basis.					

Sample Description: BM1 Treated 720 kGy with Ethanol additive Soil
Chevron

LL Sample # SW 7684756
LL Group # 1520439
Account # 19947

Project Name: Chevron

Collected: n.a.

Submitted: 11/21/2014 09:30
Reported: 11/26/2014 14:53

Texas A & M University
Mechanical Engineering
3123 TAMU
College Station TX 77843

ETHAN

CAT No.	Analysis Name	CAS Number	Dry Result		Dry Method Detection Limit	Dilution Factor
GC Volatiles	**SW-846 8015B modified**		**mg/kg**		**mg/kg**	
12989	C10-C12	n.a.	11		2.1	257.2
12989	C5-C6	n.a.	N.D.		2.1	257.2
12989	C6-C8	n.a.	N.D.		2.1	257.2
12989	C8-C10	n.a.	4.1	J	2.1	257.2
12989	Total GRO (C5-C12)	n.a.	18		2.1	257.2
	Reporting limits were raised due to sample foaming.					
GC Petroleum Hydrocarbons	**MA DEP EPH 5/04**		**mg/kg**		**mg/kg**	
07062	Aliphatics >C10 - C12	n.a.	N.D.		110	1
07062	Aliphatics >C12 - C16	n.a.	N.D.		110	1
07062	Aliphatics >C16 - C35	n.a.	1,900		110	1
07062	Aromatics >C10 - C12	n.a.	N.D.		110	1
07062	Aromatics >C12 - C16	n.a.	N.D.		110	1
07062	Aromatics >C16 - C21	n.a.	140		110	1
07062	Aromatics >C21 - C35	n.a.	1,300		110	1
	The recovery for the sample surrogate(s) is outside the QC acceptance limits as noted on the QC Summary. The client was contacted and the data reported.					
GC Petroleum Hydrocarbons	**SW-846 8015B**		**mg/kg**		**mg/kg**	
02729	>C12-C14	n.a.	N.D.		71	10
02729	>C14-C16	n.a.	N.D.		71	10
02729	>C16-C18	n.a.	N.D.		71	10
02729	>C18-C20	n.a.	150	J	71	10
02729	>C20-C22	n.a.	240		71	10
02729	>C22-C24	n.a.	320		71	10
02729	>C24-C26	n.a.	430		71	10
02729	>C26-C28	n.a.	520		71	10
02729	>C28-C30	n.a.	660		71	10
02729	>C30-C32	n.a.	630		71	10
02729	>C32-C34	n.a.	700		71	10
02729	>C34-C36	n.a.	810		71	10
02729	>C36-C38	n.a.	540		71	10
02729	>C38-C40	n.a.	740		71	10
02729	DRO >C12-C22	n.a.	470		71	10
02729	ORO >C22-C40	n.a.	5,400		71	10
02729	Total TPH	n.a.	5,800		71	10
Wet Chemistry	**SM 2540 G-1997**		**%**		**%**	
00111	Moisture	n.a.	N.D.		0.50	1
	Moisture represents the loss in weight of the sample after oven drying at 103 - 105 degrees Celsius. The moisture result reported is on an as-received basis.					

Sample Description: BM1 Treated 720 kGy with Citrus Oil additive Soil
Chevron

LL Sample # SW 7684757
LL Group # 1520439
Account # 19947

Project Name: Chevron

Collected: n.a.

Submitted: 11/21/2014 09:30
Reported: 11/26/2014 14:53

Texas A & M University
Mechanical Engineering
3123 TAMU
College Station TX 77843

CITRU

CAT No.	Analysis Name	CAS Number	Dry Result		Dry Method Detection Limit	Dilution Factor
GC Volatiles		**SW-846 8015B modified**	**mg/kg**		**mg/kg**	
12989	C10-C12	n.a.	310		4.1	509.68
12989	C5-C6	n.a.	N.D.		4.1	509.68
12989	C6-C8	n.a.	N.D.		4.1	509.68
12989	C8-C10	n.a.	13	J	4.1	509.68
12989	Total GRO (C5-C12)	n.a.	320		4.1	509.68
GC Petroleum Hydrocarbons		**MA DEP EPH 5/04**	**mg/kg**		**mg/kg**	
07062	Aliphatics >C10 - C12	n.a.	N.D.		120	1
07062	Aliphatics >C12 - C16	n.a.	N.D.		120	1
07062	Aliphatics >C16 - C35	n.a.	1,400		120	1
07062	Aromatics >C10 - C12	n.a.	N.D.		120	1
07062	Aromatics >C12 - C16	n.a.	N.D.		120	1
07062	Aromatics >C16 - C21	n.a.	N.D.		120	1
07062	Aromatics >C21 - C35	n.a.	1,100		120	1
	The recovery for the sample surrogate(s) is outside the QC acceptance limits as noted on the QC Summary. The client was contacted and the data reported.					
GC Petroleum Hydrocarbons		**SW-846 8015B**	**mg/kg**		**mg/kg**	
02729	>C12-C14	n.a.	N.D.		65	10
02729	>C14-C16	n.a.	N.D.		65	10
02729	>C16-C18	n.a.	N.D.		65	10
02729	>C18-C20	n.a.	N.D.		65	10
02729	>C20-C22	n.a.	94	J	65	10
02729	>C22-C24	n.a.	170	J	65	10
02729	>C24-C26	n.a.	190	J	65	10
02729	>C26-C28	n.a.	410		65	10
02729	>C28-C30	n.a.	470		65	10
02729	>C30-C32	n.a.	510		65	10
02729	>C32-C34	n.a.	500		65	10
02729	>C34-C36	n.a.	520		65	10
02729	>C36-C38	n.a.	780		65	10
02729	>C38-C40	n.a.	410		65	10
02729	DRO >C12-C22	n.a.	210		65	10
02729	ORO >C22-C40	n.a.	4,000		65	10
02729	Total TPH	n.a.	4,200		65	10
Wet Chemistry		**SM 2540 G-1997**	**%**		**%**	
00111	Moisture	n.a.	N.D.		0.50	1
	Moisture represents the loss in weight of the sample after oven drying at 103 - 105 degrees Celsius. The moisture result reported is on an as-received basis.					

Sample Description: BM1 Treated 720 kGy with KCl additive Soil
Chevron

LL Sample # SW 7684758
LL Group # 1520439
Account # 19947

Project Name: Chevron

Collected: n.a.

Submitted: 11/21/2014 09:30
Reported: 11/26/2014 14:53

Texas A & M University
Mechanical Engineering
3123 TAMU
College Station TX 77843

KCL--

CAT No.	Analysis Name	CAS Number	Dry Result		Dry Method Detection Limit	Dilution Factor
GC Volatiles		**SW-846 8015B modified**	**mg/kg**		**mg/kg**	
12989	C10-C12	n.a.	9.0	J	2.0	252.02
12989	C5-C6	n.a.	N.D.		2.0	252.02
12989	C6-C8	n.a.	N.D.		2.0	252.02
12989	C8-C10	n.a.	3.1	J	2.0	252.02
12989	Total GRO (C5-C12)	n.a.	14		2.0	252.02
GC Petroleum Hydrocarbons		**MA DEP EPH 5/04**	**mg/kg**		**mg/kg**	
07062	Aliphatics >C10 - C12	n.a.	N.D.		120	1
07062	Aliphatics >C12 - C16	n.a.	N.D.		120	1
07062	Aliphatics >C16 - C35	n.a.	780		120	1
07062	Aromatics >C10 - C12	n.a.	N.D.		120	1
07062	Aromatics >C12 - C16	n.a.	N.D.		120	1
07062	Aromatics >C16 - C21	n.a.	N.D.		120	1
07062	Aromatics >C21 - C35	n.a.	470		120	1
	The recovery for the sample surrogate(s) is outside the QC acceptance limits as noted on the QC Summary. The client was contacted and the data reported.					
GC Petroleum Hydrocarbons		**SW-846 8015B**	**mg/kg**		**mg/kg**	
02729	>C12-C14	n.a.	N.D.		82	10
02729	>C14-C16	n.a.	N.D.		82	10
02729	>C16-C18	n.a.	N.D.		82	10
02729	>C18-C20	n.a.	N.D.		82	10
02729	>C20-C22	n.a.	N.D.		82	10
02729	>C22-C24	n.a.	82	J	82	10
02729	>C24-C26	n.a.	130	J	82	10
02729	>C26-C28	n.a.	190	J	82	10
02729	>C28-C30	n.a.	260		82	10
02729	>C30-C32	n.a.	300		82	10
02729	>C32-C34	n.a.	430		82	10
02729	>C34-C36	n.a.	420		82	10
02729	>C36-C38	n.a.	490		82	10
02729	>C38-C40	n.a.	600		82	10
02729	DRO >C12-C22	n.a.	92	J	82	10
02729	ORO >C22-C40	n.a.	2,900		82	10
02729	Total TPH	n.a.	3,000		82	10
Wet Chemistry		**SM 2540 G-1997**	**%**		**%**	
00111	Moisture	n.a.	N.D.		0.50	1
	Moisture represents the loss in weight of the sample after oven drying at 103 - 105 degrees Celsius. The moisture result reported is on an as-received basis.					

Sample Description: BT Sludge Treated 1000kGy Soil
Chevron

LL Sample # SW 7684759
LL Group # 1520439
Account # 19947

Project Name: Chevron

Collected: n.a.

Submitted: 11/21/2014 09:30
Reported: 11/26/2014 14:53

Texas A & M University
Mechanical Engineering
3123 TAMU
College Station TX 77843

BT-SL

CAT No.	Analysis Name	CAS Number	Dry Result		Dry Method Detection Limit	Dilution Factor
GC Volatiles	**SW-846 8015B modified**		**mg/kg**		**mg/kg**	
12989	C10-C12	n.a.	7.4	J	2.1	251.26
12989	C5-C6	n.a.	7.7	J	2.1	251.26
12989	C6-C8	n.a.	19		2.1	251.26
12989	C8-C10	n.a.	7.8	J	2.1	251.26
12989	Total GRO (C5-C12)	n.a.	42		2.1	251.26
GC Petroleum Hydrocarbons	**MA DEP EPH 5/04**		**mg/kg**		**mg/kg**	
07062	Aliphatics >C10 - C12	n.a.	N.D.		6,300	5
07062	Aliphatics >C12 - C16	n.a.	N.D.		6,300	5
07062	Aliphatics >C16 - C35	n.a.	120,000		6,300	5
07062	Aromatics >C10 - C12	n.a.	N.D.		2,500	2
07062	Aromatics >C12 - C16	n.a.	N.D.		2,500	2
07062	Aromatics >C16 - C21	n.a.	18,000		2,500	2
07062	Aromatics >C21 - C35	n.a.	44,000		2,500	2
GC Petroleum Hydrocarbons	**SW-846 8015B**		**mg/kg**		**mg/kg**	
02729	>C12-C14	n.a.	N.D.		3,000	100
02729	>C14-C16	n.a.	4,300	J	3,000	100
02729	>C16-C18	n.a.	15,000		3,000	100
02729	>C18-C20	n.a.	31,000		3,000	100
02729	>C20-C22	n.a.	35,000		3,000	100
02729	>C22-C24	n.a.	35,000		3,000	100
02729	>C24-C26	n.a.	23,000		3,000	100
02729	>C26-C28	n.a.	22,000		3,000	100
02729	>C28-C30	n.a.	20,000		3,000	100
02729	>C30-C32	n.a.	17,000		3,000	100
02729	>C32-C34	n.a.	15,000		3,000	100
02729	>C34-C36	n.a.	15,000		3,000	100
02729	>C36-C38	n.a.	19,000		3,000	100
02729	>C38-C40	n.a.	22,000		3,000	100
02729	DRO >C12-C22	n.a.	86,000		3,000	100
02729	ORO >C22-C40	n.a.	190,000		3,000	100
02729	Total TPH	n.a.	280,000		3,000	100
Wet Chemistry	**SM 2540 G-1997**		**%**		**%**	
00111	Moisture	n.a.	4.5		0.50	1

Moisture represents the loss in weight of the sample after oven drying at 103 - 105 degrees Celsius. The moisture result reported is on an as-received basis.

General Sample Comments

State of Texas Lab Certification No. T104704194-13-10

All QC is compliant unless otherwise noted. Please refer to the Quality Control Summary for overall QC performance data and associated samples.